

UNIVERSITY OF WARMIA AND MAZURY IN OLSZTYN

Technical Sciences

20(1) 2017



PUBLISHER UWM

Editorial Board

Ceslovas Aksamitauskas (Vilnius Gediminas Technical University, Lithuania), Olivier Bock (Institut National de L'Information Géographique et Forestière, France), Stefan Cenkowski (University of Manitoba, Canada), Adam Chrzanowski (University of New Brunswick, Canada), Davide Ciucci (University of Milan-Bicocca, Italy), Sakamon Devahastin (King Mongkut's University of Technology Thonburi in Bangkok, Thailand), German Efremov (Moscow Open State University, Russia), Mariusz Figurski (Military University of Technology, Poland), Maorong Ge (Helmholtz-Zentrum Potsdam Deutsches GeoForschungsZentrum, Germany), Dorota Grejner-Brzezinska (The Ohio State University, USA), Janusz Laskowski (University of Life Sciences in Lublin, Poland), Arnold Norkus (Vilnius Gediminas Technical University, Lithuania), Stanisław Pabis (Warsaw University of Life Sciences-SGGW, Poland), Lech Tadeusz Polkowski (Polish-Japanese Institute of Information Technology, Poland), Arris Tijsseling (Technische Universiteit Eindhoven, Netherlands), Vladimir Tilipalov (Kaliningrad State Technical University, Russia), Alojzy Wasilewski (Koszalin University of Technology, Poland)

Editorial Committee

Marek Markowski (Editor-in-Chief), Piotr Artiemjew, Kamil Kowalczyk, Wojciech Sobieski, Piotr Srokosz, Magdalena Zielińska (Assistant Editor), Marcin Zieliński

Features Editors

Piotr Artiemjew (Information Technology), Marcin Dębowski (Environmental Engineering), Zdzisław Kaliniewicz (Biosystems Engineering), Grzegorz Królczyk (Materials Engineering), Marek Mróz (Geodesy and Cartography), Ryszard Myhan (Safety Engineering), Wojciech Sobieski (Mechanical Engineering), Piotr Srokosz (Civil Engineering), Jędrzej Trajer (Production Engineering)

Statistical Editor

Paweł Drozda

Executive Editor

Mariola Jezierska

The Technical Sciences is indexed and abstracted in BazTech (<http://baztech.icm.edu.pl>) and in IC Journal Master List (<http://journals.indexpopernicus.com>)

The Journal is available in electronic form on the web sites
<http://www.uwm.edu.pl/techsci> (subpage Issues)
<http://wydawnictwo.uwm.edu.pl> (subpage Czytelnia)

The electronic edition is the primary version of the Journal

PL ISSN 1505-4675
e-ISSN 2083-4527

© Copyright by Wydawnictwo UWM • Olsztyn 2017

Address

ul. Jana Heweliusza 14
10-718 Olsztyn-Kortowo, Poland
tel.: +48 89 523 36 61
fax: +48 89 523 34 38
e-mail: wydawca@uwm.edu.pl

Contents

W. LUDWIG, T. MAĆZKA – <i>Determination of Cores Electrification During the Flow in the Modified Wurster Apparatus</i>	5
S. FRANCIK, N. PEDRYC, A. KNAPCZYK, A. WÓJCIK, R. FRANCIK, B. ŁAPCZYŃSKA-KORDON – <i>Bibliometric Analysis of Multiple Criteria Decision Making in Agriculture</i>	17
A. SKOTNICKA-SIEPSIAK – <i>Comparing Selected Parameters of a Two-Dimensional Turbulent Free Jet on the Basis of Experimental Results, Digital Simulations, and Theoretical Analyses</i>	31
Z. MARSZAŁEK – <i>Performance Test on Triple Heap Sort Algorithm</i>	49
A. RYCHLIK, K. LIGIER – <i>Fatigue Crack Detection Method Using Analysis of Vibration Signal</i>	63
W. SOBIESKI, S. LIPIŃSKI – <i>The Analysis of the Relations Between Porosity and Tortuosity in Granular Beds</i>	75
S. ULLAH KHAN, N. ALI – <i>Unsteady Hydromagnetic Flow of Oldroyd-B Fluid Over an Oscillatory Stretching Surface: a Mathematical Model</i>	87



DETERMINATION OF CORES ELECTRIFICATION DURING THE FLOW IN THE MODIFIED WURSTER APPARATUS

Wojciech Ludwig¹, Tadeusz Mączka²

¹ Department of Chemical Engineering
Wrocław University of Technology

² Senior R&D Specialist,
Institute of Power Systems Automation, Wrocław

Received 17 June 2016, accepted 14 December 2016, available online 16 December 2016.

Key words: electrification, cores, Wurster, spout-fluid bed.

Abstract

The purpose of this paper was presentation of the value of cores electrification during their flow in the modified Wurster apparatus, applied for dry encapsulation of pharmaceutical materials. Previous works of the authors dealt with vulnerability of the particles of different diameter, produced by SYNTAPHARM (Cellets 1000, 700 and 100) on electrification in laboratory conditions. The presented work gives the results of examination on particles electrification in real conditions of their stable circulation in a column. The measurement system, that was applied, allowed determination of electrification potential and electrification current. Those quantities, which are the measures of charge accumulation on cores were determined for several particles (Cellets 1000, 700 and 500) with the different humidity, for different mass of the bed and spouting gas velocities.

Symbols:

- d – particles diameter [μm]
- I – particles electrification current [μA]
- m – mass of a bed circulating in a column [g]
- U – particles electrification potential [kV]
- \dot{V} – volumetric flow rate of the spouting gas [l/min]
- X – initial humidity of the bed [%]
- ρ – bulk density of particles [kg/m^3]

Introduction

In the course of fluidization and spouting of particles built of dielectric material the occurrence of the phenomena connected with their electrostatic charging is practically unavoidable. The first reports describing those kind of phenomena appeared in the literature in forties of the twentieth-century and from that time many researchers dealt with this subject (PARK et al. 2002, MEHRANI et al. 2005). It is justified, because electrostatic charging of the bed very often affects its flow hydrodynamics in decisive way. High value of electrostatic charge collected on moving particles leads to series of negative processes. The most important among them is particles agglomeration on the walls of the equipment and its internals (control and measuring elements), which entails the necessity of frequent apparatus stopping and its cleaning. Under the influence of electrostatic forces large agglomerates could be created inside the bed, reducing an efficiency and productivity of some unit processes e.g. drying or coating. Uncontrolled electric discharging leads frequently to the damage of control and measurement instruments and creates fire or explosion risks (CHENG et al. 2012).

Mechanism of charge creation on the particles moving in a bed is quite complex and it has not been explained completely yet. The electric charge is created in the course of particles mutual friction or the friction between particles and the walls of the column, alternatively during particles collision with equipment elements. There is also effect between continuous and dispersed phases (ionization of fluidizing gas) (MEHRANI et al. 2005, MOUGHRABIAH et al. 2009). Literature review provides great deal of information concerning the methods of the measurement of charge, its dependence on a bed parameters, fluidizing air and the equipment construction. However all those data concern only classical or circulating fluidized beds and model-based particles, made frequently of glass and plastic (polyethylene, polypropylene, polystyrene) (GUARDIOLA et al. 1996, CHENG et al. 2012). There is a lack of a report describing electrostatic phenomena in a spouted bed apparatus, although this equipment is successfully applied for years in many branches of economy e.g. in drying and pharmaceutical industry.

Among many known equipment applied to particles (cores) and tablets coating, spouted bed apparatus seems to be the optimal construction (TEUNOU, PONCELET 2002). In the fifties of the twentieth-century coating was realized in spouted bed apparatuses, in which spraying nozzle was placed in the upper part of the chamber with a bed. Although both the yield of such a process and the quality of produced coat were low. Since that apparatuses with a spraying device, placed in the bottom part of the bed were introduced. In this system probability of collisions of particles with drops of coating solution and the yield

of the process are higher, drying time is shorter, although high risk of agglomeration takes place, because of high concentration of wetted particles close the nozzle (WURSTER 1950). Some type of modification of the design described above is the Wurster apparatus (WURSTER 1950, WURSTER, LINDLOF 1966). Wurster apparatus is a spouting device with a draft tube and an additional fluidizing air stream (spout-fluid bed). At the bottom of the chamber there is a mesh used to distribute hot air stream. A spraying nozzle is positioned in the center of the distributor, placed at the bottom of the bed. Coating solution is sprayed through the nozzle or several nozzles and deposited upon particles at the time, when they flow through the entrainment zone. Every particle obtains a small part of the coat during its flow through the spraying zone. Particles are dried inside draft tube, flow into fountain zone, and next in the annulus they settle down again to the entrainment zone. Repeated movement (regular circulation) of particles leads to creation of a solid layer on their surface. Wurster apparatus is considered as the best device for periodical coating of grain materials (TEUNOU, PONCELET 2002, KARLSSON et al. 2006).

Wurster apparatus of unique construction was designed and built during former research. It enables obtaining very high particles velocity and because of that high coating yield (SZAFRAN et al. 2012). Unfortunately, proposed design solution causes several negative phenomena connected with cores electrification. It occurs during particles friction with the walls of the draft tube and the apparatus as well as during rapid impact on deflector. It leads to agglomeration of the particles and accumulation of the bed on the wall surface of the equipment, which interfere with circulation and reduce effectiveness of coating process. The authors have carried out investigations on counteracting those negative phenomena. One of the preparatory stages is the work presented here.

The purpose of the work presented in this paper was examination of the impact of the process variables (spouting velocity, mass of the bed) and particles humidity and diameter on electrification of a bed in the modified Wurster apparatus, together with an elaboration of a simple method of electrostatic effects measurement, with minor interfering in equipment construction. On this basis it will be possible to draw conclusions on restrictions or elimination of uncontrolled electrostatic particles charging during their circulation in the apparatus.

Experimental equipment

All the measurements were carried out in the installation presented in Figure 1. Air was pressed by rotary-screw compressor 1, equipped with refrigeration aggregate (2) and went through filters system (3, 4 and 5), which

removed oil droplets and through pressure reducer (6) enabling flow rate control. Afterwards gas flowed through rotameter (7) to the bed spouting nozzle in conical bottom of the apparatus (8) made of aluminum.

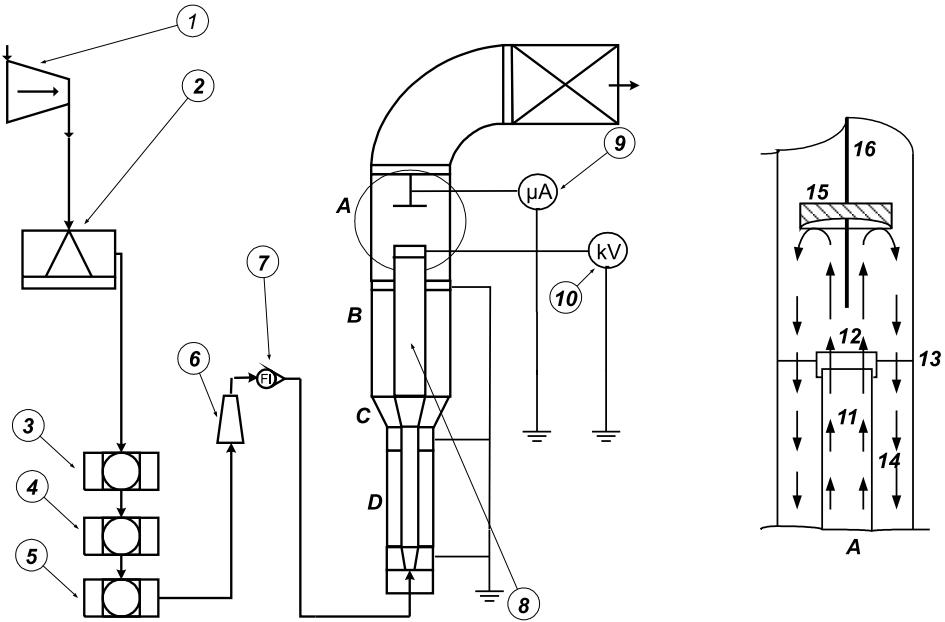


Fig. 1. Schematic diagram of experimental installation with details of the upper segment of the apparatus (arrows show trajectories of particles): 1 – compressor, 2 – freeze-air drying unit, 3 – coarse air filter, 4 – accurate air filter, 5 – carbon air filter, 6 – pressure reducer, 7 – rotameter, 8 – spout-fluid bed column (A – upper segment with the deflector, B – middle segment, C – cone with the spraying nozzles, D – lower segment with the spouting gas nozzle), 9 – microammeter, 10 – kilovoltmeter, 11 – draft tube, 12 – clamp, where the voltmeter was connected, 13 – mounting of the clamp, 15 – deflector, 16 – mounting of the deflector, where the ammeter was connected

The column (Fig. 1) consisted of three main parts: cylindrical glass segments A, B and D, aluminum cone C, in the axis of which the nozzles introducing air, plasticizer and coating substance were placed. Plasticizer and coating agent were not used in the examination presented in this paper. Above and below the lower segment of the apparatus there were aluminum rings with apertures applied for particles loading and removal. Draft tubes were placed in the segments axes, and joined together with the use of aluminum clamps. The upper segment A was equipped with deflector (15), which constricted escaping of the particles outside the installation. Electrostatic kilovoltmeter (10) (C196) was connected to upper, electrically isolated clamp (12) of the draft tube (11) using the high-voltage cable, to enable voltage measurement. Microammeter (9)

(Metex M-3270), which measured electrification current of striking particles, was connected to electrically isolated metal element, supporting aluminum deflector (16). All metal elements of the column, except those applied for measurements, were grounded to prevent uncontrolled electrical discharge.

Measurements were carried out at constant temperature 25°C, changing volumetric flow rate of spouting gas at constant bed mass (500 g) or changing bed mass at constant volumetric flow rate of spouting gas (1200 liters/min.) for different initial humidity of the particles (Tab. 1). Cellets® cores made of microcrystalline cellulose, produced by SYNTAPHARM and used in pharmaceutical industry were applied as particles (Tab. 2).

Table 1
Ranges of operating variables

Parameter	Minimum value	Maximum value
Bed humidity [%]	0	15
Spouting gas volume flow rate [l/min]	930	1200
Mass of the bed [g]	200	900

Table 2
Properties of investigated particles

Particles	d [μm]	ρ [kg/m^3]	Sphericity	Geldart class
Cellets® 500	500–710	800	0.95	A
Cellets® 700	700–1000	800	0.95	B
Cellets® 1000	1000–1400	800	0.95	B

Specific mass of particles, which were electrically uncharged and possessed specific humidity, was introduced into experimental equipment and then volumetric flow rate of the spouting gas was set up, making the bed stable circulation. After the time necessary to stabilization of measured quantities (5 min) electrification potential was read out as well as electrification current. Subsequently, the gas flow was stopped and the bed was electrically discharged through the grounded bottom of the apparatus made of metal. In the next stage another portion of the bed (100 g) was added or another circulation velocity was established (changing the pressure of the gas by 0.5 bar). Particles of specific humidity were prepared by the material saturation with water. Material humidity measurement was made applying gravimetric method with the use of moisture analyzer Radwag MAX 50.

Results and discussion

As a result of examination the dependences between electrification potential and electrification current for different particles were obtained, depending on the velocity of the spouting gas (particle velocity) and the mass of the bed with different initial humidity. Electrification potential achieved high values in the range of 13–41 kV, while electrification current varied in the range of 0.5–3.1 μA .

Together with the growth of the bed mass electrification potential increased, however the differences were higher at the beginning of measurements series – at smaller amount of the circulating bed (Fig. 2). It could be caused by the growth of particles concentration, which led to smaller electrification by friction on apparatus walls. Together with the growth of the mass of the bed there is also augmentation of its quantity collected on the grounded bottom of the apparatus, as movable packed bed, which makes longer the residence time of particles in this zone and favors their electrical discharging. Along with growth of the volumetric flow rate of the spouting gas, and as a result the augmentation of the particles velocity, the electrification potential decreased (Fig. 3), which was probably caused by the lower contact time of the particles with the apparatus walls. The growth of electrification potential with the growth of initial humidity of the bed was observed (Fig. 2, 3), despite the humid bed circulates better, because its charge relaxation time is short and greater electric charge could be quickly taken away (quick discharging).

Together with the growth of the bed humidity electrification current grew (Fig. 4, 5), which is connected with the drop of particles resistivity (from about $10^9 \Omega\text{m}$ to $10^5 \Omega\text{m}$) and relaxation time (from about 10^{-1} s to 10^{-5} s) (MĄCZKA 2015), which causes the growth of the charge exchange rate. Along with the growth of the volumetric flow rate of spouting air there is a growth of electrification current, which is related to the growth of the particles impact velocity on the deflector. Together with the growth of the bed mass the electrification current grew, achieving the maximum value for the bed mass between 600 and 800 g (Fig. 6). At the mass of about 600 g the number of cores in the fountain is so high, that some part of them do not reach the deflector, which causes reduction of electrification current. Besides that, there is augmentation of the bed mass in the bottom of the apparatus, which leads to its partial discharging.

Together with the decrease of particles diameter both electrification potential and electrification current increased (Fig. 6, 7). However in the first case the differences between particles are small especially with small masses of the bed. More significant differences arise only with masses of the bed greater

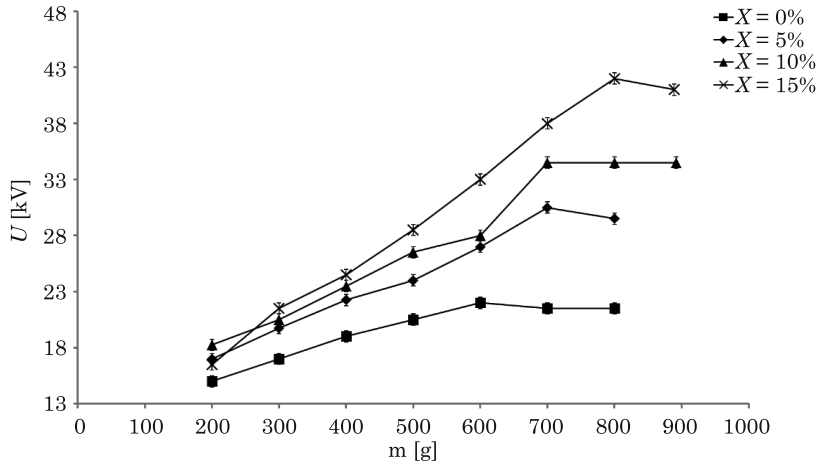


Fig. 2. Dependence of electrification potential on the mass of bed for its different initial humidity ($\dot{V} = 1200$ l/min, Cellets® 1000)

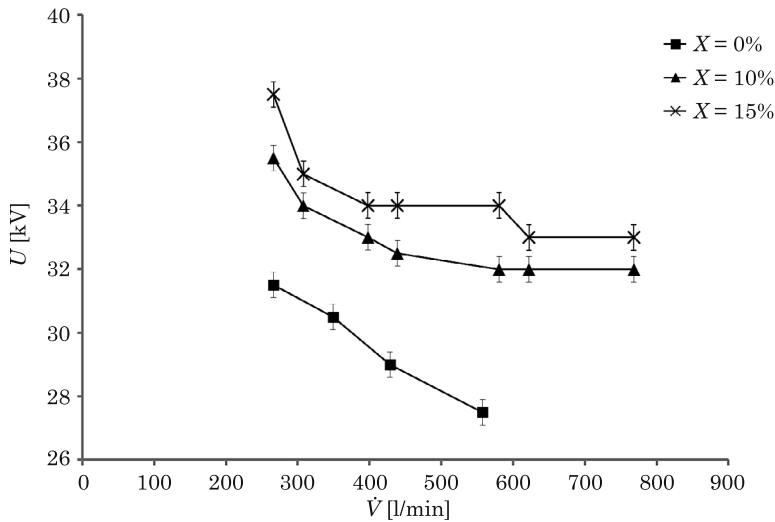


Fig. 3. Dependence of electrification potential on the volumetric flow rate of the spouting gas for different initial humidity of the bed ($m = 500$ g, Cellets® 1000)

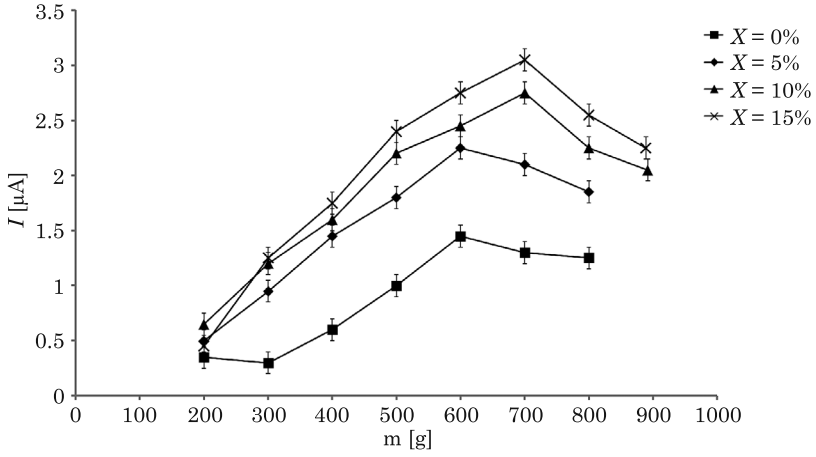


Fig. 4. Dependence of electrification current on the mass of bed for its different initial humidity ($\dot{V} = 1200$ l/min, Cellets® 1000)

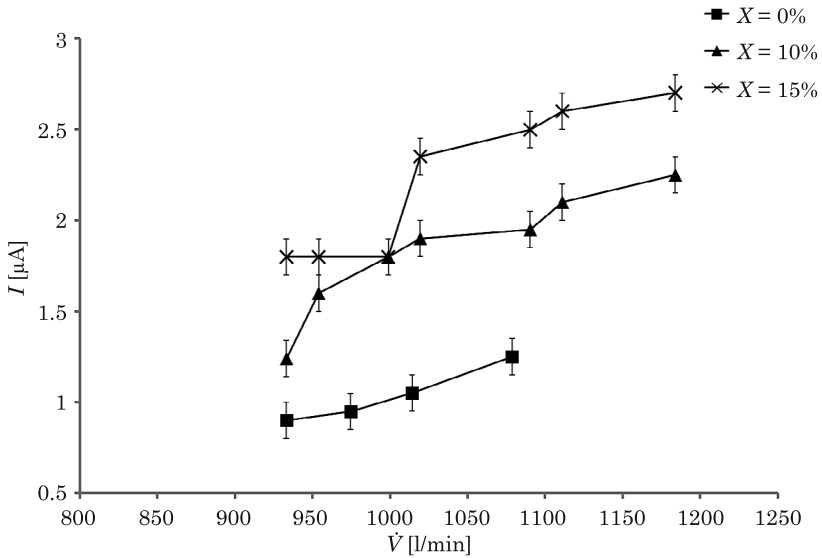


Fig. 5. Dependence of electrification current on the volumetric flow rate of the spouting gas for different initial humidity of the bed ($m = 500$ g, Cellets® 1000)

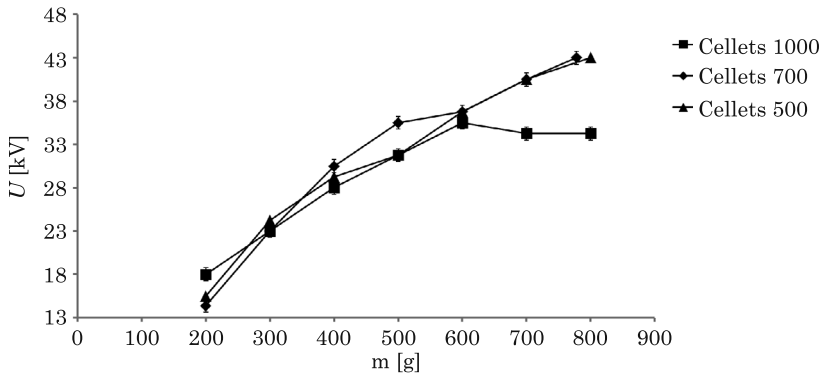


Fig. 6. Dependence of electrification potential on the bed mass for different particles ($\dot{V} = 1200$ l/min, $X = 0\%$)

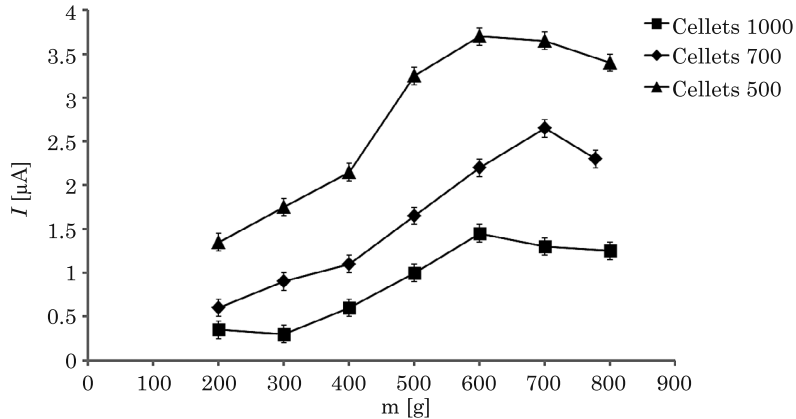


Fig. 7. Dependence of electrification current on the bed mass for different particles ($\dot{V} = 1200$ l/min, $X = 0\%$)

than 400 g. Particles with smaller diameter develop larger surface, and because of that they can accumulate greater charge, additionally at the same time higher number of them strike on the deflector.

Conclusions

Parameters of electrification such as electrification potential and electrification current were determined applying relatively simple measuring system, taking advantage of elements of the inner part of the apparatus, without any significant changes of the equipment construction.

It was established that the potential difference in the column, despite grounding of its metal elements, achieved very high values – from a dozen or so to tens of kilovolts, which confirmed the primary hypothesis on electrostatic mechanisms of negative phenomena such as material sticking to inner parts of the column, which often precluded the correct work of the equipment. The measurement device, that was applied, unfortunately did not enable to determine directly the basic quantity from the point of view of electrostatics – the amount of electric charge collected in the bed. It could be calculated on the base of gathered data and additionally knowing the concentration and particles velocity in the draft tube. At this stage of preliminary research authors did not have the possibility to determine those two parameters.

Owing to this fact, in further part of examination, it is predicted to rebuild the equipment at its lower part, in order to determine the total electrical charge, applying Faraday cage method. On this base it will be possible to draw final conclusions, concerning optimal hydrodynamic parameters and modification of the bed properties, that constrict uncontrolled electrical charging of the cores.

Acknowledgements

The authors wish to thank SYTAPHARM company for supply of the Cellets® particles.

The studies were funded by the Polish National Science Centre within the framework of the research grant UMO-2013/09/B/ST8/00157.

References

- CHENG Y., LAU D.Y.J., GUAN G., FUSHIMI C., TSUTSUMI A., WANG C.H. 2012. *Experimental and Numerical Investigations on the Electrostatics Generation and Transport in the Downer Reactor of a Triple-Bed Combined Circulating Fluidized Bed*. Industrial and Engineering Chemistry Research, 51: 14258–14267.
- GUARDIOLA J., ROJO V., RAMOS G. 1996. *Influence of particle size, fluidization velocity and relative humidity on fluidized bed electrostatics*. Journal of Electrostatics, 37: 1–20.
- KARLSSON S., BJOERN I.N., FOLESTAD S., RASMUSON A. 2006. *Measurements of the particle movement in the fountain region of a Wurster type bed*. Powder Technology, 165: 22–29.
- MAĆZKA T. 2015. *Study on the electrostatic properties of cores*. Report no. 504-002104-026-ZT/TM-25/2015, Wrocław Electrotechnical Institute.
- MEHRANI P., BI H.T., GRACE J.R. 2005. *Electrostatic charge generation in gas-solid fluidized beds*. Journal of Electrostatics, 63: 165–173.
- MOUGHRAHIAH W.O., GRACE J.R., BI X.T. 2009. *Effects of Pressure, Temperature, and Gas Velocity on Electrostatics in Gas – Solid Fluidized Beds*. Industrial Engineering Chemical Research, 48: 320–325.
- PARK A.H., BI H., GRACE J.R. 2002. *Reduction of electrostatic charges in gas-solid fluidized beds*. Chemical Engineering Science, 57: 153–162.

-
- SZAFRAN R.G., LUDWIG W., KMIEĆ A. 2012. *New spout-fluid bed apparatus for electrostatic coating of fine particles and encapsulation*. Powder Technology, 225: 52–57.
- TEUNOU E., PONCELET D. 2002. *Batch and continuous bed coating- review and state of the art*. Journal of Food Engineering, 53: 325–340.
- WURSTER D.E. 1950. *Means of applying coatings to tablets or like*. Journal of the American Pharmaceutical Association, 48(8): 451.
- WURSTER D.E., LINDLOF J. A. 1966. *Particle coating apparatus*. US patent, 3241529.



Quarterly peer-reviewed scientific journal

ISSN 1505-4675
e-ISSN 2083-4527

TECHNICAL SCIENCES

Homepage: www.uwm.edu.pl/techsci/



BIBLIOMETRIC ANALYSIS OF MULTIPLE CRITERIA DECISION MAKING IN AGRICULTURE

***Sławomir Francik¹, Norbert Pedryc¹, Adrian Knapczyk¹,
Artur Wójcik¹, Renata Francik²,
Bogusława Łapczyńska-Kordon¹***

¹ Department of Mechanical Engineering and Agrophysics
University of Agriculture in Krakow

² Department of Bioorganic Chemistry
Jagiellonian University Medical College

Received 7 October 2016, accepted 14 December 2016, available online 15 December 2016.

Key words: Multiple Criteria Decision Making, Multiple Criteria Decision Analysis, bibliometric analysis, research trends, Agriculture.

A b s t r a c t

Development trends (Research Trends) in scientific research on the methods of Multiple Criteria Decision Making (MCDM) and Multiple Criteria Decision Analysis (MCDA) in agriculture are analyzed. Established bibliometric techniques are applied. MCDA/MCDM methods are being very intensively developed in recent years, as evidenced by the number of scientific papers published annually in renowned scientific journals indexed in the Web of Science (WoS) database. In the years 1979–2015 a total of 1,355 scientific articles were collected in the database. The number of articles published annually increased rapidly after 2005. Besides, the annual number of citations of the publications is increasing. Research on MCDA/MCDM is conducted in many research areas. In the years 1984–2015 the Web of Science database accumulated 27 scientific publications on MCDA/MCDM in agriculture area. Therefore, it can be concluded that the MCDA/MCDM issues are currently not sufficiently analyzed in relation to agriculture. In the future this subject will probably be further developed, an increasing number of scientists will conduct research on the MCDA/MCDM and the annual number of articles published in the field will increase.

Correspondence: Sławomir Francik, Katedra Inżynierii Mechanicznej i Agrofizyki, Uniwersytet Rolniczy w Krakowie, ul. Balicka 120, 30-149 Kraków, e-mail: Slawomir.Francik@ur.krakow.pl

Introduction

Decision making is an integral part of human activity in all areas. Choosing the best option (optimal decision) is most often very difficult due to incomplete knowledge of the situation requiring a decision – a collection of all factors (dependent and independent of an evaluator), affecting the decision by the decision-maker in the decision-making process (KSIĄŻEK 2011). The most common decisions must be taken in conditions of uncertainty and taking into account many, often contradictory, criteria. Modeling a decision-making situation, one can differently assess importance of specific factors and aggregate variables. Solving such problems is the subject of the so-called multiple criteria decision analysis – MCDA (Multiple Criteria Decision Analysis). It is defined as a set of methods and mathematical tools to enable comparison of variants of decision, taking into account different and often conflicting criteria (PIWOWARSKI 2009, ŻAK 2014, KRUSZYŃSKI 2014). This area is also called multiple criteria decision making (MCDM – Multiple Criteria Decision Making).

It is considered that the beginning of the multiple criteria decision analysis (MCDA) was a scientific conference *Multiple Criteria Decision Making* organized by Cochrane and Zeleny in 1972 at Columbia University in South Carolina, USA (FIGUEIRA et al. 2005). Since then, there has been a rapid development of research on methods of multi-criteria decision analysis.

Decision making is closely related to a range of activities in agriculture. Owners of farms have to make decisions that are related to the organization of agricultural production, choice of technology, selection and operation of machinery and equipment, as well as the economics. Thus, providing the tools that allow to make the best decisions is an important task for scientists. As one of the tools are MCDA/MCDM methods, it is vital to determine the current state of research in applications of MCDA/MCDM in agriculture and to identify the development trends related to that research.

The aim of the paper was to analyse development trends (Research Trends) in scientific research on the methods of Multiple Criteria Decision Making (MCDM) and Multiple Criteria Decision Analysis (MCDA) in agriculture.

One way of attaining the objective is to use established bibliometric techniques. A bibliometric method was used in this research. An additional aim of this paper was to analyze the existing MCDA/MCDM methods and their classification.

Classification of MCDA/MCDM methods

MCDA/MCDM methods are used to solve different kinds of decision-making problems. According to the criterion: the purpose of decision-making, multicriteria decision problems are divided into three (GRABAŃSKI 2015, KRUSZYŃSKI 2014) or four (PIWOWARSKI 2009, ROY 2005) groups:

- $P.\alpha$ – choice problematic – multi-criteria optimization – determining the best variant of the decision-making,
- $P.\beta$ – sorting problematic – the allocation of variants to specific categories,
- $P.\gamma$ – ranking problematic – ordering variants, classifying equally good variants,
- $P.\delta$ – description problematic – description of potential variants.

Due to the dynamic development of methods used to support decision makers in solving multi-criteria decision-making problems, there are difficulties in their unambiguous classification – different authors use different classification criteria. One of the most frequently cited is the classification of the methods into three groups (ŻAK 2014, KRUSZYŃSKI 2014, VINCKE 1992, SEIXEDO, TERESO 2010):

Group I – methods of Multi Attribute Utility Theory (MAUT), the so-called American school of multi-criteria decision support (B. Roy synthesis method to a single criterion, bypassing incomparability of the variants – e.g. UTA, AHP);

Group II – methods of outranking, so-called European / French / school of multi-criteria decision support (B. Roy methods of outranking synthesis, taking into account incomparability of the variants – e.g. ELECTRE I-IV, Promethee I, II and Oreste);

Group III – interactive methods or multi-objective mathematical programming models, (B. Roy dialogue methods of local assessment in different iterations – e.g. LBS STEM).

A similar classification of MCDA methods has been used in the book *Multiple Criteria Decision Analysis: State Of The Art Surveys*, edited by J. Figueiry, S. Greco and M. Ehrgott, published by Springer Publishing House (FIGUEIRA et al. 2005):

- Outranking Methods: ELECTRE Methods, PROMETHEE Methods, Other Outranking Approaches,
- methods based on Multiattribute Utility and Value Theories: UTA Methods, Analytic Hierarchy and Analytic Network Processes, MACBETH,
- Non-Classical MCDA Approaches.

A more extensive breakdown of methods of multi-criteria decision making (MCDM) is shown in Figure 1 (SOBCZYK et al. 2011, PIWOWARSKI 2009).

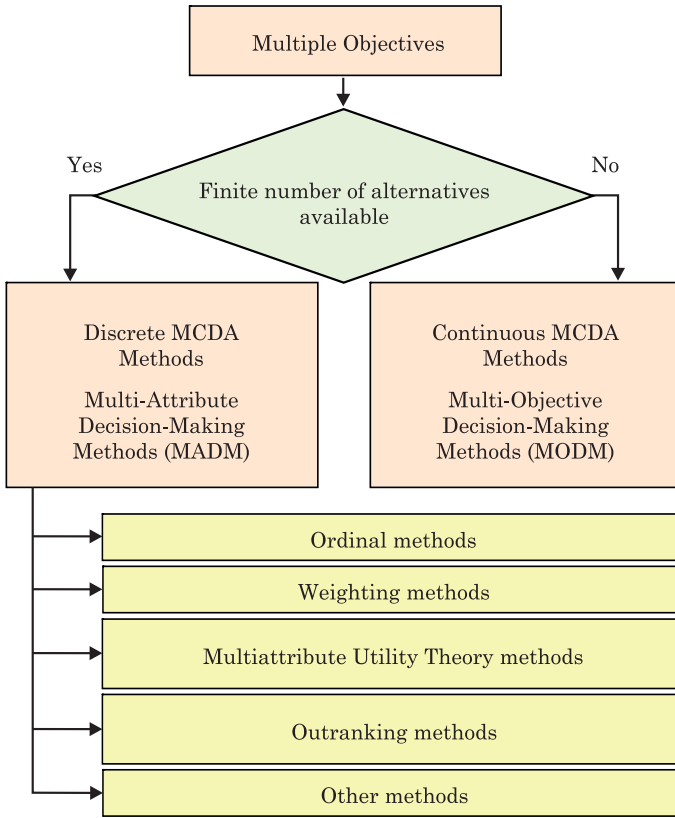


Fig. 1. Classification of multi-criteria decision support methods

Source: authors' own analysis based on PIWOWARSKI (2009), KODIKARA (2008), SOBCZYK et al. (2011)

PIWOWARSKI and KODIKARA divided discrete MCDA methods into five groups (PIWOWARSKI 2009, KODIKARA 2008, SOBCZYK et al. 2011) while Trzaskalik distinguishes seven groups of methods among the methods of decision support in multicriteria discrete decision-making (TRZASKALIK 2014a, TRZASKALIK 2014b):

- Additive Methods,
- The AHP method (Analytical Hierarchy Process) and related methods,
- Verbal Methods,
- ELECTRE Methods,
- PROMETHEE Methods,
- Use of reference points,
- Interactive Methods.

Bibliometric method

Bibliometry was introduced by Pritchard in 1969 as a method of mathematical and statistical analysis applied to books and other communication media. Citation and content analyses are now widely used bibliometric techniques (SUN et al. 2012). Broadus defined bibliometry as a quantitative analysis of physically published units or bibliographic units (TSAI 2012).

Bibliometric research techniques are divided into evaluative and descriptive. Descriptive bibliometric techniques allow for the observation of trends in the development of science and technology, the identification of relevant actors on the stage of innovation and a better understanding of the specifics of individual areas of research (KLINCEWICZ et al. 2012).

Bibliometric techniques have many advantages. The most important is the ability to conduct quantitative analyses objectified based on the codified knowledge – measurable, objectified, consistent and accessible data, HICKS et al. (2002). Hence, bibliometrics is an effective and important tool to determine the trends of research in various fields of science (AKHAVAN et al. 2016, ELLEGAARD, WALLIN 2015, KADEMANI et al. 2013, KUMARI 2013, PENG et al. 2015, YANG et al. 2013, SUN et al. 2012).

As confirmed by some publications (KLINCEWICZ et al. 2012, ELLEGAARD, WALLIN 2015), research institutions, universities as well as individual scientists are interested in systematic observation of technological development and research trends.

The results of bibliometric analyses are now often used, particularly in the areas of basic and applied sciences (ELLEGAARD, WALLIN 2015).

Analyses of publications were conducted, among others, and trends set in the areas of scientific research in relation to:

- knowledge management (AKHAVAN et al. 2016),
- materials science (KADEMANI et al. 2013),
- synthetic organic chemistry (KUMARI 2013),
- digital elevation model – DEM (PENG et al. 2015),
- engineering (UCAR et al. 2014),
- solid waste (YANG et al. 2013).

Bibliometrics can be successfully used to determine trends in the field of agriculture and forestry (KLINCEWICZ et al. 2012).

Bibliometric analysis requires the selection of a database, on the basis of which publications will be obtained. One of the most widely used databases for bibliometric analysis of publications in the Web of Science (WoS), which contains articles with the highest level of quality – from magazines with a significant impact factor (AKHAVAN et al. 2016, ELLEGAARD, WALLIN 2015, HU et al. 2010, KADEMANI et al. 2013, PENG et al. 2015, SUN et al. 2012, TSAI 2012,

YANG et al. 2013). Therefore, in this study the WoS database has been used as a data source.

Bibliometric analyses usually take place in several stages (SUN et al. 2012, TSAI 2012, VAN RAAN, VAN LEEUWEN 2002, YANG et al. 2013):

1. The assembly of data on publications (complying with adopted criteria) indexed in the selected database and creating a set of publications;

2. Classification of publications collected on the basis of search (included in the collection of publications) in terms of:

- document type,
- the characteristics of publications in different years,
- the characteristics of citations of publications in those years,
- country / territory from which the authors of the publication come,
- dominant institutions in which the research was carried out, on the basis of affiliation of the authors of the publications,
- the most important magazines in which publications were issued,
- authors with the greatest number of published articles and the highest number of citations;

3. Analysis of the results of classification.

Materials and Methods

As part of this paper a set of publications was created on the basis of search in the Web of Science Core Collection database, on the subject of articles terms: “Multiple Criteria Decision Analysis” or “Multiple Criteria Decision Making”. The search was performed on documents in English from 1945 until 2015.

After determining the number of document types, further analyses were carried out for the identified scientific publications (Document Types: Article). The distribution in time for a number of scientific publications and the number of citations of these publications in the years 1979–2015 was made. The main “Research Areas” were identified, as well as main “Web of Science Categories”, “Countries/Territories” the authors of the publication came from, scientific institutions the authors are affiliated with (Organizations) and the authors who have published the largest number of articles.

Then, the subset in the Research Area: Agriculture was separated from the accumulated set of publication. For those publications we determined:

- distribution of the number of scientific publications in time and the number of citations of those publications,
- the major categories of the Web of Science,
- country / state the authors of the publications came from,
- research institutions the authors are affiliated with and the authors who have published the largest number of articles.

Results

As a result of the search in the Web of Science Core Collection (topic: Multiple Criteria Decision Analysis or Multiple Criteria Decision Making; the period from 1945 to 2015) 2021 records/documents were identified. Among the documents found, articles were the most numerous – 1355, followed by proceedings papers – 663. Other documents include: books reviews – 35, publication reviews – 34, meeting abstracts – 11, notes – 5 books – 4, letters – 2 and discussions – 1. The first publication appeared in 1979.

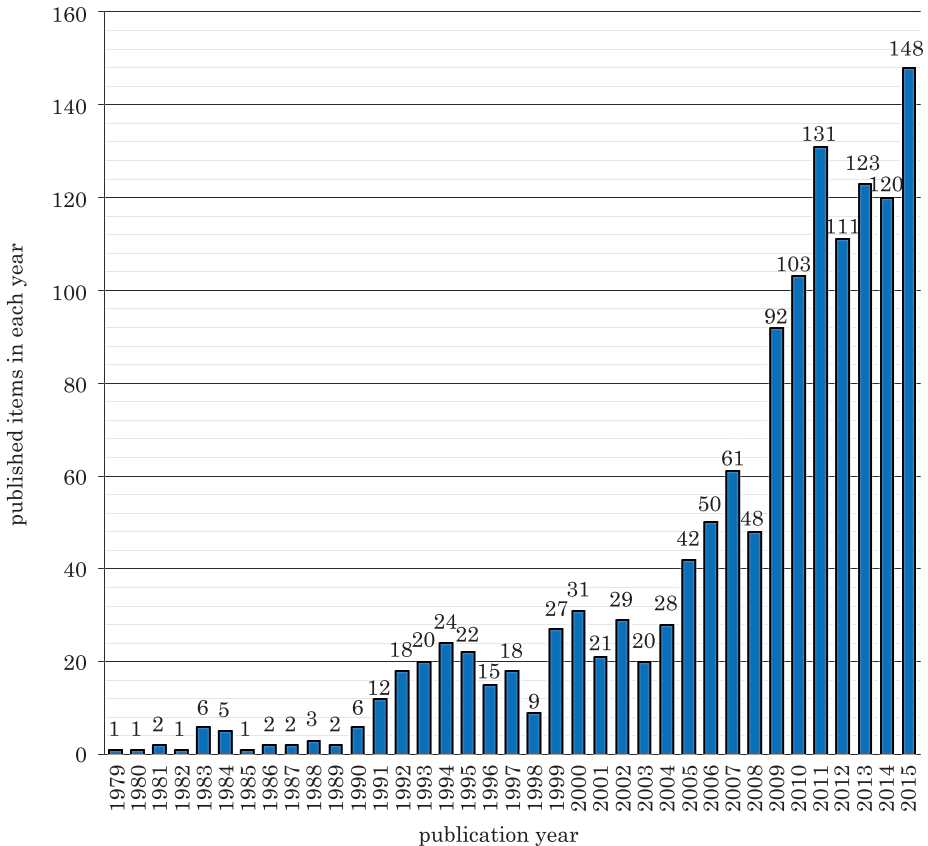


Fig. 2. The number of scientific articles indexed in the Web of Science Core Collection database, published in different years

Analysing the change in the number of scientific articles published in different years (Fig. 2) is it possible to distinguish four periods:

I from 1979 to 1990 – the average number of publications 2.7.

II from 1991 to 2004 – the average number of publications 21.0.

III from 2005 to 2009 – the average number of publications 58.6.

IV from 2010 to 2015 – the average number of publications 122.7.

The importance of the multi-criteria decision analysis (Multiple Criteria Decision Analysis) or multi-criteria decision-making (Multiple Criteria Decision Making) is evidenced not only by the number of scientific publications but also by the number of citations of these publications in the Web of Science Core Collection database (WoS-CC). In the years 1981 to 2015 the total number of citations was more than 23,000 (23,167). The number has been rising very sharply since 2005 (Fig. 3).

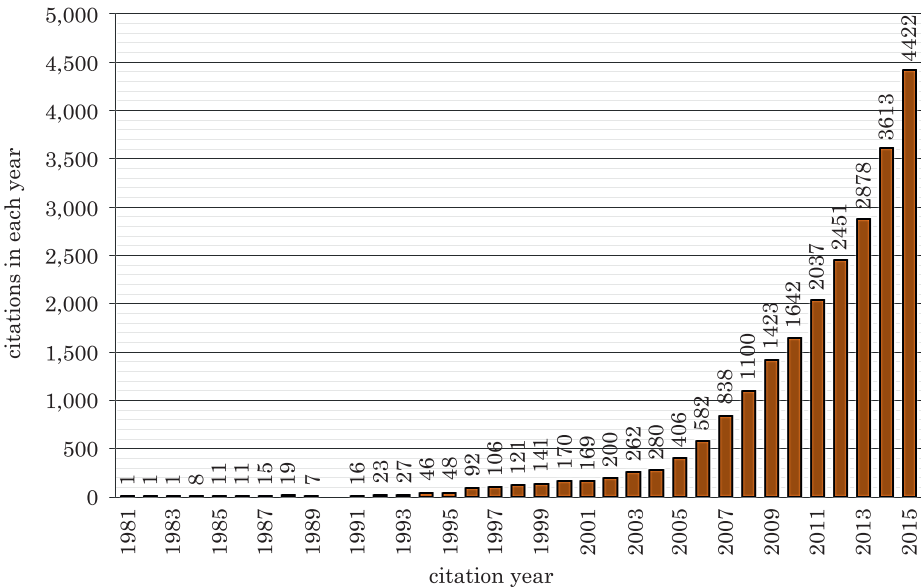


Fig. 3. The number of citations of scientific articles found in the Web of Science Core Collection database in different years

The most frequently cited publication (Tab. 1) had 603 citations (to year 2015) and the average number of citations during the year amounted to more than 50.

The accumulated set of 1,335 publications included 62 research areas, with most publications in the area of: Computer Science – 512, Operations Research And Management Science – 510, Engineering – 424 and Business Economics – 329.

A similar range is related to the use of Web of Science Categories. Most of the publications belonged to the categories: operational research and management science – 519, computer science artificial intelligence – 312, Management – 239 and Computer Science Interdisciplinary Applications – 157.

The most cited publications on MCDA/MCDM in the years 1981–2015

Table 1

Authors	Title	Publication year	Journal	TC	AvC
Opricovic S., Tzeng G.H.	<i>Compromise solution by MCDM methods: A comparative analysis of VIKOR and TOPSIS.</i>	2004	European Journal of Operational Research, 156(2): 445–455	603	50.3
Chen C.T., Lin C.T., Huang S.F.	<i>A fuzzy approach for supplier evaluation and selection in supply chain management. By:..</i>	2006	International Journal of Production Economics, 102(2): 289–301	411	41.1
Tzeng G.H., Chiang C.H., Li C.W.	<i>Evaluating intertwined effects in e-learning programs: A novel hybrid MCDM model based on factor analysis and DEMATEL.</i>	2007	Expert Systems With Applications, 32(4): 1028–1044	252	28.0

TC – total number of citations

AvC – average number of citations per year

In the analyzed set of publications the most frequently published were authors from Taiwan (294) USA (229) and the People's Republic of China (150). Polish authors had 38 publications.

Most of the publications were affiliated to the National Chiao Tung University, Hsinchu, Taiwan – 66, Kainan University, Taoyuan, Taiwan – 57, Vilnius Gediminas Technical University, Vilnius, Lithuania – 45. As regards the Polish scientific institutions, most of the publications were affiliated to the Polish Academy of Science, Warsaw, Poland – 13, the Poznan University of Technology, Poznan, Poland – 11 and Technical University Czestochowa, Czestochowa, Poland – 8.

The author of the most numerous publications is TZENG Gwo-Hshiung (Graduate Institute of Urban Planning, National Taipei University, New Taipei City & Institute of Management of Technology, National Chiao Tung University, Hsinchu, Taiwan) – 59. Slightly lower results are achieved by: CHEN Ting-Yu (Department of Industrial and Business Management, Graduate Institute of Business and Management, College of Management, Chang Gung University, Taiwan) – (31) ZAVADSKAS Edmundas Kazimieras (Department of Construction Technology and Management, Vilnius Gediminas Technical University, Vilnius, Lithuania) – 24 and Carlos ROMERO (Department of Forest Economics and Management, Forestry School, Technical University of Madrid, Madrid, Spain) – 23. Among Polish authors, with the best results are achieved by: KALISZEWSKI Ignatius (Systems Research Institute, Polish Academy of Science, Warsaw, Poland) and SLOWINSKI

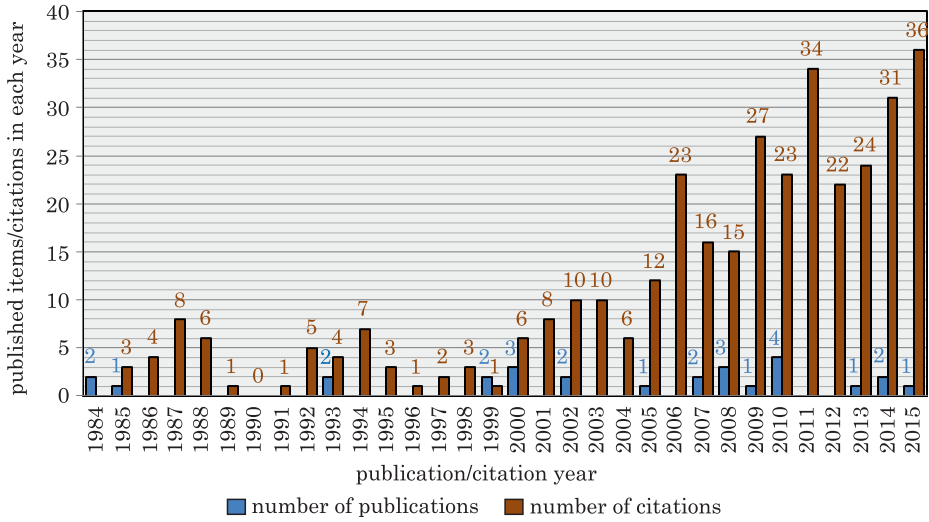


Fig. 4. The number of publications and citations in the Research Area Agriculture

Roman (Institute of Computing Science, Poznan University of Technology, Poznan & Systems Research Institute, Polish Academy of Science, Warsaw, Poland) – 8 publications each.

A subset of publications in the Research Area: AGRICULTURE has 27 scientific articles. The first two publications appeared in 1984. After analysing the change in the number of scientific articles published in different years (Fig. 4), two periods can be distinguished:

I from 1984 to 1998 – the average number of publications 0.3 (5 publications),

II from 1999 to 2015 – the average number of publications 1.3 (22 publications).

Between 1985 and 2015 the total number of citations was 352, while the number of citations in a year has clearly increased since 2005. The most cited publication (Tab. 2) had 46 citations (to year 2015) and the average number of citations per year was 4.2.

The analyzed subset of the publication is contained mainly in such WoS (Web of Science Categories) categories as Agriculture Multidisciplinary – 14, Agricultural Economics Policy – 6, Economics – 4, Agricultural Engineering – 3 and Computer Science Interdisciplinary Applications – 3.

In the analyzed subset of publications, the most widely published authors came from England (6), Spain (6) United States (4) Iran (3) and the Netherlands (3).

Most publications were affiliated with (University Of Reading, Reading, UK) – 6 (Universidad De Cordoba) – 4 (Wageningen University Research

Table 2

The most cited publications on MCDA/MCDM in the Research Area Agriculture in the years 1984-2015

Authors	Title	Publication year	Journal	TC	AvC
Gilliams S., Raymaekers D., Muys B., Van Orshoven J.	<i>Comparing multiple criteria decision methods to extend a geographical information system on afforestation</i>	2005	Computers and Electronics in Agriculture, 49(1): 142–158	46	4.3
Rehman T., Romero C.	<i>The application of the MCDM paradigm to the management of agricultural systems – some basic considerations</i>	1993	Agricultural Systems, 41(3): 239–255	42	1.8
Romero C., Rehman T.	<i>Goal programming and Multiple Criteria Decision – Making in farm-planning an expository analysis</i>	1984	Journal of Agricultural Economics, 35(2): 177–190	31	1.0
Rehman T., Romero C.	<i>Multiple – Criteria Decision-Making techniques and their role in livestock ration formulation</i>	1984	Agricultural Systems, 15(1): 23–49	30	0.9

TC – total number of citations

AvC – average number of citations per year

Center) – 3 (Polytechnic University Of Madrid) – 2 and (University of Tehran) – 2.

The authors of the largest number of publications in the analyzed subset are REHMAN Tahir (Department of Agriculture, University of Reading, Reading, UK) – 6 publications and ROMERO Carlos (Department of Forest Economics and Management, Forestry School, Technical University of Madrid, Madrid, Spain) – 5 publication.

Poland is represented only by 1 publication. Its co-author was Piech Bozena (Department of Economics, Organization & Management, Agricultural Academy of Szczecin, Szczecin, Poland): Piech B; Rehman T. 1993. *Application of multiple criteria decision-making methods to farm-planning – A case-study*. Agricultural Systems, 41(3): 305–319.

Most of the publications from the analyzed subset were published in the following journals: Agricultural Systems (6), Computers And Electronics In Agriculture (3) and the Journal Of Agricultural Economics (2).

Conclusions

Summing up the results, it can be concluded that:

Up to now very large number of MCDA/MCDM methods have been designed and new ones are constantly being developed. This causes problems because the classification of the methods has not been harmonized and different authors offer different classifications.

MCDA/MCDM methods are being very intensively developed in recent years, as evidenced by the number of scientific papers published annually in renowned scientific journals indexed in the Web of Science database. In the years 1979–2015 a total of 1,355 scientific articles was collected in the WoS database. A rapid increase in the number of articles published during the year started after 2005. In 2015 there were 148 publications on methods of MCDA/MCDM the Web of Science database. Besides, the annual number of citations of the publications is increasing.

Research on MCDA/MCDM is conducted in many research areas. A set of 1,335 publications gathered from Web of Science resources consisted of 62 Research Areas, with most of the publications in the area of: information technology (Computer Science) – 512 and operations research and management science (Operations Management Science Research) – 510.

MCDA/MCDM methods are also the subject of research in the field of agriculture (Research Areas: Agriculture). However, until 2015 the Web of Science database accumulated only 27 scientific publications on MCDA/MCDM in this field, which accounts for just 2% of the total articles focused on MCDA/MCDM methods (1,355 articles). Therefore, we can conclude that research on MCDA/MCDM methods in agriculture is not widely performed, despite the presence of many decision-making problems. This can be explained by the fact that new methods of decision support are developed mainly in the area of operations research and management science. In the next stage, they are disseminated in the area of information technology. Therefore, application of new methods for decision support in agriculture is delayed. Another reason for the low level of interest in those methods may also be the nature of decision-making in agricultural production, namely, decisions are usually made by a single person. As a result, decisions are taken on basis of experience and less complex computational methods.

We can, however, expect that with the development of information technology, universal access to computers and user-friendly computer programs, the application of computationally complex methods will gradually become more and more wide-spread. The increase in the number of citations that can be observed since the year 2000 seems to confirm a growing interest in scientific methods MCDA/MCDM for agriculture.

It can be assumed that in the future this subject will be developed, an increasing number of scientists will conduct research on the MCDA/MCDM and the number of articles published during the year will increase.

Acknowledgement

This research was financed by the Ministry of Science and Higher Education of the Republic of Poland.

References

- AKHAVAN P., EBRAHIM N.A., FETRATI M.A., PEZESHKAN A. 2016. *Major trends in knowledge management research: a bibliometric study*. *Scientometrics*, 107: 1–16. doi:10.1007/s11192-016-1938-x.
- ELLEGAARD O., WALLIN J.A. 2015. *The bibliometric analysis of scholarly production: How great is the impact?* *Scientometrics*, 105: 1809–1831. doi:10.1007/s11192-015-1645-z.
- FIGUEIRA J., GRECO S., EHRGOTT M. 2005. *Introduction*. In: *Multiple Criteria Decision Analysis: State of the Art Surveys*. Eds. J. Figueira, S. Greco, M. Ehrgott. Springer Science, Business Media, Boston.
- GRABAŃSKI S. 2015. *Wyznaczenie lokalizacji centrum dystrybucji. Modelowanie z wykorzystaniem systemów geoinformacji*. Uniwersytet Ekonomiczny w Poznaniu.
- HICKS D., KROLL P., NARIN F., THOMAS P., RUEGG R., TOMIZAWA H., SAITOH Y., KOBAYASHI S. 2002. *Quantitative Methods of Research Evaluation Used by the U.S. Federal Government*. NISTEP Study Material.
- KADEMANI B.S., SAGAR A., SURWASE G., BHANUMURTHY K. 2013. *Publication trends in materials science: A global perspective*. *Scientometrics*, 94: 1275–1295. doi:10.1007/s11192-012-0835-1.
- KLINCWICZ K., ZEMIGAŁA M., MIJAŁ M. 2012. *Bibliometria w zarządzaniu technologiami i badaniami naukowymi*. Ministerstwo Nauki i Szkolnictwa Wyższego, Warszawa.
- KODIKARA P.N. 2008. *Multi-Objective Optimal Operation of Urban Water Supply Systems*. PhD Thesis. Victoria University, Australia.
- KRUSZYŃSKI M. 2014. *Metodyka wielokryterialnego wspomagania decyzji w problematyce zarządzania transportem miejskim*. Politechnika Poznańska.
- KSIĄŻEK M. 2011. *Analiza porównawcza wybranych metod wielokryterialnych oceny przedsięwzięć inwestycyjnych*. *Budownictwo i Inżynieria Środowiska*, 2: 555–561.
- KUMARI L. 2013. *Trends in synthetic organic chemistry research. Cross-country comparison of Activity Index*. *Scientometrics*, 67: 467–476. doi:10.1556/Scient.67.2006.3.8.
- PENG Y., LIN A., WANG K., LIU F., ZENG F., YANG L. 2015. *Global trends in DEM-related research from 1994 to 2013: a bibliometric analysis*. *Scientometrics*, 105: 347–366. doi:10.1007/s11192-015-1666-7.
- PIWOWARSKI M. 2009. *Wielokryterialna analiza decyzyjna w systemach GIS*. *Polskie Stowarzyszenie Zarządzania Wiedzą. Seria: Studia i Materiały*, 18: 123–134.
- RAAN A.F. VAN, LEEUWEN, T. VAN. 2002. *Assessment of the scientific basis of interdisciplinary, applied research*. *Research Policy*, 31: 611–632. doi:10.1016/S0048-7333(01)00129-9.
- ROY B. 2005. *An Overview of MCDA Techniques Today*. In: *Multiple Criteria Decision Analysis: State of the Art Surveys*. Eds. J. Figueira, S. Greco, M. Ehrgott. Springer Science, Business Media, Inc., Boston, pp. 2–24.
- SEIXEDO C., TERESO A.P. 2010. *A multicriteria decision aid software application for selecting MCDA software using AHP*. 2nd International Conference on Engineering Optimization, September 6–9, Lisbon, Portugal, pp. 1–11.
- SOBCZYK E.J., WOTA A., KREZOLEK S. 2011. *Zastosowanie matematycznych metod wielokryterialnych do wyboru optymalnego wariantu źródła pozyskania węgla kamiennego*. *Gospodarka Surowcami Mineralnymi/Mineral Resources Management*, 27: 51–68.

- SUN J., WANG M.H., HO Y.S. 2012. *A historical review and bibliometric analysis of research on estuary pollution*. Marine Pollution Bulletin, 64: 13–21. doi:10.1016/j.marpolbul.2011.10.034.
- TRZASKALIK T. 2014a. *Wielokryterialne wspomaganie decyzji. Metody i zastosowania*. PWE, Warszawa.
- TRZASKALIK T. 2014b. *Wielokryterialne wspomaganie decyzji. Przegląd metod i zastosowań*. Zeszyty Naukowe Politechniki Śląskiej. Seria: Organizacja i Zarządzanie, 74: 239–263.
- TSAI H.H. 2012. *Global data mining: An empirical study of current trends, future forecasts and technology diffusions*. Expert Systems with Applications, 39: 8172–8181. doi:10.1016/j.eswa.2012.01.150.
- UCAR I., LÓPEZ-FERNANDINO F., RODRIGUEZ-ULIBARRI P., SESMA-SANCHEZ L., URREA-MICÓ V., SEVILLA J. 2014. *Growth in the number of references in engineering journal papers during the 1972–2013 period*. Scientometrics, 98, 1855–1864. doi:10.1007/s11192-013-1113-6.
- VINCKE P. 1992. *Multicriteria Decision-Aid*. John Wiley & Sons, Chichester.
- YANG L., CHEN Z., LIU T., GONG Z., YU Y., WANG J. 2013. *Global trends of solid waste research from 1997 to 2011 by using bibliometric analysis*. Scientometrics, 96: 133–146. doi:10.1007/s11192-012-0911-6.
- ŻAK J. 2014. *Metodyka wielokryterialnego wspomagania decyzji w transporcie i logistyce*. Logistyka, 3: 7141–7155.



COMPARING SELECTED PARAMETERS OF A TWO-DIMENSIONAL TURBULENT FREE JET ON THE BASIS OF EXPERIMENTAL RESULTS, DIGITAL SIMULATIONS, AND THEORETICAL ANALYSES

Aldona Skotnicka-Siepsiak

Institute of Building Engineering
University of Warmia and Mazury

Received 27 September 2016, accepted 27 December 2016, available online 28 December 2016.

Key words: 2D free jet, turbulent jet, CFD, spreading rate, velocity profiles, Coandă effect.

Abstract

The presented experimental and digital examinations of a two-dimensional turbulent free jet are a first phase of in the study of the Coandă effect and its hysteresis. Additionally, basing on theoretical analyses, selected results for a turbulent jet have been also mentioned, considering theoretical assumptions for the wall layer. As the result, on the basis of experimental, digital, and analytical methods, a review of characteristic jet properties has been prepared, which includes a jet spreading ratio, its cross and longitudinal sections, and turbulence level. The jet spreading ratio has been expressed as a non-linear function of the $x : b$ relative length.

Introduction

The carried-out examinations aimed at identifying properties of a two-dimensional turbulent free jet basing on the results of obtained laboratory measurements, theoretical calculations, and CFD simulations carried out with the *FloVent* calculating application. They have been performed for the Reynolds number ranging from 10,000 to 38,000.

Correspondence: Aldona Skotnicka-Siepsiak, Instytut Budownictwa, Zakład Budownictwa Ogólnego i Fyzyki Budowli, Uniwersytet Warmińsko-Mazurski, ul. Heweliusza 4, 10-724 Olsztyn, phone: 89 523 45 76, e-mail: aldona.skotnicka-siepsiak@uwm.edu.pl

As for the comparison of the obtained laboratory and theoretical results, we had a large set of previously conducted research analyses at our disposal. Our actions focused on confirming the convergence of our own results and previously carried-out examinations by other authors. The issue of estimating how the results of the digital simulations in *FloVent* may be applied was the next phase of our work; however, we did not have any previous results by other scientists here. In spite of the fact that the *FloVent* application was created mostly for assessing the issues of ventilation, it is mainly used for engineering purposes, in analyses of air distribution assessment, heat transfer, and heat comfort.

The scope of this article makes a first phase of the research works that assume an analysis of the Coandă effect hysteresis and its practical application at improving the air mix in systems based on the dilution principle (WIERCIŃSKI, GROMOW 2002).

The Coandă effect is named after Henri Marie Coandă whose research resulted in an American patent no. 2052869 “Device for Deflecting a Stream of Elastic Fluid Projected into an Elastic Fluid” in 1936 (Coanda 1936). The discovered phenomenon was applied widely: in 1938 in the USA (Coanda 1938), Henri Coandă patented a flying saucer, which he called “Aerodina Lenticulara”. The constructor treated the mechanism as the one in which future applications of the discovered phenomenon would be the most important for aviation. Previously, the project has been an inspiration for constructors and scientists (HAQUE et al. 2015, MIRKOV, RASUO 2012a, b).

Presently, the Coandă effect has found its way to many technical solutions: from ordinary tools as electric toothbrushes to sports cars or frequent uses in aviation (WIERCIŃSKI, GROMOW 2002). The big application scale of that phenomenon is confirmed by the resources of the United States Patent and Trademark Office where the amount of 3,164 patent applications is displayed when searched for the patents applied after 1976 and referring to the keyword “Coandă”.

However, until proposing final solutions is possible, we have focused on an initial case for us when a two-dimensional turbulent jet of diffused air is considered. Such a jet appears very often in practical ventilation issues. For instance, it is generated by slot diffusers. In the cases where a movement of the air flowing out of a diffuser takes place in an air medium that remains in relative stillness and is not limited by surfaces of the partitions forming a room, we can talk about a turbulent free jet (SZYMAŃSKI, WASILUK 1999). The Coandă effect may occur as a result of the closeness of a barrier, the angle that the jet flows, or the influence of another air jet (FAGHANI, ROGAK 2012). Adhesion of the air jet, e.g. to the surface of a ceiling, resulting from an inducted vortex and higher vacuum on one side when dimension a does not

exceed 50–30 thicknesses of the jet has been presented in the first case in Figure 1. A similar effect may be expected when angle h is less or equal to 45° (Fig. 1) (RECKNAGEL et al. 1994).

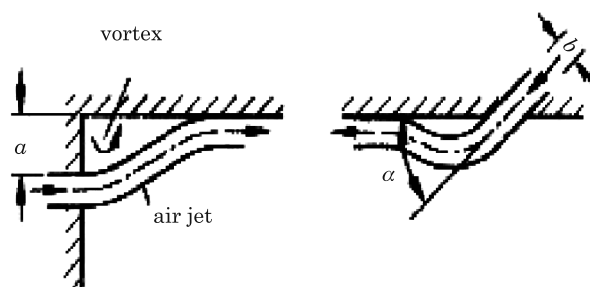


Fig. 1. The Coandă effect with air jets
Source: FAGHANI, ROGAK (2012).

By causing adhesion and sliding, the Coandă effect changes the designed air distribution in a room and it was usually perceived as an unfavourable phenomenon. Presently, the Coandă effect is used frequently in a planned way and is intended at the stage of conceptualization and implementation of air division in ventilated or air-conditioned rooms. Works by VON HOFF et al. (2012) or VALENTIN et al. (2013) may be provided here as an illustrations.

We hope that we are capable of using the potential of that phenomenon basing on the Coandă effect hysteresis in the construction of a diffuser. An unstable jet of air that alternatively adheres and comes unstuck of a barrier is to cause an improvement of the air mix and a decrease of speed and temperature gradients averaged in time for a room (WIERCIŃSKI, GROMOW 2002).

Literature Review

A turbulent isothermal jet of air was subjected to the analysis. The value of $Re_{kr} = 1,200$ was accepted as a limit of the laminar movement for plane slots.

Upon leaving the nozzle, the turbulent air jet starts to spread gradually which entails an increase of its cross section and a decrease of velocity. Moreover, a movement of air particles in the transverse direction towards the direction of the jet is observed in the turbulent jet, which effects in transporting the particles outside the main mass of the jet. The particles transport kinetic energy to the bordering layers of the surrounding air and grab some particles from the surrounding air towards the jet.

Four zones of the following properties may be distinguished in the air jet:

Zone I: initial – characterized by the unchangeability of its axial velocity. In it, a jet core can be separated where the initial velocity is sustained. The smaller the vortices of the jet are, the longer zone is.

Zone II: transitory – a distribution of velocities characteristic for turbulent free jets is shaped in its cross-section profile. Its length depends on the construction of a diffuser.

Zone III: basic – there is a proportional decrease of its axial velocity in relation to the length from the outlet

Zone IV: dominant influence of viscous forces – together with a rapid decrease of its axial velocity, the jet stops along its primary axis.

In the case of a plane jet, a decrease of its axial velocity is much smaller than in the case of a round one, which results its farther reach.

According to the information in the article by NEWMAN (1961), the static pressure in the jet is the same everywhere, thus the jet momentum is constant regardless of a distance from the nozzle. A flow in defined length x along the jet, for a jet from the slot with width b and core velocity U , may be as well formed by a bigger slot with width b' and a lower value of velocity in the jet core U' , located somewhere along the flow of the jet.

$$\rho U^2 b' = J = \rho U^2 b \quad (1)$$

where:

ρ – density,

U, U' – velocity at the nozzle outlet,

b, b' – width of the diffusion slot,

J – value of jet momentum in relation to the width unit of the nozzle.

The value of mean velocity u in distance y from the middle of the jet depends on jet momentum J , fluid density ρ , and the x, y localization in the accepted frame of reference. When moving further from the stable area, e.g. with participation of free turbulences, it may be assumed that the change in the fluid viscosity is of no significant influence on the flow or on the large-scale vortices.

The value of localization $y_{m:2}$, for which the mean velocity measured perpendicularly to the jet axis reaches the $u = 1/2 u_m$, value of a half of the maximal velocity in a given cross-section of profile velocity may be accepted as a measure of the jet spreading in a local frame of reference towards direction y , measured perpendicularly to the jet axis.

For all the x values in the accepted frame of reference, the following similarity for the profiles of velocity diffusion is accepted:

$$\frac{u}{u_m} = F\left(\frac{y}{y_{m:2}}\right) \quad (2)$$

According to the Görtler's assumptions, it can be accepted that turbulent viscosity ϵ is constant across the flow for every x value and proportional to the $u_m y_{m:2}$ value. The solution is formed as follows:

$$u = u_m \sec h^2 \frac{0.88y}{y_{m:2}} = \left\{ \frac{3 J \sigma}{4 \rho x} \right\}^{\frac{1}{2}} \sec h^2 \frac{\sigma y}{x} \quad (3)$$

where:

σ – constant,

u_m – maximal velocity value in a given section.

The above dependence occurs for the conditions when $y < 1.3 y_{m:2}$; in other cases it provides slightly too high results. The flow is not independent from slot width b until the $x : b$ value reaches 25. The results by Bourque provide the value of $\sigma = 12$ close to the nozzle that falls down to the value of 7.5 for large $x : b$ values. When accepting the value of $\sigma = 7.7$, we obtain:

$$y_{m:2} : x = 0.88 : \sigma = 0.114$$

$$\rho u_m^2 x : j = 3\sigma : 4 = 5.78 \quad (4)$$

$$\epsilon : u_m y_{m:2} = 1 : 3.52 \rho = 0.037$$

where:

ϵ – turbulent viscosity.

Localization of value $y_{m:2}$, for which the velocity measured perpendicularly to the jet axis reaches the $u = 1/2 u_m$ value of a half of the maximal velocity in a given cross-section velocity profile complies also to:

$$\frac{y_{m:2}}{b} = K_1 \left(\frac{x}{b} + K_2 \right) \quad (5)$$

where:

K_1, K_2 – coefficient.

Coefficient K_1 is a measure of the jet spreading ratio, and using the following dependency:

$$x_0 = -K_2 b \quad (6)$$

it is possible to identify a localization of a virtual origin of jet x_0 (KOTOSOVINOS 1976). Information on localization of the virtual origin is equivocal. Some part of the researchers place it in front of the nozzle, others – behind it.

Attention should also be paid that directly behind the nozzle there is an area of the jet core, the length of which is approximately $6b$, which in the case of our calculations – for a diffusion slot with the width of $b = 20$ mm – means that the reach of the core area is up to the length of about $x_0 = 0.12$ m (RAJARATNAM 1976). In that area the dependencies indicated above will not occur.

Description of Measuring Post

The laboratory measurements were taken at a measuring post in the laboratory of the Department of Building Engineering and Building Physics at the University of Warmia and Mazury in Olsztyn. The experimental results were performed as a part of the doctoral thesis, whose topic was “Hysteresis of the Coanda effect”. Prof. Zygmunt Wierciński was the supervisor of the doctoral dissertation in the Institute of Fluid-Flow Machinery Polish Academy of Sciences. The examinations were performed in a chamber with dimensions of $385 \times 200 \times 229$ cm where a case made of transparent Plexiglas slates was fixed on a steel rack, which eliminated influences of the external environment on the conducted experiment. The air was delivered to the system by a sucking duct, 250 mm in diameter and 530 cm in length, placed 40 cm above the floor. On its inlet, the duct was equipped with an air intake, 400 mm in diameter, with a regulated flow. The duct was also equipped with a measuring orifice plate with impulse orifices in lengths D and $D/2$ to measure the static pressure. The orifices were connected to a pressure transducer by elastic hoses. A diffuser in the shape of the Witoszyński nozzle with regulated cross-section was mounted on the pressing side of the ventilator. The stable height of the nozzle was $h = 60$ cm. The experiments were performed for the nozzle width of $b = 2.0$ cm.

The experimental examinations were carried out for six measuring sessions characterized by various values of airflow for the Reynolds number ranging from about 10,000 to about 38,000. The symmetry centre in the frontal plane of the diffusion orifice of the Witoszyński nozzle forms the beginning of the frame. The accepted theoretical axis of the x jet is convergent with the axis of symmetry of the aforementioned nozzle, the width of which was 0.02 mm. All

the measurements were performed in plane $z = 0$ in the middle of the nozzle that was 0.60 m tall.

The scheme of the described measuring post has been presented in the Figure 2 below.

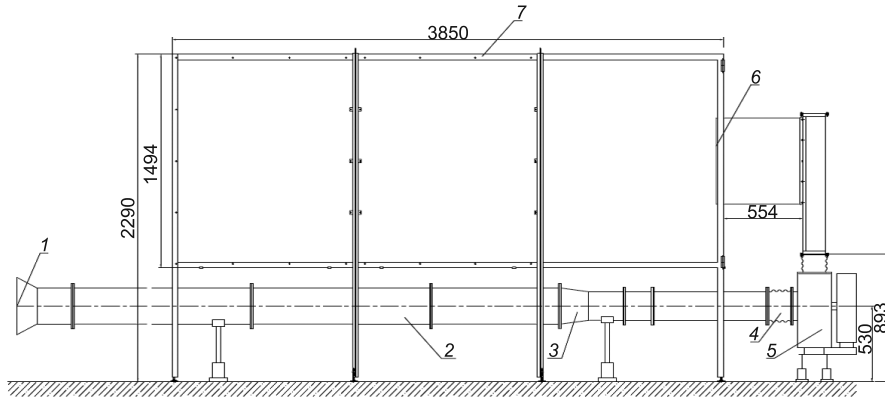


Fig. 2. Scheme of measuring post – side view: 1 – air intake with the flow regulated by a rotating element, 2 – sucking duct, 3 – orifice plate for measuring static pressure, 4 – ventilator, 5 – elastic joints, 6 – the Witoszyński nozzle, 7- measuring post case made of a rack and Plexiglas slates

Distributions of the arithmetical mean for the velocity and the turbulence level of a turbulent free jet were examined using a thermo-anemometer ATU 2001.

In the above measuring system, we applied a dynamic measuring net that, while assuming optimization of the measuring points, was adjusted to the varied distribution of velocities in the examined air jet. The measurements were taken in 11 measuring lines parallel to each other. Vertically, they were localized in the axis of symmetry of the air diffusion. The first measuring line was directly behind the nozzle in the minimal length of $x : b = 0.5$, which was allowed for by the construction of the stand of the thermo-anemometric probe. The measurement was taken in the jet core. The following measuring lines were situated every 0.10 m away from the nozzle towards direction x , until the final value of $x : b = 50.0$ was reached. Every measuring line was characterized by its specific width resulting from the velocities identified at the measuring post. The measurements for every measuring line were carried out in a local frame of reference toward direction $\pm y$, until the velocity values lower than 1 m/s were recorded.

Table 1 contains a list of values for the ventilator capacities, the velocities at the outlet from the nozzle identified on the basis of measurements taken with the orifice plate and the hot wire, as well as the value of the Reynolds number for every measuring session.

Table 1
Values of ventilator capacities, air velocities at the nozzle outlet and the Reynolds

Measuring session	Ventilator capacity [m ³ /s]	Air velocity at nozzle outlet		Reynolds number [-]
		based on measurements with orifice place	based on measurements with thermoanemometer	
		[m/s]	[m/s]	
1	0.338	28.19	28.02	37,343
2	0.250	20.90	20.78	27,685
3	0.152	12.67	12.86	16,784
4	0.127	10.56	10.18	13,983
5	0.107	8.88	8.63	11,768
6	0.096	7.98	7.98	10,570

The values of the Reynolds number were calculated according to the formula:

$$\text{Re} = \frac{U \cdot b}{\nu} \quad (7)$$

where:

U – velocity at the nozzle outlet,

b – width of the diffusion slot,

ν – coefficient of kinematic viscosity.

Due to the fact that the measuring post was situated in a confined space of the laboratory room, from which the circulatory air for the measuring system was collected, it was accepted for simplicity reasons that the measuring system is an isothermal one.

Measuring Net for the Turbulent Free Jet

Using the Computational Fluid Dynamics (CFD), a digital model of the aforementioned laboratory post was created and simulations were conducted, which made it possible to examine distributions of the arithmetic mean for the velocity and turbulences of a turbulent free jet. The simulations were carried out using the *FloVent* application by *Mentor Graphics*.

The examinations were conducted for each of the six measuring sessions, for the air capacity in the system identified experimentally and for the diffusion slot $b = 20$ mm wide.

A measuring net consisting of about 500,000 meshes was used in the simulation. In the area where the parameters of the turbulent free jet were analysed the net was concentrated and the dimensions of a mesh were $x = 5$ mm, $y = 20$ mm, $z = 30$ mm (the directions according to the *FloVent* scheme). The dimensions of the area were $x = 1.20$ m, $y = 0.62$ m, $z = 1.00$ m. As for the remaining area of the measuring post, the meshes did not exceed 75 mm in every direction.

The application provides three models of turbulence: *Capped LVEL*, *LVEL Algebraic*, and *LVEL K-Epsilon*. The *LVEL K-Epsilon* model was used for the simulations as it is the one that had been verified in the largest number of engineering calculations and, according to the producer's information, it provided the best results. The model is also characterized by simplicity and stability.

The calculations were performed by a computer equipped with a CPU 2.61 GHz and 3.25 GB of RAM. The running time for a single simulation was about 2.5 hours.

Calculation Results

The calculations of the jet momentum carried out according to formula (1) provided the results: $Re = 37,343 \rightarrow 18.60$ kg/s²; $Re = 27,685 \rightarrow 10.42$ kg/s²; $Re = 16,784 \rightarrow 3.73$ kg/s²; $Re = 13,983 \rightarrow 2.61$ kg/s²; $Re = 13,983 \rightarrow 1.86$ kg/s² and $Re = 10,570 \rightarrow 1.49$ kg/s². The jet momentum is a constant value, regardless of the length from the nozzle.

In order to analyse the distribution of velocities in the jet, for the diffusion slot with the width of $b = 20$ mm, the u_m value of the maximal velocity was verified in particular measuring planes basing on the experimental data. Generally, the assumption that maximal values in particular measuring planes were within jet axis $x : b = 0.0$ was confirmed. The distribution of velocity was identified using formula (3). Values of the σ parameter shown in Table 2, were accepted for calculations. In our case, the mean value of the σ coefficient out of the area of the jet core ($x : b = 10.0 \div 50.0$) was 8.10. It is a higher value than the ones given in the literature (NEWMAN 1961). A higher accordance occurred for sessions 4, 5, and 6 that were characterized by lower values of $Re = 10,000 \div 15,000$.

The analysis of theoretical calculations and the CFD simulation of the u_m values of the maximum velocity in particular measuring planes, which were

obtained on the basis of laboratory measurements, indicates that the average difference in the obtained values of u_m for particular measuring plates is 1.9% for comparable research methods. When comparing the results obtained by theoretical calculations and laboratory measurements, the maximal differences in the u_m value of the maximum velocity did not exceed 0.7%, and the average difference was 0.2%. A comparison of the data obtained by measurements and CFD simulations provides worse results. In spite of a satisfactory mean value of deviations on the level of 3.6%, some quite huge deviations of up to 10.6% may be observed in particular profiles.

Table 2
Values of the σ parameter accepted in calculations; width of the diffusion slot $b = 20$ mm

$x : b [-]$	Values of the σ parameter [-] for measuring session:					
	1 Re = 37,343	2 Re = 27,685	3 Re = 16,784	4 Re = 13,983	5 Re = 11,768	6 Re = 10,570
0.5	0.66	0.67	0.69	0.62	0.63	0.66
5.0	6.40	6.60	6.00	5.20	5.60	5.40
10.0 ÷ 50.0	8.47	8.30	8.78	8.07	7.38	7.58

The analysis of the relation between the u_m value of the axial velocity in particular measuring planes and the U value at the outlet of the nozzle for selected measuring sessions is presented in Figure 3.

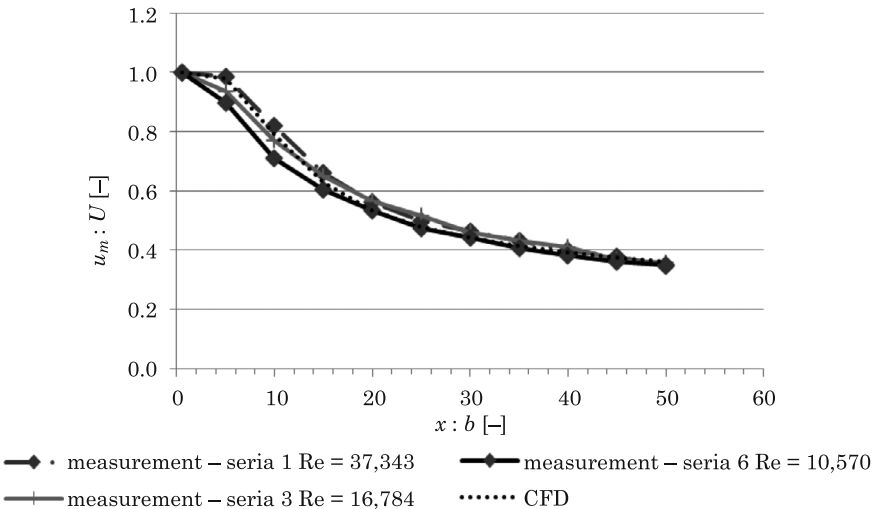


Fig. 3. Correlation between the u_m value of the axial velocity in measuring planes and the U value at the outlet of the nozzle for selected measuring sessions 1, 3 and 6

The course of the curve mirroring the results of the CFD simulation is unchangeable for all the measuring sessions. A very high convergence of the results obtained by laboratory measurements and theoretical calculations makes it possible to accept the convergence of the curves mirroring the results. However, they are different for particular measuring sessions. For measuring sessions with the higher values of the Reynolds number, it is visible that the results obtained by the CFD simulations are understated in the middle part of the jet. As the Reynolds number decreases, an increase in the CFD simulation results is visible for the first three measuring planes. As for the further measuring planes, understating of the obtained results of simulations is visible, as well as accordance of the results for the last two measuring sessions. In the case of the lowest values of the Reynolds number, the convergence occurs in the middle part of the jet; however, in the remaining areas, the simulation results are overstated in relation to the laboratory results and the ones obtained from theoretical calculations.

An examination of the decrease in the u_m value of axial velocity in particular measuring planes may be also conducted on the basis of the following formula:

$$\frac{u_m}{U} = \sqrt{\frac{b}{m \cdot x}} \quad (8)$$

where:

m – mixed number.

The value of mixed number obtained in such a way is $m = 2.00$ for the first measuring plane localized directly behind the nozzle at $x = 0.01$ m in the area of the jet core, regardless of the manner of identification of the u_m axial velocity in particular measuring planes. In the next measuring plane, for $x = 0.10$ m, there occurs a significant decrease in the value of the m coefficient. As for the results of the CFD simulations, the value $m = 0.21$ was obtained, regardless of the Reynolds number. In the case of the mixed coefficient determined on the basis of laboratory examinations and theoretical calculations the following dependency is visible: as the value of the Reynolds number increases, the value of the m coefficient decreases. In the following planes, in spite of small fluctuations, the value of the m coefficient is equalized. As for the results obtained by the CFD simulations, it is $m = 0.16$ for all the measuring sessions. In the case of the remaining examination methods, the previously observed dependency between the values of the Reynolds number and the m coefficient is observed. The values of mixed number m for three selected measuring sessions are shown in Table 3.

The analysis of the turbulence level based on laboratory examination confirms the fact that the measurement in the first measuring plane for $x : b = 0.5$ is situated in the diffused air jet core. The measurements taken in the following planes indicate that the jet is shaped gradually, while the measurement in the second plane for $x : b = 5.0$ points out at the localization in the transitory zone of the jet. The jet spread increases together with the increase of the length from the diffuser, with the simultaneous decrease of the turbulence level. However, lacks of total similarity and fully shaped turbulence profiles are visible, which is to be obtained for our diffusion slot with the width of $b = 20$ mm on exceeding the length of $x : b > 65.0$ from the nozzle according to the rule defined by RAJARATNAM (1976). The described dependencies are presented in Figure 4.

Table 3

Values of mixed number m

$x : b [-]$	Value of mixed number $m [-]$ for measuring session:								
	1 Re = 37,343			3 Re = 16,784			6 Re = 10,570		
	Measurement	Theoretical Calculation	CFD Simulation	Measurement	Theoretical Calculation	CFD Simulation	Measurement	Measurement	Measurement
0.5	2.00	2.00	2.00	2.00	2.00	2.00	2.00	2.00	2.00
5.0	0.21	0.21	0.21	0.23	0.23	0.21	0.25	0.25	0.25
10.0 ÷ 50.0	0.16	0.16	0.16	0.16	0.16	0.16	0.18	0.18	0.18

When examining spreading of the jet, in a local frame of reference towards the y direction measured perpendicularly to the jet axis, localization $y_{m:2}$ was considered, for which the mean velocity measured perpendicularly to the jet axis reaches the $u = 1/2 u_m$ value for a half of the maximum velocity in a given cross-section profile of velocity. The values may be accepted as convergent ones, apart from the areas of the jet core and the transitory zone (the first two measuring planes) that were omitted in the further analysis. In the case of comparing the $y_{m:2}$ localization identified on the basis of the measurement data and theoretical calculations, the average difference in the obtained coordinates is ± 7 mm ($y : b = 0.35$). It is noteworthy that the worst matches in the studied scope occur in measuring sessions 5 and 6 (the average difference in the obtained coordinates is ± 12 mm $-y : b = \pm 0.6$). The convergence of the results obtained from the laboratory measurement and the CFD simulations appears to be slightly worse. The average difference in the obtained localization coordinates towards direction y is ± 8 mm ($y : b = \pm 0.4$). Regardless of the applied calculation methods, the maximum difference in the obtained localiz-

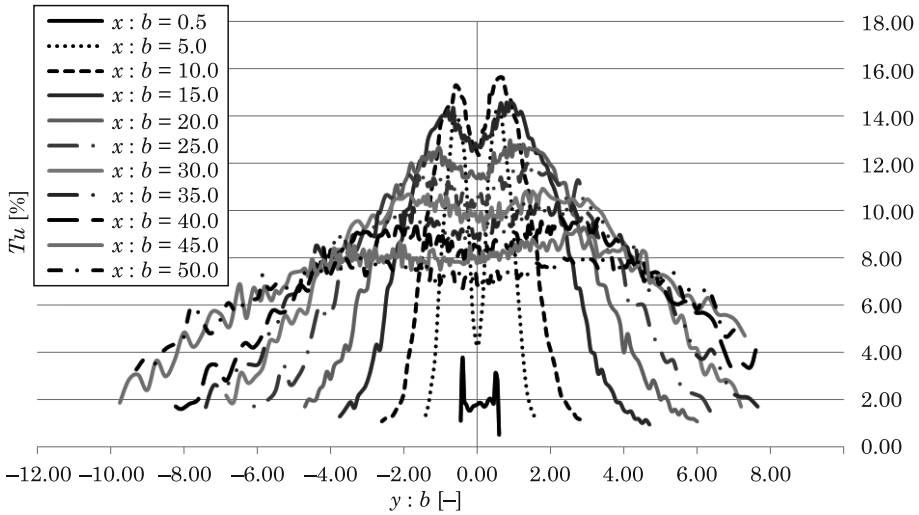


Fig. 4. Turbulence level Tu based on the laboratory examinations for a diffusion slot with the width of $b = 20$ mm; measuring session no 1 $Re = 37,343$

ation coordinates towards direction y does go beyond ± 3.5 cm ($y : b = \pm 1.75$). A very high convergence of the $y_{m:2}$ localization is visible for the results obtained by the CFD simulation. It is virtually the same for all the measuring sessions regardless of the noted various $u = \frac{1}{2} u_m$ values for velocity.

The described dependencies are illustrated by the sample Figure 5.

In spite of the convergence of the identified u_m maximum velocity in the measuring plane situated directly behind the diffuser at $x : b = 0.5$, the shape of the curve illustrating the distribution of the velocity is divergent when laboratory, theoretical, and CFD simulation results are compared. This entails the fact that the localization of the $u = \frac{1}{2} u_m$ value for a half of the maximum velocity is also divergent. It is a result of the fact that the first measuring plane was localized in the area of the jet core, where it still was not shaped and was not convergent with the theoretical description of the jet shape. In the measuring planes at lengths of $x : b > 5.0$, the image of the already-shaped jet is in accordance with the theoretical assumptions (Fig. 5); however there is a divergence visible here for the u_m values of the maximum velocity determined by the CFD simulations and the remaining methods. In the case presented on the graph, it is about 5.5%.

Basing on the identified localization of the $u = \frac{1}{2} u_m$ value for a half of the maximum velocity, the jet spreading angle was analysed by applying three methods of examining velocity distribution (Tab. 4).

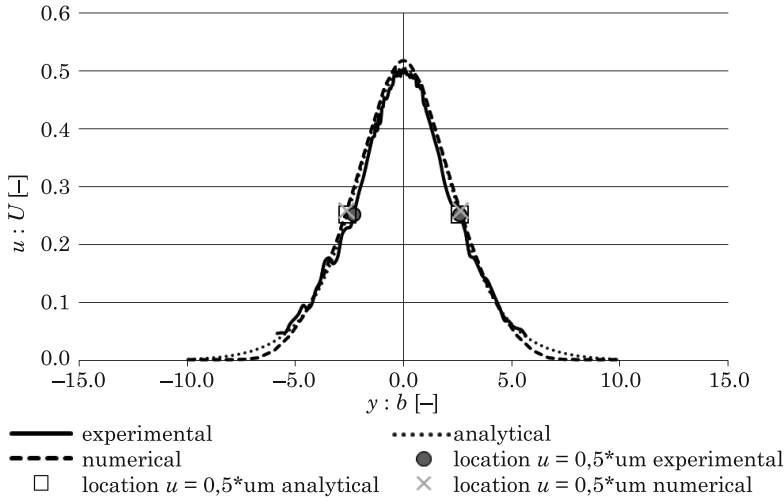


Fig. 5. Velocity values for the slot width of $b = 20$ mm; the measuring plane at the length of $x : b = 25.0$; measuring session 2: $Re = 27,685$

Table 4

Specification	Jet expansion angle α [°]					
	Jet expansion angle α [°] for measuring sessions 1-6					
	1 Re = 37,343	2 Re = 27,685	3 Re = 16,784	4 Re = 13,983	5 Re = 11,768	6 Re = 10,570
Laboratory measurement	12.05	13.72	15.55	15.49	14.24	13.84
Theoretical calculation	12.55	13.82	11.47	11.49	14.42	12.15
CFD simulation	13.14	13.14	13.13	13.13	13.13	13.13

For the measuring sessions no 1, 2 and 5, the values of the jet spreading angle determined from the results of the theoretical calculations are convergent with the laboratory results. In the remaining cases, some huge divergences, up to 4° , are visible. A general trend for a decrease of the spreading angle together with an increase of the Reynolds number is visible in the laboratory results. As for the results obtained in the CFD simulations, the value of spreading angle $\alpha = 13.1^\circ$ is obtained for all the measuring sessions.

The analysis of the virtual jet origin localization requires considering the values of coefficients K_1 and K_2 according to formulas (5) and (6) presented before. As the results of theoretical calculations and simulations are not comparable with the laboratory results for the first two measuring planes, those planes were omitted in the further analysis.

In the case of the laboratory measurements that we carried out, provided that the first two measuring planes were omitted in the analysis, the virtual jet origin was always localized behind the diffuser ($K_2 < 0$). The analysis of the results obtained by theoretical calculations for the first three measuring sessions indicates that the localization of the virtual jet origin is behind the nozzle; however, the remaining three cases indicate that its localization is in front of it. As for the results obtained from the CFD simulations, the virtual jet origin is located in front of the nozzle, practically in the same point each time for all the measuring sessions. Figure 6 presents those dependencies.

It is noteworthy that the results obtained by theoretical calculations correspond in the best way with the linear dependency trend of coefficients K_1 and K_2 identified on the basis of the literature data (KOTSOVINOS 1976). The values of the K_1 jet spreading coefficient that we obtained by analysing the laboratory measurements are higher than the data from the literature (KOTSOVINOS 1976).

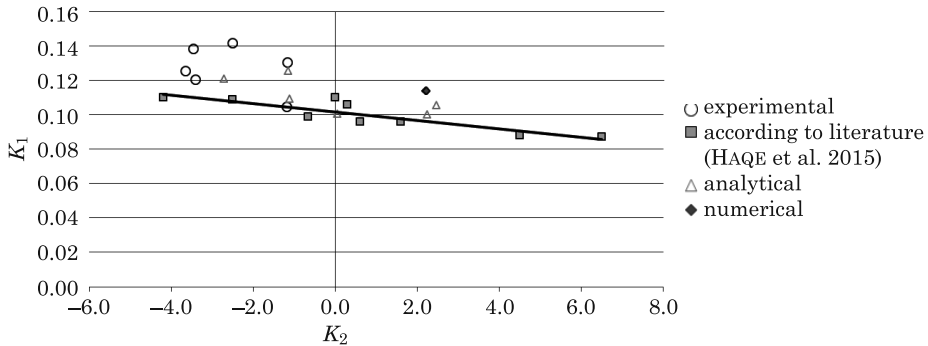


Fig. 6. Dependency between coefficients K_1 and K_2

In own research, $K_1 = 0.105 \div 0.142$ and $K_2 = -3.65 \div -1.17$ for laboratory examination. In case of theoretical calculations the coefficient $K_1 = 0.100 \div 0.126$ and $K_2 = -2.71 \div 2.47$. For numerical investigations the $K_1 = 0.114$ while $K_2 = 2.22 \div 2.23$. Those results have a good compatibility with the literature (KOTSOVINOS 1976) referring

The obtained results of the σ parameter analysed in the context of the dependency: $y_{m:2} : x = 0.88 : \sigma = 0.114$ cited in formula (5) after (NEWMAN 1961) show a convergence for the area of a formed turbulent jet. In the case of measuring sessions with the lowest values of the Reynolds number, the probability of the obtained results is the highest.

Table 5

Analysis of distribution of the $0.88 : \sigma$ value for particular measuring sessions

$x : b [-]$	Values of $0.88 : \sigma [-]$ for measuring session:					
	1 Re = 37,343	2 Re = 27,685	3 Re = 16,784	4 Re = 13,983	5 Re = 11,768	6 Re = 10,570
0.5	1.333	1.313	1.275	1.419	1.397	1.333
5.0	0.138	0.133	0.147	0.169	0.157	0.163
10.0 ÷ 50.0	0.104	0.106	0.100	0.109	0.119	0.116

The thesis that the distribution of an increased value of the localization for which the mean velocity measured perpendicularly to the jet axis reaches the $u = 1/2 u_m$ value for a half of the maximum velocity in a given velocity cross-section profile for the analysed turbulent jets is not precisely linear, cited after (KOTSOVINOS 1976), was also confirmed.

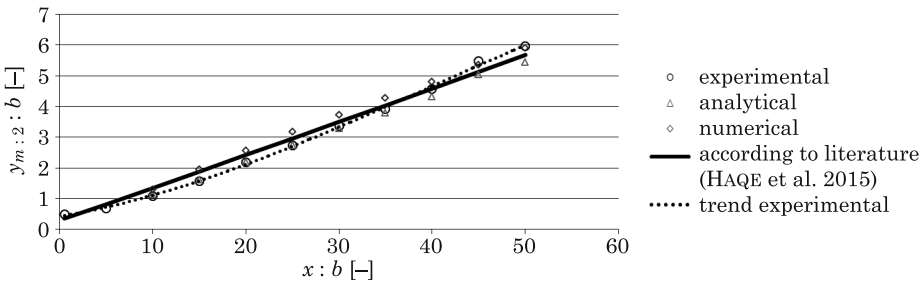


Fig. 7. Distribution of the $y_{m:2}$ localizations to b along the jet for the mean results of all the measuring sessions

Following (KOTSOVINOS 1976), presented in Figure 7 is a curve of the following formula:

$$\frac{y_{m:2}}{b} = 0.228 + 0.0913 \frac{x}{b} + 0.00005101 \left(\frac{x}{b}\right)^2 + 0.000000331 \left(\frac{x}{b}\right)^3 \quad (9)$$

according to which the characteristics of the distribution was presented by the author. The trend line charted for the mean results of own laboratory results is described by the formula:

$$\frac{y_{m:2}}{b} = 0.4317 + 0.0489 \frac{x}{b} + 0.0021 \left(\frac{x}{b}\right)^2 + 0.00002 \left(\frac{x}{b}\right)^3 \quad (10)$$

It diverges from the curve defined in the literature; however, attention should be paid at the fact that the analyses that we have conducted apply only to the area of $x \leq 50 b$, while in the literature (KOTSOVINOS 1976) the area is four times longer.

Conclusions

The obtained results confirm a possibility to examine the properties of a two-dimensional turbulent free jet on the basis of the obtained laboratory measurements, theoretical calculations and CFD simulations carried out by the *FloVent* calculating application.

The conducted examinations did not make it possible for us to find a satisfactory answer to the question of virtual jet origin localization. The results based on digital examinations indicate that it is localized in front of the diffusion nozzle. However, the results based on the laboratory measurements and theoretical calculations do not provide an unequivocal answer indicating localizations both behind and in front of the nozzle. The obtained values of the K_1 coefficient are the most convergent with the results by Flora & Goldschmidt, Heskestad, Kotsovinos, Mih & Hoopes, or Nakaguchi cited from the literature (KOTSOVINOS 1976).

References

- BOURQUE C., NEWMAN B.G. 1959. *Reattachment of a Two-Dimensional Incompressible Jet to an Adjacent Plane Plate*. Aeronaut. Quarterly, 11: 201.
- COANDA H. 1936. *Device for deflecting a stream of elastic fluid projected into an elastic fluid*. United States Patent 2052869. <http://www.freepatentsonline.com/2052869.html> (access: 09.12.2016).
- COANDA H. 1938. *Propelling device*. United States Patent 2108652. <http://www.freepatentsonline.com/2108652.html> (access: 09.12.2016).
- FAGHANI E., ROGAK S.N. 2012. *Application of CFD and Phenomenological Models in Studying Interaction of Two Turbulent Plane Jets*. International Journal of Mechanical Engineering and Mechatronics, 1(1).
- FÖRTHMANN E. 1934. *Über turbulente Strahlausbreitung*. Ing.-Archiv, 5(42).
- GÖRTLER H. 1942. *Berechnung von Aufgaben der freien Turbulenz auf Grund eines neuen Näherungssatzes*. ZAMM, 22: 244.
- HAQUE E., HOSSAIN S., ASSAD-UZ-ZAMAN M., MASHUD M. 2015. *Design and construction of an unmanned aerial vehicle based on Coanda effect*. Proceedings of the International Conference on Mechanical Engineering and Renewable Energy (ICMERE2015), 26–29 November, Chittagong, Bangladesh.
- HOEFF T. VAN, BLOCKEN B., DEFRAEYE T., CARMELET J., VAN HELST G.J.F. 2012. *PIV measurements and analysis of transitional flow in a reduced-scale model: Ventilation by a free plane jet with Coanda effect*. Building and Environment, 56: 301–313.
- KOTSOVINOS N.E. 1976. *A Note on the Spreading Rate and Virtual Origin of a Plane Jet*. The Journal of Fluid Mechanics, 77(2): 305–311.
- MIRKOV N., RASUO B. 2012. *Manoeuvrability of an UAV with Coanda effect based lift production*. 28th International Congress of the Aeronautical Sciences.

- MIRKOV N., RASUO B. 2012. *Numerical simulation of air jet attachment to convex walls and applications*. 28th International Congress of the Aeronautical Sciences.
- NEWMAN B.G. 1961. *The Deflexion of Plane Jet by Adjacent Boundaries – Coandă Effect*. Pergamon Press, Oxford.
- RAJARATNAM N. 1976. *Turbulent Jets*. Elsevier Scientific Publishing Company, Amsterdam – Oxford – New York.
- RECKNAGEL H., SPRINGER E., HÖNNMANN W., SCHRAMEK E.R. 1994. *Poradnik ogrzewanie i klimatyzacja*. EWFE, Gdańsk.
- REICHARDT H. 1943. *On a New Theory of Free Turbulence*. J. Roy. Aero. Soc., 47: 167.
- SZYMAŃSKI T., WASILUK W. 1999. *Wentylacja użytkowa poradnik*. IPPU Masta, Gdańsk.
- VALENTÍN D., GUARDO A., EGUSQUIZA E., VALERO C., ALAVEDRA P. *Use of Coandă nozzles for double glazed facades forced ventilation*. Energy and Buildings, 62: 605–614.
- WIERCIAŃSKI Z., GROMOW E. 2002. *Polepszenie rozdziału powietrza w pomieszczeniu wentylowanym za pomocą niestacjonarnego efektu Coandă*. Ciepłownictwo Ogrzewnictwo Wentylacja, 10.



Quarterly peer-reviewed scientific journal

ISSN 1505-4675
e-ISSN 2083-4527

TECHNICAL SCIENCES

Homepage: www.uwm.edu.pl/techsci/



PERFORMANCE TEST ON TRIPLE HEAP SORT ALGORITHM

Zbigniew Marszałek

Institute of Mathematics
Silesian University of Technology

Received 19 November 2016, accepted 16 January 2017, available online 19 January 2017.

Key words: computer algorithm, data sorting, data mining, analysis of computer algorithms.

Abstract

Rapid information search in large data sets is one of the most important issues. Quite often it leads sorting strings stored in different cultures, languages. In this work the author presents a modified triple heap algorithm to sort strings for large data sets. Triple heap algorithm is the subject of research and demonstrating its usefulness in applications.

Introduction

Recent years have seen a substantial increase in computer capacity. Computers have become faster and began to store large data sets. The result is that we are forced to organize data sets in such a way that they can be efficiently processed. A special role is played here sorting algorithms giving the opportunity to operate on large data sets. Development of database structures enforces new versions of algorithms for specific applications. A modified version of the sort algorithm (WOZNIAK et al. 2013, 2016) allows the sorting of large data sets for specific issues. It is particularly convenient if we do not have a sufficiently large memory to duplicate the data, as required by the triple merge algorithm (WEGNER, TEUHOLA 1989) and derivatives (MARSZALEK 2016).

Correspondence: Zbigniew Marszałek, Zakład Matematyki Obliczeniowej i Informatyki, Instytut Matematyki, Politechnika Śląska, ul. Kaszubska 23, 44-100 Gliwice, phone: 32 237 13 41, e-mail: Zbigniew.Marszalek@polsl.pl

Also various approaches to other sorting algorithms are widely examined in the recent years, i.e. multi-pivot quicksort was examined for efficiency of pivot operations during sorting (AUMÜLLER et al. 2016). Similarly effects of partitioning were discussed for applications of quicksort (AUMÜLLER, DIETZFELBINGER 2013). Other research (WILD et al. 2016, NEBEL et al. 2016) proposed interesting approaches to improve some strategies for preprocessing input data before sorting. This paper presents a modification of the triple heap algorithm for sorting strings, and compares its efficiency to the traditional heap algorithm.

Related work

Sorting of search results is one of the most commonly used methods for the preparation of reports and quick information retrieval. In many of the works presented are algorithms for sorting of large data sets. In practical solutions we meet the need of effective memory management and use of algorithms that do not use additional resources i.e. for distributed gaming system (POLAP et al. 2015a, b). Some system models need efficient technology to store the data (DAMASEVICIUS et al. 2016, GABRYEL 2016) of different types, what can be of further processing in expertise (DAMASEVICIUS et al. 2016a, b). Experimental tests allow you to find the best solutions with the best possible computational complexity and apply them in practice. There are various methods useful in data mining (ARTIEMJEW et al. 2016, ARTIEMJEW 2014, 2015, NOWICKI et al. 2016), which are implemented in some special system data architectures like Boltzmann machine (MLECZKO et al. 2016). The paper presents a modified algorithm to sort through mounds used for sorting strings.

Big data sets

In large databases stored information is collected from the respective structures of different sources. These data are then processed so that it would be possible to quickly search information and efficient processing in order to produce the required reports. Information processing illustrated by Figure 1. It shows that the collected information is gathered mostly on external media and are given the appropriate classification and ordering. To organize large sets of data are used for stable algorithms with low computational complexity, allowing efficient operation in NoSQL databases. For comparison methods are carried out tests to check the operating time using a CPU (Central Processing Unit) and clock cycles (clock rate). This enables an efficient comparison algorithms.

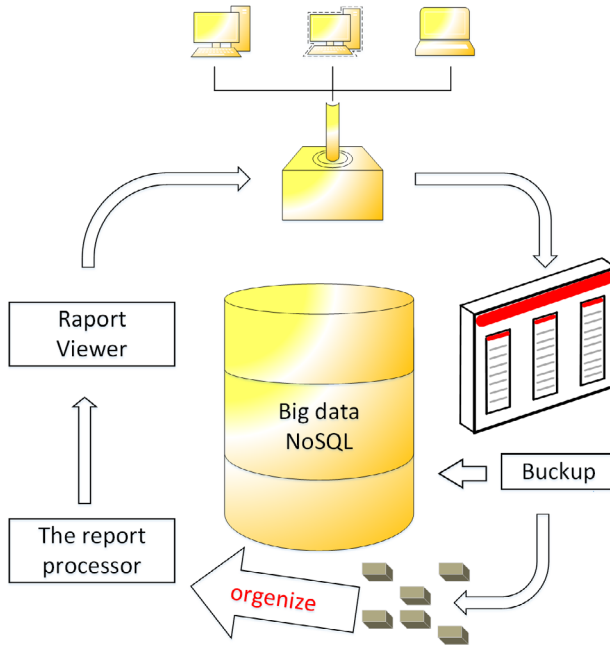


Fig. 1. Big data NoSQL database management system

Algorithms and statistical research

The statistical tests of time algorithms carried out tests for 100 samples for each dimension of the task of sorting. In each sample for a given dimension of the first tasks are random length strings of up to 8 characters, and then are inserted into chains of random capital letters of the English alphabet. For example, generated 10 sample string is shown in Figure 2.

The statistical tests were used methods such as in NOWICKI et al. (2016). A statistical average of n -element set of samples a_1, \dots, a_n defined by the formula

$$\bar{a} = \frac{1}{n} (a_1 + \dots + a_n).$$

The standard deviation is defined by the formula:

$$\sigma = \sqrt{\frac{\sum_{i=1}^n (a_i - \bar{a})^2}{n - 1}},$$

where:

- n – the number of elements in the sample,
- α_1 – value of the random variable in the sample,
- $\bar{\alpha}$ – the arithmetic mean of the sample.

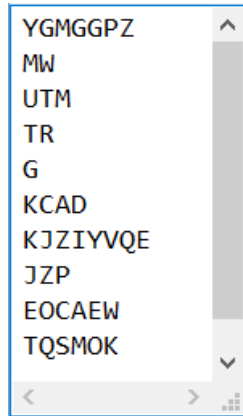


Fig. 2. Randomly generated sample for 10 strings

To determine the algorithms with the lowest time complexity they will be compared to the average time they work for large data sets. The standard deviation is characterized by the dispersion between time sorting. If we can determine the worst-case time sorting and its magnitude is the same as the average time of sort, we can say that statistical studies reflect the behavior of the algorithm in practice.

Another important factor in statistical surveys is the coefficient of variation talking about the stability of the algorithm. It is determined by formula:

$$V = \frac{\sigma}{\bar{\alpha}},$$

where:

- σ – standard deviation of random variables in tests,
- $\bar{\alpha}$ – the arithmetic mean of the sample.

The analysis methods for sorting sets of random samples taken 10, 100, 1,000, 10,000, 100,000, 1,000,000 and 10,000,000 elements. The results are presented in graphs.

Triple Heap Sort Algorithm – THSA

The algorithms used in NoSQL databases as possible require low computational complexity. The methods of handling the data source and do not require additional resources are of particular interest. Let us now to present modified triple heap sort algorithm for sorting strings stored in Unicode. Strings a_i $i = 0, \dots, n - 1$ present in the form of triple tree where the node number is the index of the string Figure 3.

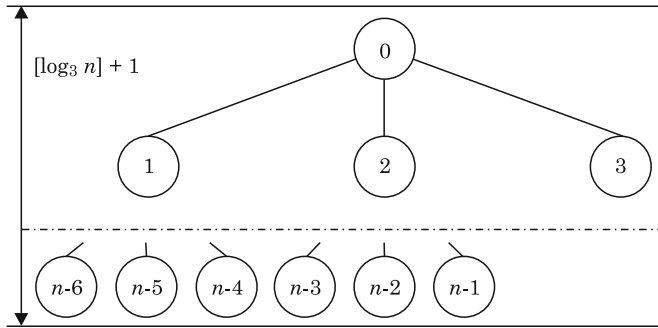


Fig. 3. Triple tree of strings

Sorting strings start of construction of the heap, i.e. Strings arrangement in such a way as to satisfy the conditions:

$$a[i] \geq a[3 \cdot i + 1] \quad i = 0, \dots, \left\lfloor \frac{n-2}{3} \right\rfloor \tag{1}$$

$$a[i] \geq a[3 \cdot i + 2] \quad i = 0, \dots, \left\lfloor \frac{n-2}{3} \right\rfloor \tag{2}$$

$$a[i] \geq a[3 \cdot i + 3] \quad i = 0, \dots, \left\lfloor \frac{n-2}{3} \right\rfloor \tag{3}$$

The relationship most equality is understood the same as the stacking order of words in the dictionary of a language of culture. Starting to build the heap from node $\left\lfloor \frac{n-2}{3} \right\rfloor$, we know that elements indexed from $n - 1$ down to $\left\lfloor \frac{n-2}{3} \right\rfloor + 1$ and they don't have descendants. We begin construction of the heap

with the $\left\lceil \frac{n-2}{3} \right\rceil$ having at least one descendant node. Next we are passing all nodes values up to the node with the index zero each time applying Algorithm 1. This algorithm is pushing the element off the root of the parent into the bottom as far as possible. It is held in this way. We sort the biggest value to be in a node from descendant nodes of the parent chosen according to (1) – (3). Next a value of the node of the parent is being compared with the nodes of the descendant. If the descendant node stores the value greater than the node of the parent, the value is changed and the algorithm gets up to the chosen descendant node. Then the same algorithm is applied for the parent to the moment when the parent isn't storing the greater value from a child or the parent doesn't have any children. Passing all nodes values up we receive a sorted heap. In the root the biggest value is sorted. We change this top node value with the value of last element of the heap and then reduce the number of elements in the heap by one. Again we apply the Algorithm 2 pushing the element off the root possibly far into the bottom to receive all elements sorted. Therefore the sequence on the stack is sorted by proposed THSA in the same table of strings, what make the method very efficient for big data system.

THEOREM 1. Height of triple heap, built of n elements is

$$k = \lceil \log_3 n \rceil + 1 \quad (4)$$

Where heap height k is understood as number of levels in the heap and n is a number of all elements in the heap.

Proof. Each heap level k has from $1 = 3^0$ to 3^k elements. Therefore according to heap divisions we can estimate number of all elements in the heap as

$$1 + 3 + \dots + 3^{k-1} + 3^k = \frac{1}{2} (3^{k+1} - 1) \quad (5)$$

In the last level of the heap do not have to be a complete number of leaves. Nevertheless we can write down that $r \leq 3^k$ that satisfy the equation

$$1 + 3 + \dots + 3^{k-1} + r = n \quad (6)$$

Now we can estimate n

$$n = r + 1 + 3 + \dots + 3^{k-1} \leq \frac{1}{2} (3^{k+1} - 1) \quad (7)$$

$$\log_3 (2n + 1) \leq (k + 1) \log_3 3 = (k + 1) \quad (8)$$

$$\log_3 (2n + 1) - \log_3 3 \leq k \quad (9)$$

$$\log_3 \left(\frac{2n+1}{3} \right) \leq \min_{k \in N} k \quad (10)$$

Given that $n \geq \frac{2n+1}{3}$ for $n \in N$ we obtain an estimate for $k \in N$

$$\log_3 \left(\frac{2n+1}{3} \right) \leq \log_3 n \leq \lceil \log_3 n \rceil + 1 = k \quad (11)$$

which proves the theorem.

THEOREM 2. Triple heap is created in a linear time.

THEOREM 3. Presented Triple Heap Sort Algorithm is sorting n elements in time

$$O(n \cdot \log_3 n) \quad (12)$$

which we give without proof.

Presented method was implemented in C++ CLR. The algorithm is divided into algorithm to re-arrange elements into triple heap Figure 4 and triple heap sort algorithm Figure 5.

```

Start
Load table  $a$ ,
Load index  $t$ ,
Load index  $r$ ,
Remember  $3 \cdot t + 1$  in  $k0$ ,
Remember  $k0+1$  in  $k1$ ,
Remember  $k0+2$  in  $k2$ ,
Remember  $a[t]$  in  $x$ ,
While  $r$  is greater than or equal to  $k2$  then do
Begin
  Remember  $k0$  in  $z$ ,
  If  $a[k1]$  is greater than  $a[z]$  then do
    Remember  $k1$  in  $z$ ,
  If  $a[k2]$  is greater than  $a[z]$  then do
    Remember  $k2$  in  $z$ ,
  If  $a[z]$  is greater than  $x$  then do
    Begin
      Remember  $a[z]$  in  $a[t]$ ,
      Remember  $z$  in  $t$ ,
      Remember  $3 \cdot t + 1$  in  $k0$ ,
      Remember  $k0+1$  in  $k1$ ,
      Remember  $k0+2$  in  $k2$ ,
    End
  Else
    Begin
      Remember  $r+1$  in  $k0$ ,
      Remember  $r+2$  in  $k1$ ,
      Remember  $r+3$  in  $k2$ ,
    End
End
If  $r$  is greater than or equal to  $k1$  then do
Begin
  Remember  $k0$  in  $z$ ,
  If  $a[k1]$  is greater than  $a[z]$  then do
    Remember  $k1$  in  $z$ ,
  If  $a[z]$  is greater than  $x$  then do
    Begin
      Remember  $a[z]$  in  $a[t]$ ,
      Remember  $z$  in  $t$ ,
    End
End
Else
Begin
  If  $r$  is greater than or equal to  $k0$  then do
    Begin
      If  $a[k0]$  is greater than  $x$  then do
        Begin
          Remember  $a[k0]$  in  $a[t]$ ,
          Remember  $k0$  in  $t$ ,
        End
      End
    End
End
Remember  $x$  in  $a[t]$ ,
Return
Stop

```

Fig. 4. Algorithm to re-arrange into triple heap

```

Start
Load table  $a$ ,
Load size of table  $a$  into  $n$ ,
Remember  $(n-2)/3$  in  $t$ ,
While  $t$  is greater than or equal to zero then do
Begin
    Proceed Algorithm to re-arrange into triple heap with table  $a$  and
    setting index of initial heap element  $t$  and index of final heap element as  $n-1$ ,
    Decrease the index  $t$  by one,
End
Remember  $n-1$  in  $t$ ,
While  $t$  is greater than zero then do
Begin
    Remember  $a[t]$  in  $x$ ,
    Remember  $a[0]$  in  $a[t]$ ,
    Remember  $x$  in  $a[0]$ ,
    Proceed Algorithm to re-arrange into triple heap with table  $a$  and
    setting index of initial heap element 0 and index of final heap element as  $t-1$ ,
    Decrease the index  $t$  by one,
End
Return
Stop

```

Fig. 5. Triple heap sort algorithm

The study triple heap sort algorithm

Performance analysis presented methods has been tested for sorting large data sets. The algorithm was implemented in C++ CLR in Visual Studio 2015 Enrprice on MS Windows Server 2008 R2. The study was conducted on 100 samples randomly generated for each dimension of the task. Tests were carried out on quad core amd opteron processor 8356 8p. The purpose of the analysis and comparison is to check whether triple heap sort algorithm is better than traditional heap sort of sorting large data sets. For the benchmark we have applied input samples of 10, 100, 1,000, 10,000, 100,000, 1,000,000 and 10,000,000 elements. Each sorting operation by examined methods was measured in time [ms] and CPU (Central Processing Unit) usage represented in tics of CPU clock.

Summary of time sorting the method is binary heap sort and triple heap sort were placed in Table 1. These results are averaged for 100 sorting samples for each of BSHA and THSA in Figures 6 and 7.

Compare the current coefficient of variation methods are binary heap and triple heap sorting of large data sets.

Table 1

Sorting results binary heap sort and triple heap sort algorithm

Elements	Method – average time sorting for 100 samples			
	binary heap sort algorithm – BHSA		triple heap sort algorithm – THSA	
	ms	ti	ms	ti
10	1	33	1	30
100	1	689	1	499
1,000	8	11,612	5	6,940
10,000	122	189,626	63	98,877
100,000	1,479	2,305,583	846	1,317,943
1,000,000	19,425	30,276,976	11,217	17,483,931
10,000,000	246,460	384,143,716	143,035	222,939,977

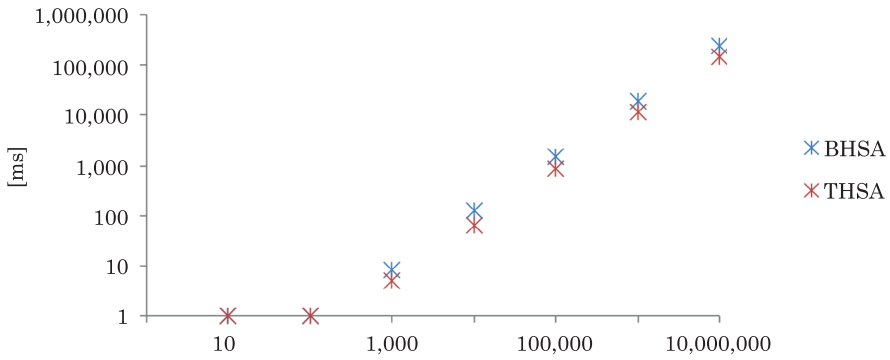


Fig. 6. Comparison of benchmark time [ms] for presented in Sec. 2 methods

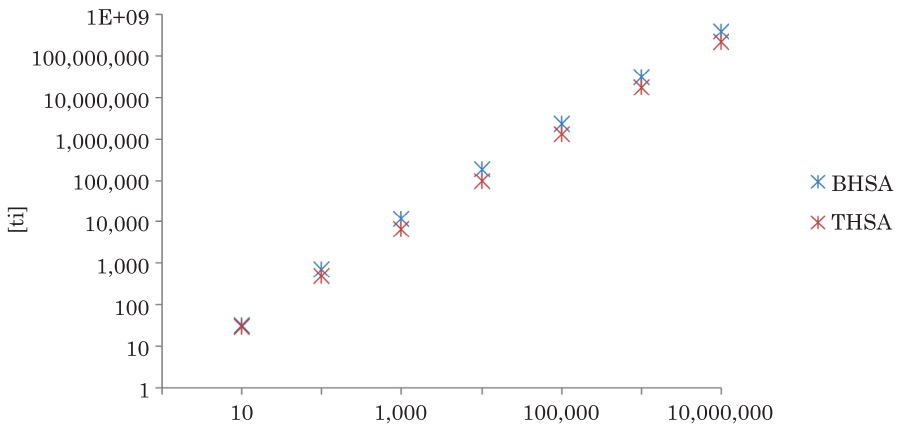


Fig. 7. Comparison of benchmark CPU operations [ti] for presented in Sec. 2 methods

Table 2

Coefficient of variation binary heap fast sort and triple heap sort

Number of elements	Coefficient of variation	
	BHSA	THSA
10	0.925820099772551	1.24162020748728
100	0.843720298643621	0.338541807177754
1,000	0.232357160225841	0.0237000571071293
10,000	0.0232357160225841	0.0244774504038522
100,000	0.00792931906914819	0.0078376227129250
11,000,000	0.00667148990227573	0.0066610364196879
110,000,000	0.00487603595021875	0.00487596419925631

Analyzing Table 2 we see that both algorithms are similar in statistical stability for large data sets. Low stability of the algorithm for a small size job due to the fact that the system operation execution exceed the sorting algorithm. As size increases the coefficient of variation task is stabilizing.

Analysis of time sorting and comparison

Analysis and comparison will describe efficiency for sorting large data sets. Let us compare both methods of assuming the duration of the binary heap sort and let us examine if the percentage is a longer duration of action triple heap sort. The results are shown in the graphs Figures 8 and 9.

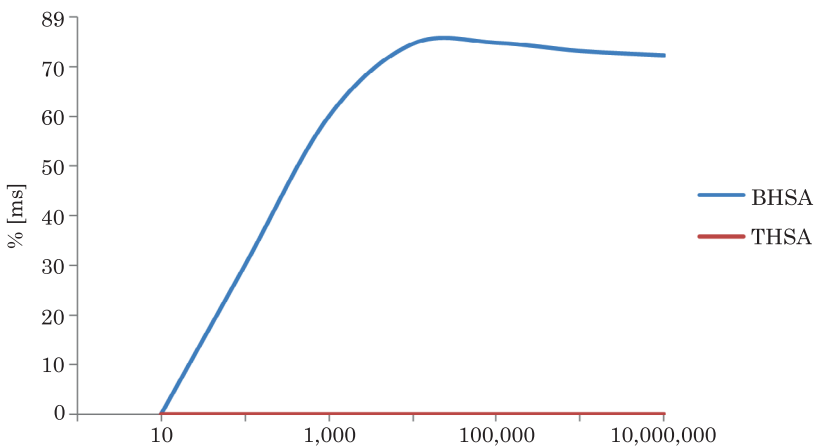


Fig. 8. Comparison of the two methods in terms of operational time [ms]

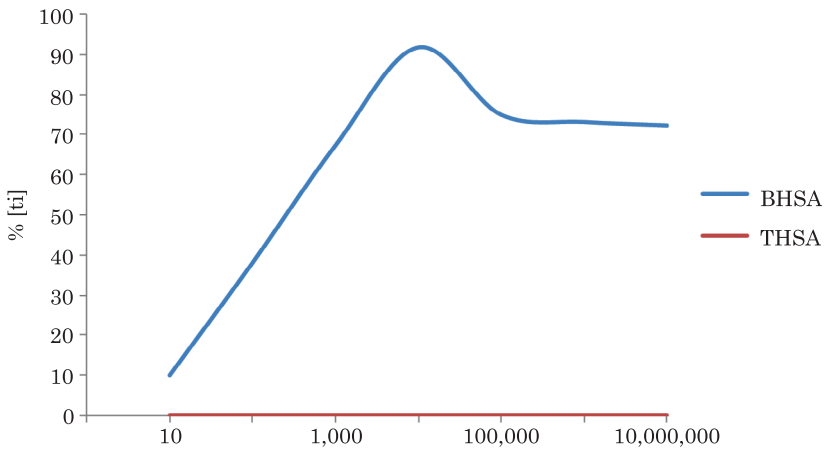


Fig. 9. Comparison of the two methods in CPU operations [ti]

The study shows that the triple heap sort method operate in a much shorter time measuring tasks from 1,000 to 10,000,000. Triple heap sorting algorithm is stable method allows sorting of large data sets stored in the form of strings in Unicode. Because it does not require additional resources, it is particularly the case when the entire job must do in the computer's memory.

Final Remarks

The article presented triple heap sort algorithm for rapid sorting of large data sets. The tests performed demonstrate the stability of the method and confirm the theoretical time complexity. Both Triple Heap Sort Algorithm and Binary Heap Sort Algorithm for fast sorting may find practical application in NoSQL databases.

References

- ARTIEMJEW P. 2014. *Rough mereology classifier vs. simple DNA microarray gene extraction methods*. International Journal of Data Mining, Modelling and Management, 6(2): 110–126. doi: 10.1504/IJDM.2014.063193.
- ARTIEMJEW P. 2015. *The Boosting and Bootstrap Ensemble for Classifiers Based on Weak Rough Inclusions*. Lecture Notes in Computer Science – RSFDGrC, 9437: 267–277. doi: 10.1007/978-3-319-25783-9.
- ARTIEMJEW P., NOWAK B.A., POLKOWSKI L.T. 2016. *A New Classifier Based on the Dual Indiscernibility Matrix*. Communications in Computer and Information Science – ICIST, 639: 380–391. doi: 10.1007/978-3-319-46254-7.

- AUMÜLLER M., DIETZFELBINGER M. 2013. *Optimal Partitioning for Dual Pivot Quicksort*. ICALP'13 Proceedings of the 40th international conference on Automata, Languages, and Programming. Part I. Eds. F.V. Fomin, R. Freivalds, M. Kwiatkowska, D. Peleg. Springer-Verlag Berlin, Heidelberg.
- AUMÜLLER M., DIETZFELBINGER M., KLAUE P. 2016. *How Good Is Multi-Pivot Quicksort?* ACM Trans. Algorithms, 13(1): 47.
- DAMASEVICIUS R., MASKELIUNAS R., VENCKAUSKAS A., WOZNIAK M. 2016a. *Smartphone User Identity Verification Using Gait Characteristics*. Symmetry 8(10): 100. doi: 10.3390/sym8100100.
- DAMASEVICIUS R., VASILJEVAS M., SALKEVICIUS J., WOZNIAK M. 2016b. *Human Activity Recognition in AAL Environments Using Random Projections*. Comp. Math. Methods in Medicine, 2016(ID 4073584): 17. doi:http://dx.doi.org/10.1155/2016/4073584.
- GABRYEL M. 2016. *The Bag-of-Features Algorithm for Practical Applications Using the MySQL Database*. Lecture Notes in Computer Science – ICAISC, 9693: 635-646. doi: 10.1007/978-3-319-39384-1.
- GRYCUK R., GABRYEL M., SCHERER R., VOLOSHYNOVSKIY S. 2015. *Multi-layer Architecture For Storing Visual Data Based on WCF and Microsoft SQL Server Database*. Lecture Notes in Computer Science – ICIST, 9119: 715-726. doi: 10.1007/978-3-319-19324-3.
- MARSZALEK Z. 2016. *Novel Recursive Fast Sort Algorithm*. Communications in Computer and Information Science – ICIST, 639: 344-355. doi: 10.1007/978-3-319-46254-7.
- MLECZKO W.K., NOWICKI R.K., ANGRYK R.A. 2016. *Rough Restricted Boltzmann Machine – New Architecture for Incomplete Input Data*. Lecture Notes in Computer Science-ICAISC, 9692: 114-125. doi: 10.1007/978-3-319-39378-0.
- NEBEL M.E., WILD S., MARTÍNEZ C. 2016. *Analysis of Pivot Sampling in Dual-Pivot Quicksort: A Holistic Analysis of Yaroslavskiy's Partitioning Scheme*. Algorithmica, 75(4): 632-683.
- NOWICKI R.K., SCHERER R., RUTKOWSKI L. 2016. *Novel rough neural network for classification with missing data*. 21st International Conference on Methods and Models in Automation and Robotics, MMAR, Miedzyzdroje, August 29 – September 1, IEEE, p. 820-825. doi: 10.1109/MMAR.2016.7575243.
- POLAP D., WOZNIAK M., NAPOLI CH., TRAMONTANA E. 2015a. *Is Swarm Intelligence Able to Create Mazes?* International Journal of Electronics and Telecommunications, 61(4): 305-310. doi: 10.1515/eletel-2015-0039.
- POLAP D., WOZNIAK M., NAPOLI CH., TRAMONTANA E. 2015b. *Real-Time Cloud-based Game Management System via Cuckoo Search Algorithm*. International Journal of Electronics and Telecommunications, 61(4): 333-338. doi: 10.1515/eletel-2015-0043.
- WEGNER L.M., TEUHOLA J.I. 1989. *The External Heapsort*. IEEE Transactions on Software Engineering, 15(7).
- WILD S., NEBEL M.E., MAHMOUD H. 2016. *Analysis of Quickselect Under Yaroslavskiy's Dual-Pivoting Algorithm*. Algorithmica, 74(1): 485-506.
- WOZNIAK M., MARSZALEK Z., GABRYEL M., NOWICKI R.K. 2013. *Modified Merge Sort Algorithm for Large Scale Data Sets*. Lecture Notes in Computer Science – ICAISC, 7895: 612-622. doi: 10.1007/978-3-642-38610-7.
- WOZNIAK M., MARSZALEK Z., GABRYEL M., NOWICKI R.K. 2016. *Preprocessing Large Data Sets by the Use of Quick Sort Algorithm*. Advances in Intelligent Systems and Computing – KICSS, 364: 111-121. doi: 10.1007/978-3-319-19090-7.



FATIGUE CRACK DETECTION METHOD USING ANALYSIS OF VIBRATION SIGNAL

Arkadiusz Rychlik, Krzysztof Ligier

Chair of Vehicle and Machine Construction and Operation
University of Warmia and Mazury in Olsztyn

Received 8 September 2016, accepted 17 January 2017, available online 19 January 2017.

Key words: fatigue cracking, diagnostic signal, force of inertia, microscopic examinations.

Abstract

This paper discusses the method used to identify the process involving fatigue cracking of samples on the basis of selected vibration signal characteristics. Acceleration of vibrations has been chosen as a diagnostic signal in the analysis of sample cross section. Signal characteristics in form of change in vibration amplitudes and corresponding changes in FFT spectrum have been indicated for the acceleration. The tests were performed on a designed setup, where destruction process was caused by the force of inertia of the sample. Based on the conducted tests, it was found that the demonstrated sample structure change identification method may be applied to identify the technical condition of the structure in the aspect of loss of its continuity and its properties (e.g.: mechanical and fatigue cracks). The vibration analysis results have been verified by penetration and visual methods, using a scanning electron microscope.

Introduction

Brackets are among the most frequently used structural elements in engineering. They are commonly used, from simple structures like pressure gauge connections in pipelines, to more sophisticated components, such as aircraft wings or airscrew vanes. Methods applied to monitor these objects in order to identify and forecast their technical condition have now become an important area of research. It is possible to prevent the damage to structures

and machine components by early detection of fatigue cracks, carried out using various non-destructive testing methods. The following conventional non-destructive test methods: penetrant testing, magnetic methods, ultrasonic testing, etc., have their constraints and are often expensive and ambiguous in evaluation of the condition. Alternative methods based on identification of the form and parameters of vibrations may constitute an effective, quick and convenient diagnostic tool for the detection of fatigue cracks in machine components and structural systems.

In the literature, structure cracks are identified in two ways: linearly and non-linearly. In the linear method, vibrations are examined in the objects, where changes of modal parameters in relation to the initial model are taken into account, whereas in the non-linear model, a crack is identified through the analysis of frequency characteristics (ANDREAS, BARAGATTI 2011, ANDREAS 2012, ANDREAS, CASINI 2016, ANDREAS et al. 2005, ANDREAS et al. 2007, ANDREAS, BARAGATTI 2012, BRODA et al. 2014b, LIU et al. 2015, MENDROK 2014, PREIBISCH et al. 2009, RADKOWSKI, SZCZUROWSKI 2012, SUDINTAS 2015).

In the linear approach, a crack is always considered as open, and it is modelled as a local flexibility (GUDMUNSON 1998). Crack size and location are examined and characterised through changes of modal parameters including: natural frequency (OSTACHOWICZ, KRAWCZUK 1991), damping factor (PANTELIU et al. 2001) or modulus of rigidity (GIBSON 2000, KAŻMIERCZAK et al. 2013). However, this approach has two primary constraints. First, a change in natural frequency is significant only for large crack sizes (CHENG et al. 1996), and second, a measured natural frequency shift cannot be unequivocally attributed to cracking itself, since it may be also generated by other factors, as wear, relaxation, etc. (ANDREAS, BARAGATTI 2009, ANDREAS et al. 2016, BIAŁKOWSKI, KRĘŻEL 2015).

In the non-linear model it is generally recognised that vibration theory is correlated with modal parameters of a system, that is: natural frequency, damping, and forms of vibrations. In other words, it is a physical system consisting of physical structure properties (mass, rigidity and damping). These model parameters are homogeneous systems described by differential equations of the model physical motion expressed with reference to its mass, damping and rigidity, acceleration, speed and displacement. As a result of this, all changes in modal parameters are directly proportional to the change in physical property of the modelled object due to damage (ANDREAS, CASINI 2016).

The problem of identifying structural damage on the basis of vibrations was raised by numerous authors (BRODA et al. 2014a, OH et al. 2015, JASSIM et al. 2013, KLEPKA et al. 2014, TAO et al. 2014, TROCHIDIS et al. 2014, TROJNAR et al. 2014, XU 2014, ZHOU 2006). Object vibration parameters are defined in this

approach, and structural damage identification is the function of change in object structural properties, such as rigidity and mass. The presence of damage affects both vibration signal response and dynamic properties of a given structure. Dynamic properties of the structure include: natural frequencies, shapes and damping mode indicators. These properties are used as indicators of damage in the structure being tested. Early detection of structural damage allows for timely maintenance and repairs, extending the system service life.

In order to ensure safety and structural reliability it is necessary to perform long-term, medium-term and short-term monitoring of the structure technical condition in the operating process. One of the basic dynamic properties is rigidity, which may lead to changes in the shape and frequency reduction mode, and to damping coefficient increase.

The paper presents an attempt to use vibration signal analysis to detect the loss in sample structure continuity.

Measurement setup

Laboratory tests were carried out using the measurement setup shown in Figure 1. The setup consists of a reciprocating motion generator (crank gear), to which a clamp holding the samples is fixed.

The setup allows for the generation of sample oscillatory motion at specific frequency (f) and constant displacement amplitude. Due to the oscillatory motion and one-side fixing of a sample, generated forces of inertia cause its elastic strains.

The following sensors were employed to identify dynamic parameters of the system: two piezoelectric sensors for vibration accelerations (ICP-100) and a rotational speed sensor for the shaft of inverter-controlled driving motor. A multi-channel KSD-400 recorder based on the NI 6343 card supported by LabVIEW was used for the purposes of acquired data recording, visualisation and analysis.

Visual assessment was carried out in two stages. Initial process involved identification of cracks through penetrant testing according to the PN EN ISO 3452-1:2013-08E and PN EN ISO 3059:2013-06E standards. The second stage of surface evaluation for selected samples was performed with a JEOL JSM 5310LV type scanning electron microscope, working in a digital configuration.

No sample surface polishing was applied, so as to maintain surface condition of sheet metal used for structural components and to show the impact of surface condition on the occurrence of cracks.

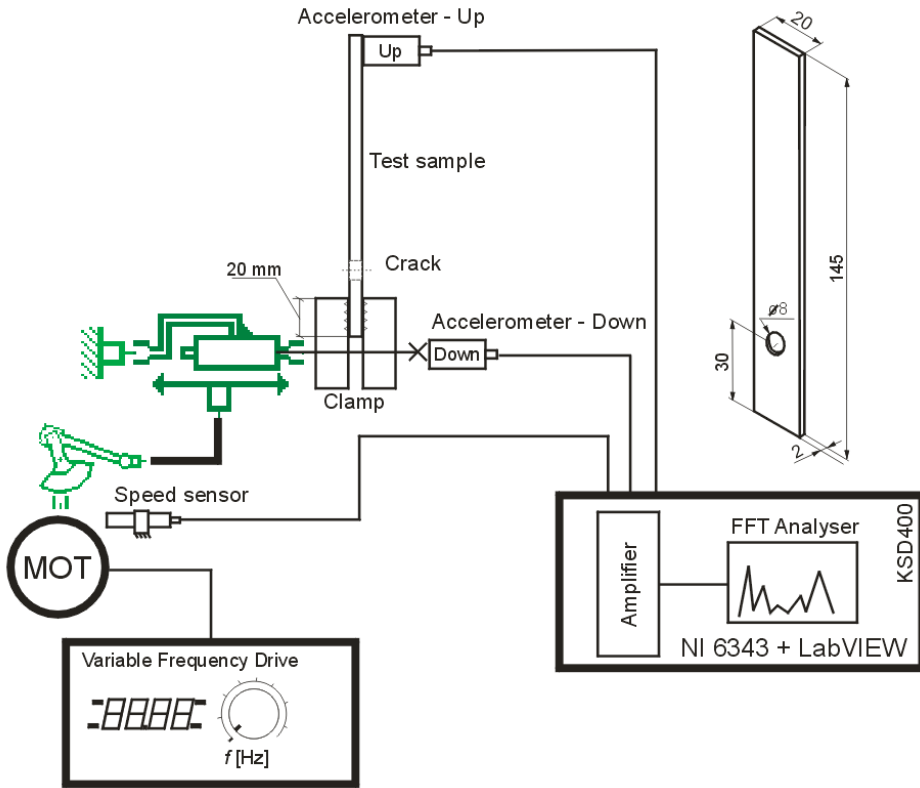


Fig. 1. The structure of setup for experimental tests and general view of test sample

The tested object

The tested object was a flat rectangular sample shown in Figure 1. A notch in the form of a hole was made in the sample, where stresses were accumulating during the tests due to the smallest cross-section of the whole sample. The used samples were made of 1.4301 stainless steel and S235JR steel. The sample surface was left untreated following manufacturing process. The surface roughness was assessed using the Hommel Tester T1000E, profile measurement gauge, according to the ISO 4287/1 standard.

The surface roughness is considered as an important factor influencing fatigue strength. Many researchers have carried out much work to evaluate the effects of the surface roughness on fatigue (ALANG et al. 2011, KYRRE et al. 2008). In those works mostly R_a is used as a roughness parameter. Due to the fact that in the study of fatigue resistance local changes of surface

topography are important, it was decided to include the Rz parameter, to characterize surface of the samples. Sample roughness parameters are specified in Table 1.

Table 1
Surface roughness parameters for the tested samples

Material	Roughness parameters [μm]	
	Ra	RzI
1.4301	0.17	1.9
S235JR	0.87	6.22

The progress and results of tests

The experimental research was carried out for the frequency ranging from 20 Hz to 50 Hz. However, the paper shows the results of research for the frequency of 30 Hz only. The reason of that was that an excitation frequency of 30 Hz was the resonance frequency for applied sample. This excitation frequency guaranteed quick progress of the sample destruction process within approx. 4,000 s.

Acceleration amplitude and the form of vibrations in frequency domain (the FFT analysis) were used to identify the sample section destruction process.

All the test results presented below were obtained for the following test parameters:

- vibration excitation frequency 30 Hz;
- sample holder displacement amplitude $A = 1$ mm (the size of displacement is caused by the crank throw);
- mass of sensor (125 g) mounted on upper end of a sample.

For selected samples the tests were interrupted at the moment of pinpointing the beginning of the sample damage process identified in the diagnostic signal trajectory. All the samples were put through penetrant testing, and those for which penetrant testing did not show any cracks, were subject to microscopic examinations.

Figure 2 shows a sample cascade amplitude-frequency trajectory of the test sample response process for an excitation frequency of 30 Hz, recorded by the acceleration sensor fitted on the sample upper end – Up (see Fig. 1).

It was observed that the progress of the sample section damage process is implemented in the following way:

- as regards initial sample condition, its vibration displacement amplitude for excitation frequency (f_0) is constant, shown as area A in Figure 2, and

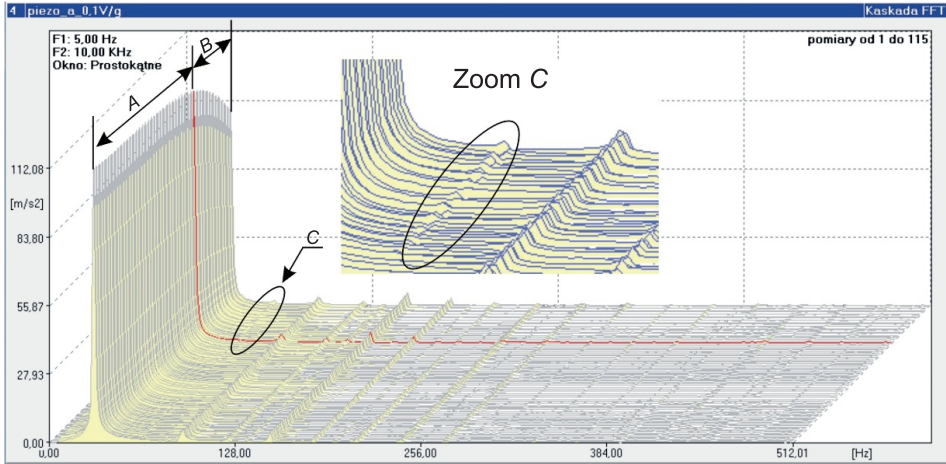


Fig. 2. Cascade view of test sample amplitude – frequency trajectory, signal recording source – acceleration sensor – Up. The red line indicates the beginning of crack in sample section notch structure. Assembly mass with acceleration sensor (125 g)

at the same time there are harmonic frequencies of higher orders visible ($3f_0 = 90$, $4f_0 = 120$ Hz, etc.) with equally constant amplitude values,

- the occurrence of a change in the condition of the sample notch section is indicated by systematic decrease of vibration acceleration amplitude for excitation frequency (shown as area B in Fig. 2) and observed increase of vibration amplitude for the second harmonic frequency (area C) – until then not identified in the vibration spectrum,

- initiation of crack in the sample notch section corresponds to the highest value of vibration acceleration amplitude for harmonic frequency (f_0). As a result of further excitation of the sample vibration, we observe a drop in the displacement amplitude compared to the nominal condition of the sample. Due to the purpose of tests, the process of further sample destruction was not identified.

The sample section destruction process progressed much the same for all tested samples, regardless of the excitation frequency, and the only difference was in the initiation time of the process of sample surface or section mechanical damage.

Visual analysis of sample damage process

The purpose of microscopic examination was to verify whether the observed changes in the amplitude of the sample vibrations are connected with cracks on the surface of the sample. Observations of the sample were carried out on the notched weakened area.

Figure 3 shows the notch zone for a sample made of S235JR steel. The sample penetrant testing did not show occurrence of any cracks. Microscopic examination of the notch area surface made it possible to observe a numerous cracks – lengths ranging from 24 to 40 μm , running perpendicular to the axis of the sample.

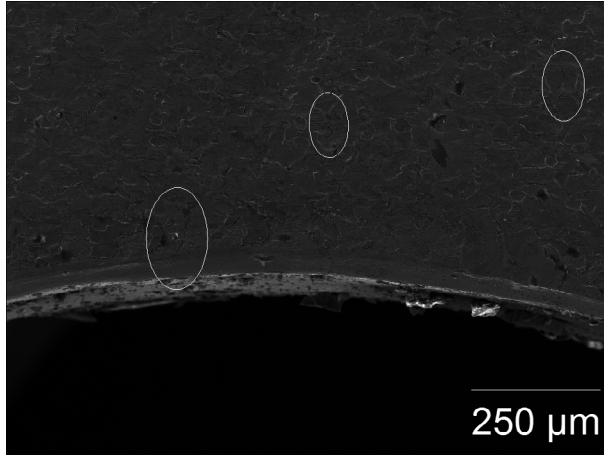


Fig. 3. View of surface – sample made of S235JR steel – cracks are marked

These cracks developed in narrowed area of the sample. The main crack was observed on both sides of the notch, starting on its edge (ca. 125 μm and 121 μm). These cracks are shown in Figures 4 and 5. The surface condition (roughness parameters was $R_a = 0.87$ and $R_z = 6.22$ μm) may have caused the initiation of other cracks in spots away from the notch.

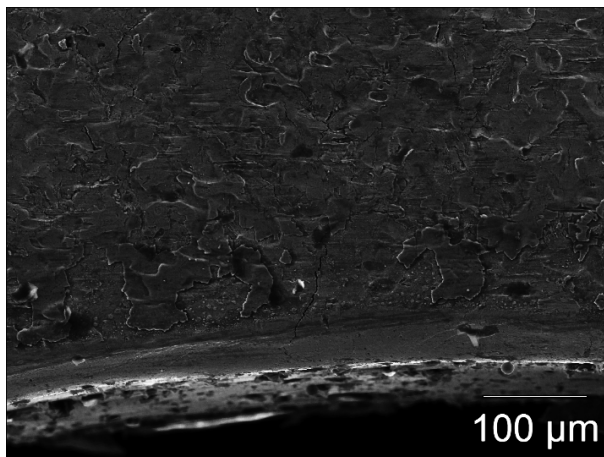


Fig. 4. The surface of a sample made of S235GJ steel with visible crack at the edge of the hole

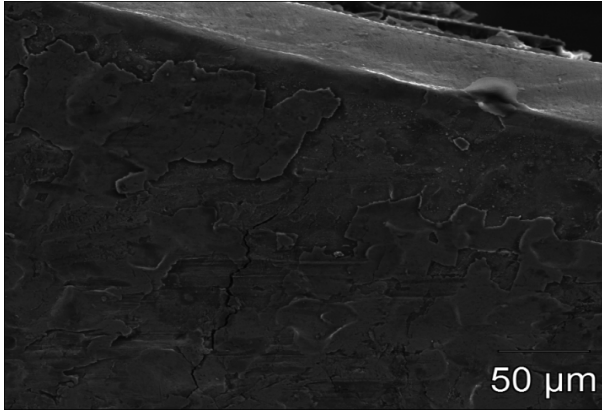


Fig. 5. The surface of a sample made of S235GJ steel with visible crack at the edge of the hole

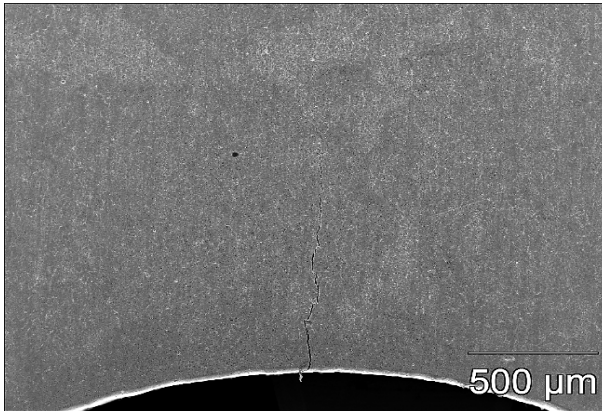


Fig. 6. Crack visible on the surface of a sample made of 1.4301 steel

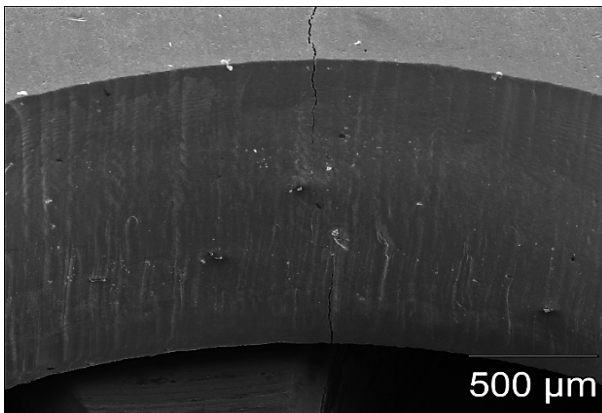


Fig. 7. Crack in cross-section of a sample made of 1.4301 steel

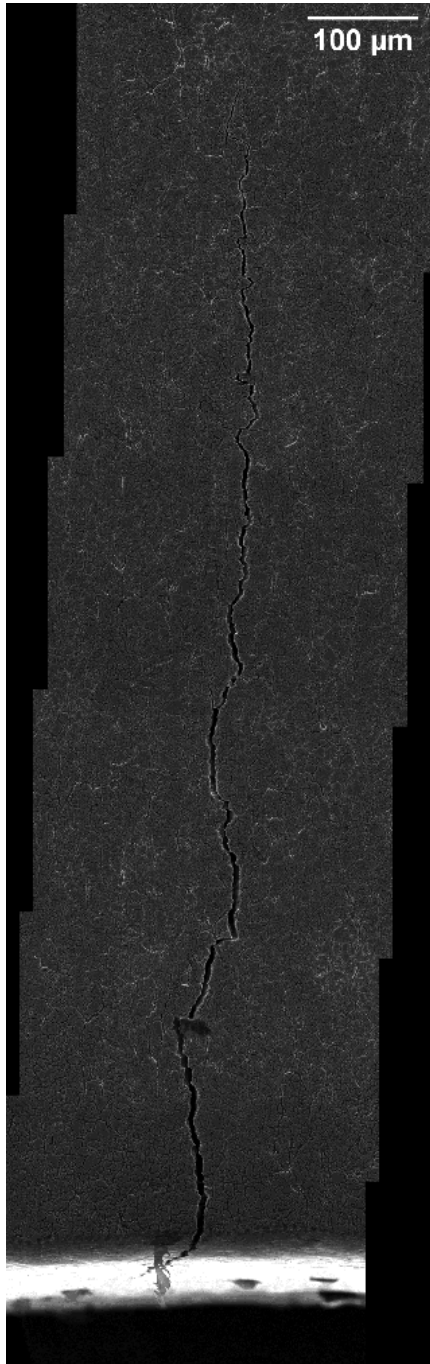


Fig. 8. Crack on the surface of sample made of 1.4301 steel

There is one crack (1 mm in length) visible on the surface of a sample made of 1.4301 stainless steel, developing from the edge of the hole (Fig. 6). In this case, the crack was visible after penetrant testing. Microscopic examinations of the surface did not show occurrence of any additional cracks accompanying the observed one.

The observed crack visible from the side of the hole is shown in Figure 7. The picture shows the crack developing inside the hole, deep into the material on both sides of the sample.

A larger zoom of the view of the whole crack is shown in Figure 8. It seems that the roughness surfaces was decisive on occurrence of cracks away from the notch edge. The microscopic observations showed that changes in the vibration amplitude of the sample are associated with the appearance of the cracks on its surface.

Conclusions

Based on the completed tests and simulations the following conclusions may be formulated:

- it is not possible to identify through penetrant testing the beginnings of the mechanical destruction processes for samples determined on the basis of distinguished signal characteristics;

- sample section destruction time is affected by the volume of mechanical work the sample section is subjected to – in other words, energy needed to destroy the sample may be defined as the area under the sample section stress curve;

- regardless of the shape and localization of the notch, the sample destruction process runs in much the same way; the only differences may occur as changes of vibration amplitude values;

- obtained test results and their further verification lets assume the suitability of the discussed vibro-acoustic method to detect material structure micro-cracks interpreted as modal parameters of the examined object.

- high surface roughness of the sample made of S235JR steel, promotes the initiation of cracks in a away from the edge of the notch. In the sample characterizing with lower roughness (1.4301 stainless steel) only one crack starting from the edge of the notch was observed.

References

- ALANG N.A., RAZAK N.A., MISKAM A.K. 2011. *Effect of Surface Roughness on Fatigue Life of Notched Carbon Steel*. International Journal of Engineering Technology IJET-IJENS, 11(1): 160–163.
- ANDREAS U. 2012. *Experimental damage detection of cracked beams by using nonlinear characteristics of forced response*. Mechanical Systems and Signal Processing, <https://www.researchgate.net/publication/258683466>.
- ANDREAS U., BARAGATTI P. 2009. *Fatigue crack growth, free vibrations and breathing crack detection of Aluminium Alloy and Steel beams*. J. of Strain Analysis for Engineering Design, 44(7): 595–608. doi: 10.1243/03093247JSA527.
- ANDREAS U., BARAGATTI P. 2011. *Cracked beam identification by numerically analysing the nonlinear behaviour of the harmonically forced response*. Journal of Sound and Vibration, 330: 721–742.
- ANDREAS U., BARAGATTI P. 2012. *Experimental damage detection of cracked beams by using nonlinear characteristics of forced response*. Mech. Syst. Signal Process., 31(8): 382–404. doi: 10.1016/j.ymsp.2012.04.007.
- ANDREAS U., BARAGATTI P., CASINI P., IACOVIELLO D. 2016. *Experimental damage evaluation of open and fatigue cracks of multi-cracked beams by using wavelet transform of static response via image analysis*. Structural Control and Health Monitoring. doi: 10.1002/stc.1902.
- ANDREAS U., CASINI P. 2016. *Identification of multiple open and fatigue cracks in beam-like structures using wavelets on deflection signals*. Continuum Mech. Thermodyn., 28: 361–378. doi: 10.1007/s00161-015-0435-4.
- ANDREAS U., CASINI P., VESTRONI F. 2003. *Frequency reduction in elastic beams due to a stable crack: numerical results compared with measured test data*. Engng. Trans., 51(1): 87–101.
- ANDREAS U., CASINI P., VESTRONI F. 2005. *Nonlinear features in the dynamic response of a cracked beam under harmonic forcing*. Proc. of DETC'05, 2005 ASME International Design Engineering Technical Conferences and Computers and Information in Engineering Conference, Long Beach, California, USA, September 24–28, Volume 6 C, pp. 2083–2089. doi: 10.1115/DETC2005-85672.
- ANDREAS U., CASINI P., VESTRONI F. 2007. *Nonlinear Dynamics of a Cracked Cantilever Beam Under Harmonic Excitation*. Int. J. of Non-Linear Mechanics, 42(3): 566–575. doi: 10.1016/j.ijnonlinmec.2006.08.007.
- BIAŁKOWSKI P., KRĘŻEL B. 2015. *Early detection of cracks in rear suspension beam with the use of time domain estimates of vibration during the fatigue testing*. Diagnostyka, 16(4): 55–62.
- BRODA D., KLEPKA A., STASZEWSKI W.J., SCARPA F. 2014a. *Nonlinear Acoustics in Non-destructive Testing – from Theory to Experimental Application*. Key Engineering Materials, 588: 192–201.
- BRODA D., STASZEWSKI W.J., MARTOWICZ A., UHL T., SILBERSCHMIDT V.V. 2014b. *Modelling of nonlinear crack-wave interactions for damage detection based on ultrasound – a review*. Journal of Sound and Vibration, 333: 1097–1118.
- CHENG S.M., WU X.J., WALLACE W. 1996. *Vibrational response of a beam with a breathing crack*. J. Sound Vib., 225(1): 201–208.
- GIBSON R.F. 2000. *Modal vibration response measurements for characterization of composite materials and structures*. Composites Science and Technology, 60: 2769–2780.
- GUDMUNSON P. 1983. *The dynamic behavior of slender structures with cross sectional cracks*. J. Mech. Phys. Solids., 31: 329–345.
- JASSIM Z.A., ALI N.N., MUSTAPHA F., ABDUL JALIL N.A. 2013. *A review on the vibration analysis for a damage occurrence of a cantilever beam*. Engineering Failure Analysis, 31: 442–461.
- KĄZMIERCZAK H., PAWŁOWSKI T., WOJNIOŁOWICZ Ł. 2013. *Quantifiable measures of the structural degradation of construction materials*. Diagnostyka, 14(4): 77–83.
- KLEPKA A., PIECZONKA L., STASZEWSKI W.J., AYMERICH F. 2014. *Impact damage detection in laminated composites by non-linear vibro-acoustic wave modulations*. Composites, Part B, 65: 99–108.
- KYRRE ÅS S., SKALLERUD B., TVEITEN B.W. 2008. *Surface Roughness Characterization for Fatigue Life Predictions Using Finite Element Analysis*. International Journal of Fatigue, 30: 2200–2209.

- LIU B., GANG T., WAN C., WANG C. LUO Z. 2015. *Analysis of nonlinear modulation between sound and vibrations in metallic structure and its use for damage detection*. *Nondestructive Testing and Evaluation*, 30(3): 277–290.
- MENDROK K. 2014. *Multiple damage localization using local modal filters*. *Diagnostyka*, 15(3): 15–21.
- OH B.K., CHOI S.W., PARK H.S. 2015. *Damage Detection Technique for Cold-Formed Steel Beam Structure Based on NSGA-II*. *Shock and Vibration*, 2015, article ID 354564. doi: <http://dx.doi.org/10.1155/2015/354564>.
- OSTACHOWICZ W.M., KRAWCZUK M. 1991. *Analysis of the effect of cracks on the natural frequencies of a cantilever beam*. *J. Sound Vib.*, 138: 191–201.
- PANTELIOS S.D., CHANDROS T.G., ARGYRAKIS V.C., DIMARAGONAS A.D. 2001. *Damping factor as an indicator of crack severity*. *Journal of Sound and Vibration*, 241: 235–245.
- PN EN ISO 3059:2013-06E: *Non-destructive testing – Penetrant testing and magnetic particle testing – Viewing conditions*.
- PN EN ISO 3452-1:2013-08E: *Non-destructive testing – Penetrant testing and magnetic particle testing - General principles*.
- PREIBISCH S., SAALFELD S., TOMANCAK P. 2009. *Globally optimal stitching of tiled 3D microscopic image acquisitions*. *Bioinformatics*, 25(11): 1463–1465.
- RADKOWSKI S., SZCZUROWSKI K. 2012. *Use of vibroacoustic signals for diagnosis of prestressed structures*. *Eksploatacja i Niezawodność. Maintenance and Reliability*, 14(1): 84–91.
- SINHA J.K., FRISWELL M.I., EDWARDS S. 2002. *Simplified models for the location of cracks in beam structures using measured vibration data*. *Journal of Sound and Vibration*, 251(1): 13–38.
- SUDINTAS A., PAŠKEVIČIUS P., SPRUOGIS B., MASKELIŪNAS R. 2015. *Measurement of stability of a pipe system with flowing fluid*. *Journal of Measurements in Engineering*, 3(3): 87–91.
- TAO J., FENG Y., TANG K. 2014. *Fatigue crack detection for a structural hotspot*. *Journal of Measurements in Engineering*, 2(1): 49–56.
- TROCHIDIS A., HADJILEONTIADIS L., ZACHARIAS K. 2014. *Analysis of vibroacoustic modulations for crack detection: A Time-Frequency Approach Based on Zhao-Atlas-Marks Distribution*. *Shock and Vibration*, 2014, article ID 102157. doi: <http://dx.doi.org/10.1155/2014/102157>.
- TROJNAR T., KLEPKA A., PIECZONKA L., STASZEWSKI W.J. 2014. *Fatigue crack detection using nonlinear vibro-acoustic cross-modulations based on the Luxemburg-Gorky effect*. *Health Monitoring of Structural and Biological Systems 2014*, 90641F. doi: 10.1117/12.2046471.
- XU Q. 2014. *Impact detection and location for a plate structure using least squares support vector machines*. *Structural Health Monitoring*, 13(1): 5–18.
- ZHOU Z. 2006. *Vibration based damage detection of simple bridge superstructures*. PhD thesis. University of Saskatchewan Saskatoon.



Quarterly peer-reviewed scientific journal

ISSN 1505-4675
e-ISSN 2083-4527

TECHNICAL SCIENCES

Homepage: www.uwm.edu.pl/techsci/



THE ANALYSIS OF THE RELATIONS BETWEEN POROSITY AND TORTUOSITY IN GRANULAR BEDS

Wojciech Sobieski, Seweryn Lipiński

Department of Mechanics and Basics of Machine Construction
University of Warmia and Mazury in Olsztyn

Received 15 December 2015, accepted 13 December 2016, available online 27 January 2017

Key words: porous media, granular beds, porosity, tortuosity.

Abstract

In the paper, functions describing different porosity-tortuosity relations were collected, and then the tortuosity values were calculated for a one granular bed consisting of spherical particles with normal distribution of diameters. Information about the bed porosity and particle sizes was obtained from measurements conducted for an artificial granular bed, consisting of glass marbles. The results of calculations were compared with the results of two other methods of tortuosity determination, performed for the same case (details are not described in this paper): the first of them uses the Path Tracking Method, the second one – information about the velocity components in a creeping flow (the Lattice-Boltzmann Method was applied to obtain the velocity field in the flow). The main aim of our article was to test whether the functions linking tortuosity with porosity, which are available in the literature, give similar results as the methods described above. To achieve this aim, the relative errors between results of calculations for the collected formulas and values from the both previous mentioned methods were calculated.

Introduction

Tortuosity is one of the most important parameters describing the porous beds. Tortuosity τ [m/m] is defined as the ratio of the actual path length inside pore channels L_p [m] to the thickness of the porous medium L_0 [m] (BEAR 1972, DIAS et al. 2006).

$$\tau = \frac{L_p}{L_0} \quad (1)$$

Correspondence: Wojciech Sobieski, Katedra Mechaniki i Podstaw Konstrukcji Maszyn, Uniwersytet Warmińsko-Mazurski, ul. M. Oczapowskiego 11, 10-957 Olsztyn, phone: 89 523 32 40, e-mail: wojciech.sobieski@uwm.edu.pl.

The tortuosity term became widespread among others by Kozeny (KOZENY 1927, SOBIESKI 2014), who corrected the value of the hydraulic drop occurring during fluid flow through a porous body by using this parameter.

A popular relationship between tortuosity and velocity, was presented by Carman as a correction of the Kozeny formula (CARMAN 1937, SOBIESKI 2014). In a general case, the path length L_p in the formula (1) may be understood as a geometrical quantity (geometric tortuosity) or as a flow property (hydraulic tortuosity) – see Figure 1.

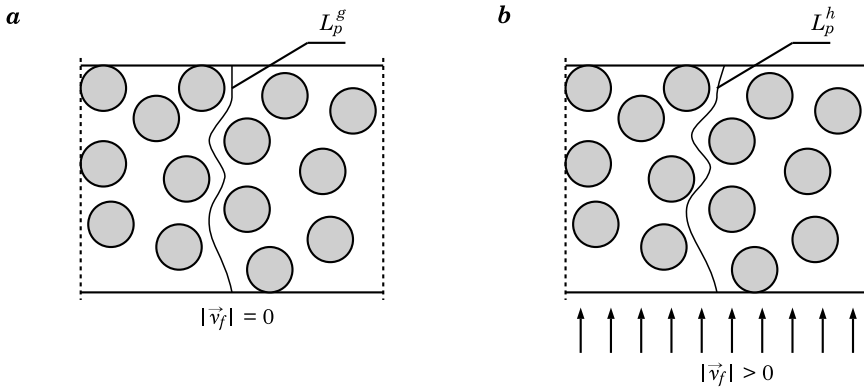


Fig. 1. The visualization of the tortuosity definition: *a* – geometric, *b* – hydraulic

The geometric tortuosity may be obtained in three different ways. The most common method is the use of a function linking it with other parameters characterizing geometry of the porous body. In this approach, it is usually assumed that the geometric tortuosity is a direct function of the porosity. In the literature, many functions may be found (derived empirically or analytically), where relationships between these quantities are proposed (YU, LI 2004, VALLABH 2009, AHMADI et al. 2014, ALLAN, SUN 2014, KONG et al. 2015). The second method involves the use of an experiment. Here, the computed tomography and image analysis (CT\IA) (WU et al. 2006, GOMMES et al. 2009, EBNER et al. 2013), acoustic methods (JOHNSON et al. 1982, KOCHAŃSKI et al. 2000, LI et al. 2010), optical methods (NWAIZU, ZHANG 2012), as well as the other methods (GAO et al. 2012) are used. In the third approach, the so-called Path Tracking Method (PTM) is used. In this method, the direction or shape of the porous space is tracked with the help of appropriate numerical algorithms (NAKASHIMA, KAMIYA 2007, STARLY et al. 2007, SOBIESKI et al. 2009). To reach it, firstly the geometry of the pore part is determined, and then its arrangement in the space is traced. When the path length L_p is known, the tortuosity may be finally calculated (SOBIESKI 2009, SOBIESKI, LIPIŃSKI 2013, SOBIESKI et al. 2016a, b).

The hydraulic tortuosity can be computed from fluid velocity fields. These fields may be obtained by means of the Computational Fluid Dynamics (CFD) method. The Lattice-Boltzmann Method (LBM) is the most popular (FENG et al. 2007, NABOVATI, SOUSA 2007, MATYKA et al. 2008, WANG 2014). Another possibility is the application of the Finite Volume Method (FVM) or the Immersed Boundary Method (IBM).

Our article is a direct continuation of the studies described in a monograph of SOBIESKI et al. (2016). In these studies, different experimental, analytical, as well as numerical tests (e.g. the Lattice Boltzmann Method and the Immersed Boundary Method) related to the same porous bed, consisting of glass marbles, were performed.

Review of the functions linking porosity with tortuosity

Table 1 shows a review of the functions which describe the porosity and tortuosity relation. Two main groups of correlation functions may be distinguished. The first group is intended for systems containing squares (in 2D

Table 1

Review of formulas for calculating the tortuosity

Source	Application	Formula
1	2	3
MAXWELL (1881) [ALLAN, SUN (2014)]	array of spheres in 3D, dilute suspension	$\tau = 1 + \frac{1}{2}(1 - e)$
RAYLEIGH (1892), [ALLAN, SUN (2014)]	array of cylinders in 2D	$\tau = 2 - e$
BARTELL, OSTERHOF (1928) [LANFREY et al. (2010), AHMADI et al. (2014)]	packed beds	$\tau = 0.5 \pi$
CARMAN (1937) [LANFREY et al. (2010), AHMADI et al. (2014)]	packed beds	$\tau = \sqrt{2}$
MACKIE, MEARES (1955) [ALLAN, SUN (2014)]	diffusion of electrolytes in membrane	$\tau = \left(\frac{2 - e}{e}\right)^2$
WEISSBERG (1963) [AHMADI et al. (2014), ALLAN, SUN (2014)]	bed of uniform spheres (applicable to overlapping, non-uniform spheres)	$\tau = 1 - 0.49 \ln e$
BEAR (1972) [DIAS et al. (2006, AHMADI et al. (2014), ALLAN, SUN (2014)]	granular beds	$\tau = \frac{1}{e^C}$, where C is a constant
KIM et al (1987) [ALLAN, SUN (2014)]	isotropic systems, $0 < e < 0.5$	$\tau = e^{-0.4}$

cont. Table 1

1	2	3
DU PLESSIS, MASLIYAH (1988), [AHMADI et al. (2014), ALLAN, SUN (2014)]	isotropic granular media	$\tau = \frac{e}{1 - (1 - e)^{2/3}}$
COMITI, RENAUD (1989) [TANG et al. (2012), AHMADI et al. (2014), ALLAN, SUN (2014)]	beds packed with spherical and cubic particles,	$\tau = 1 - C \ln e,$ where C is a constant (0.63 in TANG et al. (2012) for cubic particles, 0.41 in LANFREY et al. (2010) for packed beds)
IVERSEN, JØRGENSEN (1993) [AHMADI et al. (2014), ALLAN, SUN (2014)]	sandy marine sediments, $0.4 < e < 0.9$	$\tau = \sqrt{1 + 2(1 - e)}$
BOUDREAU (1996) [LANFREY et al. (2010), AHMADI et al. (2014), ALLAN, SUN (2014)]	packed beds	$\tau = \sqrt{1 - \ln(e^2)}$
KOPONEN et al. (1996) [TANG et al. (2012), AHMADI et al. (2014), ALLAN, SUN (2014)]	2D random overlapping mono-sized squares, $0.5 < e < 1$	$\tau = 1 + 0.8(1 - e)$
KOPONEN et al. (1997) [TANG et al. (2012), ALLAN, SUN (2014)]	2D random overlapping mono-sized squares, $0.4 < e < 0.9$	$\tau = 1 + 0.65 \frac{1 - e}{(e - 0.33)^{0.19}}$
YU, LI (2004) YU, LI (2004), TANG et al. (2012)]	2D square particles	$\tau = \frac{1}{2} \left[1 + \frac{\alpha}{2} + \alpha \frac{\sqrt{\left(\frac{1}{\alpha} - 1\right)^2 + \frac{1}{4}}}{1 - \alpha} \right]$ where $\alpha = \sqrt{1 - e}$
MATYKA et al. (2008) [KONG et al. (2015)]	2D random overlapping mono-sized squares	$\tau = 1 - 0.77 \ln(e)$
LANFREY et al. (2010) [LANFREY et al. (2010), ALLAN, SUN (2014)]	bed of spheres	$\tau = 1.23 \frac{(1 - e)^{4/3}}{e\phi^2}$ where ϕ is a shape factor
DUDA et al. (2011) [ALLAN, SUN (2014)]	2D freely overlapping squares	$\tau = 1 + (1 - e)^{1/2}$
PISANI (2011) [TANG et al. (2012), ALLAN, SUN (2014)]	random, partial overlapping shapes	$\tau = \frac{1}{1 - \phi(1 - e)},$ where ϕ is a shape factor (0.73 in TANG et al. (2012) for cubic particles)
TANG et al. (2012) [TANG et al. (2012)]	cubic particles	$\tau = \frac{3}{4} + \frac{1}{8} \sqrt{1 + \frac{1}{4} \frac{1 - e}{2 - e - 2\alpha}} +$ $+ \frac{1}{8} \sqrt{1 + \frac{1 - e}{2 - e - 2\alpha}} + \frac{1}{4} \sqrt{1 - e}$
LIU, KITANIDIS (2013) [ALLAN, SUN (2014)]	isotropic grain (spherical), staggered, $0.25 < e < 0.5$	$\tau = e^{0.28} + 0.15$

space), the second group applies to different granular beds (in 3D space). Formulas that may concern other cases are very rare. It is worth noting that besides the porosity, in some formulas, other quantities appear: a model constant or a factor related to the particle shape. In some cases, one equation may be used in both groups.

Determining the porosity of an artificial porous bed

Glass marbles (shown in Fig. 2a) were used in our investigations. An example of a granular bed consisting of such input material is shown in Figure 2b. The porosity of the bed was measured by using two graduated measuring cylinders with the volume of 250 ml. The first cylinder contained a bed sample; the second was filled with the distilled water. During the experiment, the water was slowly poured into the bed sample and the volume of pores was measured. The measurement was repeated 15 times, and in each case, the first cylinder was filled with new dry marbles. The obtained average porosity of the bed (a fraction of the volume of voids over the total volume) turned out to be equal to 0.41 ± 0.008 [-]. Obtained value is typical for loose random packing beds, which is 0.40-0.41 (RIBEIRO et al. 2010). It is worth mentioning that the obtained value is very close to the theoretical porosity (which is equal to 0.3954) of an orthorhombic system consisting of uniform spheres (COOKE, ROWE 1999).

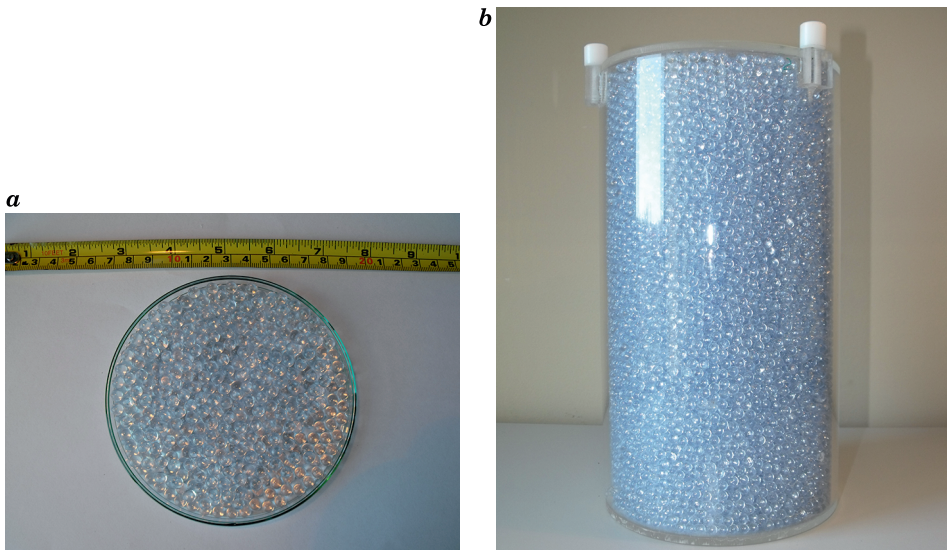


Fig. 2. The sample of glass marbles (a) and the exemplary granular bed (b)

The difference is caused by the fact that diameters in the artificial bed are not equal and the arrangement of the particles in the space is not regular.

In the next stage, 100 marbles were randomly chosen. The diameter of each marble in two random directions (perpendicular to each other) was measured with a micrometre screw with an accuracy of 0.01 mm. The average diameter of marbles was equal to 6.072 mm, with the standard deviation of 0.051 mm. The distribution of particle diameter is shown in Figure 3.

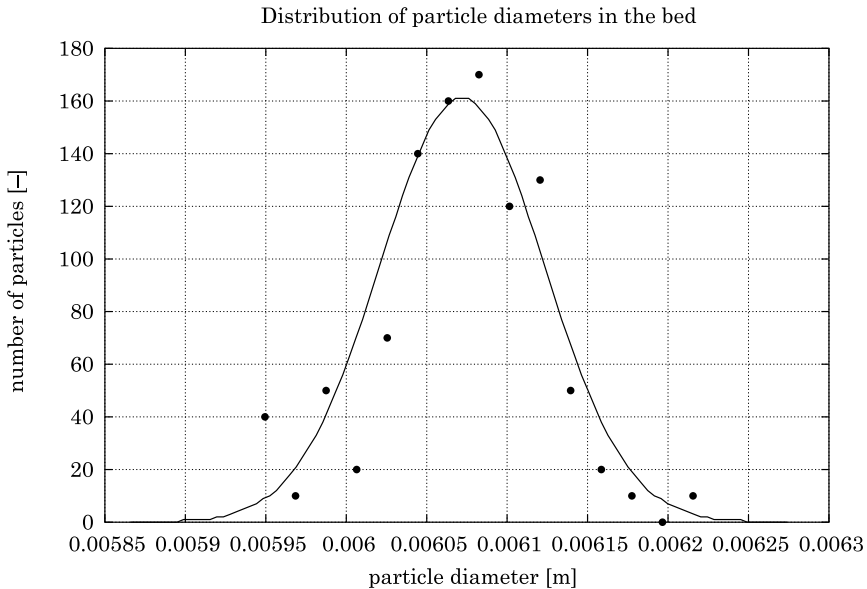


Fig. 3. The distribution of the particle diameter in the granular bed

Comparison

In the next stage of investigations, the tortuosity values for formulas collected in Table 1 and for porosity obtained in the experiment were calculated. Results of calculations are shown in Table 2. This table summarizes all results for comparison aims, although not all formulas are intended for granular beds. We can find some formulas give incorrect values. The formula (5) gives too high value of tortuosity while the formula (21) gives a non-physical result.

As it was mentioned above, the same porous bed as in our experiment, was earlier used for calculation of the geometric tortuosity with the Path Tracking Method (SOBIESKI 2009, SOBIESKI et al. 2012, *Pathfinder Project* 2013, SOBIESKI, LIPIŃSKI 2013, DUDDA, SOBIESKI 2014, SOBIESKI et al. 2016a,

Table 2

Results of calculations

No	Formula	Tortuosity	Application in the example
1	MAXWELL (1881)	1.2950	weak
2	RAYLEIGH (1892)	1.5900	not applicable
3	BARTELL, OSTERHOF (1928)	1.5708	strong
4	CARMAN (1937)	1.4142	strong
5	MACKIE, MEARES (1955)	15.0393	not applicable
6	WEISSBERG (1963)	1.4369	strong
7	BEAR (1972)	–	–
8	KIM et al (1987)	1.4285	unknown
9	DU PLESSIS, MASLIYAH (1988)	1.3826	strong
10	COMITI, RENAUD (1989)	1.3656 for C = 0.41	strong
11	IVERSEN, JØRGENSEN (1993)	1.4765	weak
12	BOUDREAU (1996)	1.6683	strong
13	KOPONEN et al. (1996)	1.4720	not applicable
14	KOPONEN et al. (1997)	1.6197	not applicable
15	YU, LI (2004)	1.6594	not applicable
16	MATYKA et al. (2008)	1.6865	not applicable
17	LANFREY et al. (2010)	1.4845 for $\phi = 1$	strong
18	DUDA et al (2011)	1.7681	not applicable
19	PISANI (2011)	1.4184 for $\phi = 1$	unknown
20	TANG et al. (2012)	1.2586 for C = 0.5	not applicable
21	LIU, KITANIDIS (2013)	0.9291	strong

Table 3

Relative errors

Formula number	τ	τ^g	τ^h	δ^g [%]	δ^h [%]
3	1.5708	1.205	1.24	30.36	26.68
4	1.4142	1.205	1.24	17.36	14.05
6	1.4369	1.205	1.24	19.24	15.88
9	1.3826	1.205	1.24	14.74	11.50
10	1.3656	1.205	1.24	13.33	10.13
12	1.6683	1.205	1.24	38.45	34.54
17	1.4845	1.205	1.24	23.20	19.72

b) as well as for calculation of the hydraulic tortuosity by application of the Lattice-Boltzmann Method. In the first method, the tortuosity value was equal to 1.205, whereas in the second method to 1.24. Both values are smaller than

all values presented in the Table 2 (besides the 21). The relative errors δ are shown in the Table 3. Geometric tortuosity τ^g and hydraulic tortuosity τ^h obtained in the former investigations were used as the reference values.

It can be assumed that the difference between the results obtained from the collected set of formulas and results of previous investigations may be caused by deviation of the particle diameters. The example presented above shows that the particles have normal distribution, but the variance is comparatively small. In many artificial beds, the diversity of particle sizes is much larger. Therefore, the formulas collected in Table 1 (obtained empirically in many cases) give higher values of tortuosity. In our opinion, this is due to the reasons described below.

When particles have different diameters, the shape of the pore space between them is more complicated. In consequence, sometimes the path may find a shorter way, but sometimes in turn it must omit the larger particles (as shown in Fig. 4). There is no doubt that it leads to a greater deviation of tortuosity values, but it is difficult to state at the current stage, which mechanism is the dominant one and so, whether the increase of the deviation of particles diameters is associated with an increase or a decrease in the average value of tortuosity in the bed. The problem of influence of the particle distribution on the path length is open and further studies are needed in this field.

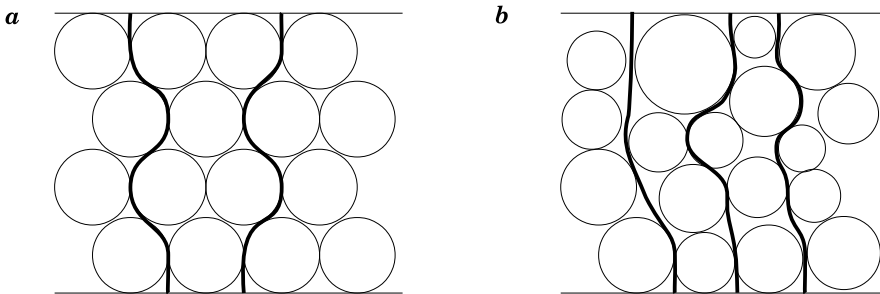


Fig. 4. Influence of the particle distribution on the path length for constant diameters (a) and diverse diameters (b)

Taking into account the fact that particle sizes in an artificial bed may be different, the porosity-tortuosity relations should have a more general form

$$\tau = f(e) \cdot f(\mu, \sigma^2) \quad (2)$$

or

$$\tau = f(e, \mu, \sigma^2) \quad (3)$$

where:

- $f(e)$ – a function linking porosity and tortuosity for a bed consisting of particles with constant diameter,
- $f(\mu, \sigma^2)$ – a correction function dependent on the average value and on its variance.

Summary and conclusions

The following conclusions can be formulated based on the above-discussed topics:

- Different mathematical formulas for determining the tortuosity may be found in the literature, but they give different results for the same data. Only for formulas designed for granular beds, the tortuosity value is within the range from 1.3654 to 1.6683. The relative error between these results is almost 20%, what is quite significant.

- In practice, it is impossible to indicate which equation in the Table 1 should be used in a specific case. Finding the next formulas does not solve this problem.

- Differences between tortuosity values obtained earlier (using the Path Tracking Method and the Lattice Boltzmann Method) and porosity-tortuosity functions available in the literature occur probably because the particle diameters in a artificial bed are not constant but they have a specific distribution.

- It can be assumed that tortuosity is probably higher in beds with higher deviation, than in beds where the particle diameters are constant.

- If the particle sizes in a granular bed are different, the porosity-tortuosity correlation functions should be corrected, for example by using a function dependent on the mean value and its variance. In this field, next investigations are needed.

References

- ALLEN R., SUN S. 2014. *Investigating the role of tortuosity in the Kozeny-Carman equation*. International Conference on Numerical and Mathematical Modeling of Flow and Transport in Porous Media, Dubrovnik, Croatia, 29 September – 3 October.
- AHMADI M.M., MOHAMMADI S., HAYATI A.N. 2011. *Analytical derivation of tortuosity and permeability of monosized spheres: A volume averaging approach*. Physical Review E., (83): 026312.
- BEAR J. 1972. *Dynamics of Fluids in Porous Media*. Courier Dover Publications, New York.
- CARMAN P.C. 1997. *Fluid Flow through a Granular Bed*. Transactions of the Institute of Chemical Engineers, Jubilee Supplement, (75): 32–48.
- COOKE A.J., ROWE R.K. 1999. *Extension of Porosity and Surface Area Models for Uniform Porous Media*. Journal of Environmental Engineering, 125(2): 126–136.

- DIAS R.P., TEIXEIRA J.A., MOTA M., YELSHIN A. 2006. *Tortuosity variation in a low density binary particulate bed*. Separation and Purification Technology, 51(2): 180–184.
- DUDDA W., SOBIESKI W. 2014. *Modification of the PathFinder algorithm for calculating granular beds with various particle size distributions*. Technical Sciences, 17(2): 135–148.
- EBNER M., CHUNG D.-W., GARCIA R.E., WOOD V. 2013. *Tortuosity Anisotropy in Lithium-Ion Battery Electrodes*. Advanced Energy Materials, 4(5): 1301278.
- FENG Y.T., HAN K., OWEN D.R.J. 2007. *Coupled lattice Boltzmann method and discrete element modelling of particle transport in turbulent fluid flows: Computational issues*. International Journal for Numerical Methods in Engineering, 72(9): 1111–1134.
- GAO H.-Y., HE Y.-H., ZOU J., XU N.-P., LIU C.T. 2012. *Tortuosity factor for porous FeAl intermetallics fabricated by reactive synthesis*. Transactions of Nonferrous Metals Society of China, 22(9): 2179–2183.
- GOMMES C.J., BONS A.J., BLACHER S., DUNSMUIR J.H., TSOU A.H. 2009. *Practical methods for measuring the tortuosity of porous materials from binary or gray-tone tomographic reconstructions*. American Institute of Chemical Engineers (AIChE) Journal, 55(8): 2000–2012.
- JOHNSON D.L., PLONA T.J., SCALA C., PASIERB F., KOJIMA H. 1982. *Tortuosity and Acoustic Slow Waves*. Physical Review Letters, 49(25): 1840–1844.
- KOCHAŃSKI J., KACZMAREK M., KUBIK J. 2000. *Determination of permeability and tortuosity of permeable media by ultrasonic method. Studies for sintered bronze*. Journal of Theoretical and Applied Mechanics, 1(39): 923–928.
- KONG W., ZHANG Q., GAO X., ZHANG J., CHEN D., SU S. 2015. *A Method for Predicting the Tortuosity of Pore Phase in Solid Oxide Fuel Cells Electrode*. International Journal of Electrochemical Science, 10(1): 5800–5811.
- KOZENY J. 1927. *Über kapillare Leitung des Wassers im Boden*. Akademie der Wissenschaften in Wien, Sitzungsberichte, 136(2a): 271–306.
- LANFREY P.-Y., KUZELJEVIC Z.V., DUDUKOVIC M.P. 2010. *Tortuosity model for fixed beds randomly packed with identical particles*. Chemical Engineering Science, 65: 1891–1896.
- LE L.H., ZHANG C., TA D., LOU E. 2010. *Measurement of tortuosity in aluminum foams using airborne ultrasound*. Ultrasonics, 50(1): 1–5.
- MATYKA M., KHALILI A., KOZA Z. 2008. *Tortuosity-porosity relation in porous media flow*. Physical Review E., 78: 026306.
- NABOVATI A., SOUSA A.C.M. 2007. *Fluid flow simulation in random porous media at pore level using the Lattice Boltzmann Method*. Journal of Engineering Science and Technology, 2(3): 226–237.
- NAKASHIMA Y., KAMIYA S. 2007. *Mathematica Programs for the Analysis of Three-Dimensional Pore Connectivity and Anisotropic Tortuosity of Porous Rocks using X-ray Computed Tomography Image Data*. Journal of Nuclear Science and Technology, 44(9): 1233–1247.
- NWAIZU C., ZHANG Q. 2012. *Characterizing Airflow paths in Grain bulks*. Paper NABEC/CSBE. Northeast Agricultural & Biological Engineering Conference Canadian Society for Bioengineering Lakehead University, Orillia, Ontario July 15–18.
- Pathfinder Project [on-line]. 2013. University of Warmia and Mazury in Olsztyn <http://www.uwm.edu.pl/pathfinder/index.php> (access: 7.02.2014).
- RIBEIRO A.M., NETO P., PINHO C. 2010. *Mean Porosity and Pressure Drop Measurements in Packed Beds of Monosized Spheres: Side Wall Effects*. International Review of Chemical Engineering, 2(1): 40–46.
- SOBIESKI W. 2009. *Calculating tortuosity in a porous bed consisting of spherical particles with known sizes and distribution in space*. Research report 1/2009, Winnipeg (Canada).
- SOBIESKI W. 2014. *The quality of the base knowledge in a research process*. Scientific Researches in the Department of Mechanics and Machine Design, University of Warmia and Mazury in Olsztyn, 2: 29–47.
- SOBIESKI W., DUDDA W., LIPIŃSKI S. 2016a. *A new approach for obtaining the geometric properties of a granular porous bed based on DEM simulations*. Technical Sciences, 19(2): 165–187.
- SOBIESKI W., LIPIŃSKI S. 2013. *PathFinder User's Guide*. University of Warmia and Mazury in Olsztyn. <http://www.uwm.edu.pl/pathfinder/index.php> (access: 7.02.2014).
- SOBIESKI W., LIPIŃSKI S., DUDDA W., TRYKOZKO A., MAREK M., WIĄCEK J., MATYKA M., GOŁĘBIEWSKI J. 2016b. *Granular Porous Media*. Department of Mechanics and Machine Design, University of Warmia and Mazury, Olsztyn.

- SOBIESKI W., ZHANG Q., LIU C. 2012. *Predicting Tortuosity for Airflow through Porous Beds Consisting of Randomly Packed Spherical Particles*. *Transport in Porous Media*, 93(3): 431–451.
- STARLY B., YILDIRIM E., SUN W. 2007. *A tracer metric numerical model for predicting tortuosity factors in three-dimensional porous tissue scaffolds*. *Computer Methods and Programs in Biomedicine*, 87(1): 21–27.
- TANG X.-W., SUN Z.-F., CHENG G.C. 2012. *Simulation of the relationship between porosity and tortuosity in porous media with cubic particles*. *Chinese Physics B*, 21(10): 100201.
- WANG P. 2014. *Lattice Boltzmann Simulation of Permeability and Tortuosity for Flow through Dense Porous Media*. *Mathematical Problems in Engineering*, Article ID 694350.
- WU Y.S., VAN VLIET L.J., FRIJLINK H.W., VAN DER VOORT MAARSCHALK K. 2006. *The determination of relative path length as a measure for tortuosity in compacts using image analysis*. *European Journal of Pharmaceutical Sciences*, 28(5): 433–440.
- VALLABH R. 2009. *Modeling Tortuosity in Fibrous Porous Media using Computational Fluid Dynamics*. PhD Thesis, North Carolina State University, Raleigh, United States.
- YU B.M., LI J.H. 2004. *A geometry model for tortuosity of flow path in porous media*. *Chinese Physics Letter*, 21(8): 1569–1571.



Quarterly peer-reviewed scientific journal

ISSN 1505-4675
e-ISSN 2083-4527

TECHNICAL SCIENCES

Homepage: www.uwm.edu.pl/techsci/



UNSTEADY HYDROMAGNETIC FLOW OF OLDROYD-B FLUID OVER AN OSCILLATORY STRETCHING SURFACE: A MATHEMATICAL MODEL

*Sami Ullah Khan*¹, *Nasir Ali*²

¹ Department of Mathematics, Comsats Institute of Information Technology, Pakistan

² Department of Mathematics and Statistics, International Islamic University, Pakistan

Received 16 April 2016, accepted 27 January 2017, available online 30 January 2017.

Key words: Oldroyd-B fluid, oscillatory stretching sheet, homotopy analysis method.

Abstract

In the present work, we have studied an unsteady, two-dimensional boundary layer flow of a magnetohydrodynamics (MHD) Oldroyd-B fluid over an oscillatory stretching surface. The problem is modeled by using constitutive equations. The number of independent variables in the governing equations are reduced by using appropriate dimensionless variables. The analytical solution is computed by using homotopy analysis method. The influences of various physical parameters such as Deborah numbers, ratio of angular frequency to stretching rate parameter and Hartmann number on time-series of velocity and transverse velocity profiles at different time instants are investigated and discussed quantitatively with the help of various graphs. It is observed that amplitude of velocity increases by increasing ratio of oscillating frequency to stretching rate parameter while decreases by increasing Hartmann number. It is further observed that the magnitude of velocity decreases by increasing Hartmann number and Deborah numbers in the terms of relaxation time parameter.

Introduction

The analysis of boundary layer flow caused by moving stretching surface has promising applications in many industrial and technological processes. These applications include metal spinning, metal extrusion, glass blowing, artificial fibers, filaments and wires and many more. Several authors have investigated the boundary layer flow of viscous fluids over stretching surfaces.

Correspondence: Sami Ullah Khan, Department of Mathematics, Comsats Institute of Information Technology, Sahiwal 57000, Pakistan, e-mail: sk_iiu@yahoo.com

CRANE (1970) computed an exact analytic solution of a viscous fluid over a linearly stretching surface. POP et al. (1996) investigated the unsteady boundary layer flow of viscous fluid over stretching surface. VARSHNEY (1979) discussed the fluctuating flow of viscous fluid over a saturated porous plate. WANG (1988) analyzed the boundary layer flow of viscous fluid over an oscillatory stretching surface by using perturbation technique. MUKHOPADHYAY et al. (2013) computed numerical solution of boundary layer flow of a Maxwell fluid over a stretching permeable surface in the presence of thermal radiation. ABBAS et al. (2009) discussed the two-dimensional boundary layer flow of a viscous fluid over an oscillatory stretching surface. ELSHEHAWAY et al. (2003) studied the effects of inclined magnetic field on the magneto fluid flow through a porous medium between two inclined wavy porous plates.

The study of hydromagnetic flow has engaged the attention of scientists and engineering due to its promising applications in the hydrodynamic processes and in the field of chemistry, physics, polymer industry and metallurgy. The electrically conducting fluid under the influence of magnetic field has prime importance in the cooling process to control the rate of cooling. Having such salient features in mind, many authors studied the MHD flows in different flow configurations (HAYAT et al. 2015, RAJU et al. 2015, ABBAS 2008).

In past few years, the study of non-Newtonian fluids has received much attention of engineers and scientists because of their practical applications in chemical and nuclear industries, polymer solutions, bioengineering engineering etc. It is well established fact that nonlinear fluids obey nonlinear relationship between shear stress and rate of deformation. Among these nonlinear fluids, Oldroyd-B fluid is the class of fluids that attracted the attentions of researchers in recent times. Oldroyd-B fluid model is one of the models which exhibit the relaxation and retardation time effects. The literature survey shows that much attention is given on steady flow of Oldroyd-B fluid over a stretching sheet. We highlight some of them. RAJAGOPAL and BHATNAGAR (1995) studied the flow of an Oldroyd-B fluid over an infinite porous plate by computing asymptotically decaying solution. SAJID et al. (2010) presented the numerical solution for two-dimensional boundary flow of an incompressible Oldroyd-B fluid over a stretching surface. Later on, HAYAT et al. (2014) investigated the three dimensional flow and heat transfer of an Oldroyd-B fluid over a bidirectional stretching surface. In another paper, HAYAT et al. (2015) used homotopy analysis method to discuss the mixed convection flow of an Oldroyd-B fluid in a doubly stratified surface. ZHENG et al. (2011) computed exact solution of generalized Oldroyd-B over accelerating infinite plate.

In all above mentioned studies, the authors studied the steady flow of Oldroyd-B fluid in the given geometries. The aim of present work is to

investigate an unsteady boundary layer flow of an Oldroyd-B fluid in presence of uniform magnetic field. The flow is induced by an oscillatory stretching sheet which stretched and oscillates periodically in its own plane. The consideration unsteady flow of Oldroyd-B fluid and magnetic field effects makes the study quite versatile and general. The results of important studies carried out previously (WANG 1988, ABBAS et al. 2008, HAYAT et al. 2010, TURKYILMAZOGLU 2013, ZHENG et al. 2013, ALI 2015, SHEIKH, ABBAS 2015, ALI et al. 2016) and can be found from this study. The dimensionless partial differential equations are solved analytically by using well known homotopy analysis method (LIAO 2004, ABBASBANDY 2007, TURKYILMAZOGLU 2009, 2012). Graphical results illustrating the behavior of velocity is shown and discussed in detail.

Mathematical Model

The flow analysis is based on the following laws.

Law of conservation of mass:

$$\operatorname{div} \mathbf{V} = 0 \quad (1)$$

Law of conservation of momentum:

$$\rho \frac{d\mathbf{V}}{dt} = \operatorname{div} \mathbf{T} + \mathbf{J} \cdot \mathbf{B} \quad (2)$$

where \mathbf{V} is the velocity vector, \mathbf{J} is the current density, \mathbf{B} is the magnetic flux vector, ρ is the density of the fluid, \mathbf{T} is the Cauchy stress tensor, d/dt represents the material derivative. We define Cauchy stress tensor

$$\mathbf{T} = -p\mathbf{I} + \mathbf{S} \quad (3)$$

where \mathbf{S} is the extra stress tensor which satisfies the following relation (HAYAT 2015):

$$\mathbf{S} + \lambda_1 \frac{D\mathbf{S}}{Dt} = \mu \left(\mathbf{A} + \lambda_2 \frac{D\mathbf{A}}{Dt} \right) \quad (4)$$

where

$$\frac{D\mathbf{S}}{Dt} = \frac{d\mathbf{S}}{dt} - \mathbf{S}\mathbf{L} - \mathbf{L}^*\mathbf{S}, \text{ for a second order tensor} \quad (5)$$

In above equations λ_1 is the relaxation time, λ_2 is the retardation time, μ is the dynamic viscosity, $*$ denotes the matrix transpose and \mathbf{A}_1 is the first Rivlin-Ericksen tensor which is defined as

$$\mathbf{A}_1 = \nabla \mathbf{V} + \nabla \mathbf{V}^* \quad (6)$$

The current density \mathbf{J} appeared in Eq. (2) is defined as

$$\mathbf{J} = \sigma (\mathbf{V} \cdot \mathbf{B}) \quad (7)$$

in which σ is the electrical conductivity.

Flow Analysis

We consider a two-dimensional and incompressible flow of electrically conducting Oldroyd-B fluid over an oscillatory stretching surface (at $\bar{y} = 0$) and fluid occupy the space $\bar{y} > 0$. We choose a cartesian coordinate system (\bar{x}, \bar{y}) . It is assumed that the sheet is stretched with velocity $u_w = b\bar{x} \sin \omega t$ (b is the stretching rate and ω is the angular frequency) in \bar{x} - direction under the action of two equal and opposite forces. Further, external magnetic field of constant magnitude B_0 is imposed in \bar{y} direction and effects of induced magnetic field are neglected under the assumption of very large magnetic diffusivity.

For flow under consideration, the appropriate velocity field is

$$\mathbf{V} = [u(\bar{x}, \bar{y}, t), v(\bar{x}, \bar{y}, t), 0] \quad (8)$$

where u and v represents the velocity components along \bar{x} and \bar{y} directions, respectively. Inserting Eq. (8) in Eqs. (1)–(7) and employing boundary layer approximations, we get the following equations

$$\frac{\partial u}{\partial \bar{x}} + \frac{\partial v}{\partial \bar{y}} = 0 \quad (9)$$

$$\begin{aligned} \frac{\partial u}{\partial t} + u \frac{\partial u}{\partial \bar{x}} + v \frac{\partial u}{\partial \bar{y}} + \lambda_1 \left(\frac{\partial^2 u}{\partial t^2} + 2u \frac{\partial^2 u}{\partial t \partial \bar{x}} + 2v \frac{\partial^2 u}{\partial t \partial \bar{y}} + u^2 \frac{\partial^2 u}{\partial \bar{x}^2} + v^2 \frac{\partial^2 u}{\partial \bar{y}^2} + 2uv \frac{\partial^2 u}{\partial \bar{x} \partial \bar{y}} \right) = \\ v \frac{\partial^2 u}{\partial \bar{y}^2} + v \lambda_2 \left(\frac{\partial^3 u}{\partial t \partial \bar{y}^2} + u \frac{\partial^3 u}{\partial \bar{x} \partial \bar{y}^2} + v \frac{\partial^3 u}{\partial \bar{y}^3} - \frac{\partial u}{\partial \bar{x}} \frac{\partial^2 u}{\partial \bar{y}^2} - \frac{\partial u}{\partial \bar{y}} \frac{\partial^2 v}{\partial \bar{y}^2} \right) - \frac{\sigma B_0^2}{\rho} \left(u + \lambda_1 \frac{\partial u}{\partial t} + v \lambda_1 \frac{\partial u}{\partial \bar{y}} \right) \end{aligned} \quad (10)$$

where ν represents the kinematic viscosity. Eq. (10) is subjected to the following boundary conditions

$$u = u_\omega = b\bar{x} \sin \omega t, v = 0, \text{ at } \bar{y} = 0, t > 0 \quad (11)$$

$$u \rightarrow 0, \frac{\partial u}{\partial \bar{y}} \rightarrow 0 \text{ as } \bar{y} \rightarrow \infty \quad (12)$$

We introduce following dimensionless variables (WANG 1988)

$$y = \sqrt{\frac{b}{\nu}} \bar{y}, \quad \tau = t\omega, \quad u = b\bar{x}f_y(y, \tau), \quad v = -\sqrt{\nu b} f(y, \tau) \quad (13)$$

The continuity Eq. (9) is identically satisfied and Eq. (10) reduces to

$$\begin{aligned} f_{yyy} + (1 + M\beta_1) ff_{yy} - S(1 + \beta_1 M) f_{y\tau} - Mf_y - f_y^2 \\ -\beta_1(S^2 f_{y\tau\tau} + 2S(f_y f_{y\tau} - ff_{yy\tau}) + f^2 f_{yyy} - 2ff_y f_{yy}) + \beta_2(Sf_{yyy\tau} + f_{yy}^2 - ff_{yyyy}) = 0 \end{aligned} \quad (14)$$

The boundary conditions in dimensionless form are

$$f_y(0, \tau) = \sin \tau, f(0, \tau) = 0 \quad (15)$$

$$f_y(\infty, \tau) \rightarrow 0, f_{yy}(\infty, \tau) \rightarrow 0 \quad (16)$$

where $\beta_1 = \lambda_1 b$ and $\beta_2 = \lambda_2 b$ are the dimensionless Deborah numbers in the terms of relaxation and retardation times, respectively, $S = \omega/b$ is the ratio of oscillating frequency to stretching rate parameter and $M = \sqrt{\sigma B_0^2 / \rho b}$ is the Hartmann number.

Series solution by homotopy analysis method

To start our simulation via the homotopy analysis method, we suggest the following initial guess for velocity profile

$$f_0(y, \tau) = \sin \tau(1 - \exp(-y)) \quad (17)$$

with linear operator

$$\mathcal{L}_f = \frac{\partial^3}{\partial y^3} - \frac{\partial}{\partial y} \tag{18}$$

with property

$$\mathcal{L}_f [C_1 + C_2 \exp(y) + C_3 \exp(-y)] = 0 \tag{19}$$

where C_i ($i = 1,2,3$) are arbitrary constants.

Zerth-order deformation problems

The zeroth-order deformation for given problem is constructed as

$$(1 - p) \mathcal{L}_f [\hat{f}(y, \tau, p) - f_0(y, \tau)] = ph_f N_f [\hat{f}(y, \tau, p)] \tag{20}$$

$$\hat{f}(0, \tau, p) = 0, \left. \frac{\partial \hat{f}(y, \tau, p)}{\partial y} \right|_{y=0} = \sin \tau, \left. \frac{\partial \hat{f}(y, \tau, p)}{\partial y} \right|_{y=0} = 0, \left. \frac{\partial^2 \hat{f}(y, \tau, p)}{\partial y^2} \right|_{y=\infty} = 0 \tag{21}$$

where $p \in [0,1]$ is an embedding parameter. The associated nonlinear operator N_f is

$$\begin{aligned} N_f [\hat{f}(y, \tau, p)] &= \frac{\partial^3 \hat{f}(y, \tau, p)}{\partial y^3} - S(1 + \beta_1 M) \frac{\partial^2 \hat{f}(y, \tau, p)}{\partial y \partial \tau} + \\ &+ S(1 + \beta_1 M) \hat{f}(y, \tau, p) \frac{\partial^2 \hat{f}(y, \tau, p)}{\partial y^2} \\ &- M \frac{\partial \hat{f}(y, \tau, p)}{\partial y} - \left(\frac{\partial \hat{f}(y, \tau, p)}{\partial y} \right)^2 \end{aligned} \tag{22}$$

$$\begin{aligned} -\beta_1 &\left(S^2 \frac{\partial^3 \hat{f}(y, \tau, p)}{\partial \tau^2 \partial y} + 2S \left(\frac{\partial \hat{f}(y, \tau, p)}{\partial y} \frac{\partial^2 \hat{f}(y, \tau, p)}{\partial y \partial \tau} - f \frac{\partial^3 \hat{f}(y, \tau, p)}{\partial y^2 \partial \tau} \right) \right) \\ &+ \hat{f}^2(y, \tau, p) \frac{\partial^3 \hat{f}(y, \tau, p)}{\partial y^3} - 2 \hat{f}(y, \tau, p) \frac{\partial \hat{f}(y, \tau, p)}{\partial y} \frac{\partial^2 \hat{f}(y, \tau, p)}{\partial y} \\ &+ \beta_2 \left(S \frac{\partial^4 \hat{f}(y, \tau, p)}{\partial y^3 \partial \tau} + \left(\frac{\partial^2 \hat{f}(y, \tau, p)}{\partial y^2} \right)^2 - \hat{f}(y, \tau, p) \frac{\partial^4 \hat{f}(y, \tau, p)}{\partial y^4} \right) \end{aligned}$$

The zeroth-order deformation problems defined above have the following solutions corresponding to $p = 0$ and $p = 1$

$$\hat{f}(y, \tau, 0) = f_0(y, \tau), \hat{f}(y, \tau, 1) = f(y, \tau) \tag{23}$$

Using Taylor’s series expansion, we can write

$$\hat{f}(y, \tau, p) = f_0(y, \tau) + \sum_{m=1}^{\infty} f_m(y, \tau) = \frac{1}{m!} \left. \frac{\partial^m \hat{f}(y, \tau, p)}{\partial p^m} \right|_{p=0} \tag{24}$$

The convergence of above series solution depends upon h_f . We assume that h_f is selected so that Eq. (24) converges at $p = 1$. Therefore

$$f(y, \tau) = f_0(y, \tau) + \sum_{m=1}^{\infty} f_m(y, \tau) \tag{25}$$

***m*th-order deformation problems**

$$\mathcal{L}_f [f_m(y, \tau) - \chi_m f_{m-1}(y, \tau)] = h_f R_m^f(y, \tau) \tag{26}$$

$$f_m(0, \tau) = 0, \frac{\partial f_m(0, \tau)}{\partial y} = 0, \frac{\partial f_m(\infty, \tau)}{\partial y} = 0, \frac{\partial^2 f_m(\infty, \tau)}{\partial y^2} = 0 \tag{27}$$

$$\begin{aligned} R_m^f(y, \tau) = & \frac{\partial f_{m-1}}{\partial y^3} - S(1 + M\beta_1) \frac{\partial^2 f_{m-1}}{\partial y \partial \tau} - M \frac{\partial f_{m-1}}{\partial y} + (1 + M\beta_1) \sum_{k=0}^{m-1} \left(f_{m-1-k} \frac{\partial^2 f_k}{\partial y^2} \right) \\ & - \beta_1 S^2 \frac{\partial^3 f_{m-1}}{\partial y \partial \tau^2} + \beta_2 S \frac{\partial^4 f_{m-1}}{\partial y^3 \partial \tau} - 2S\beta_1 \sum_{k=0}^{m-1} \left(\frac{\partial f_{m-1-k}}{\partial y} \frac{\partial^2 f_k}{\partial y \partial \tau} - f_{m-1-k} \frac{\partial^3 f_k}{\partial y^2 \partial \tau} \right) \\ & - \beta_1 \sum_{k=0}^{m-1} f_{m-1-k} \sum_{l=0}^{m-1} f_{k-1} \frac{\partial^3 f_l}{\partial y^3} + 2\beta_1 \sum_{k=0}^{m-1} f_{m-1-k} \sum_{l=0}^{m-1} \frac{\partial f_{k-l}}{\partial y} \frac{\partial^2 f_l}{\partial y^2} + \beta_2 \sum_{m=0}^{m-1} \frac{\partial f_{m-l-k}}{\partial y^2} \frac{\partial^2 f_k}{\partial y^2} \\ & - \beta_2 \sum_{k=0}^{m-1} f_{m-1-k} \frac{\partial^4 f_k}{\partial y^4} \end{aligned} \tag{28}$$

Here χ_m is defined as

$$\chi_m = \begin{cases} 0, & m \leq 1, \\ 1, & m > 1. \end{cases}$$

The general solution at m th-order deformation Eq. (26) can be defined as

$$f_m(y, \tau) = f_m^*(y, \tau) + C_1 + C_2 \exp(y) + C_3 \exp(-y) \quad (29)$$

where $f_m^*(y, \tau)$ represent the special solution.

Convergence of HAM Solution

The proper choice of the auxiliary parameters h_f is important for convergence of the HAM solution. For a particular set of parameters, the convergence region can be obtained by plotting the so-called h -curves. Figure 1 presents the regions for plausible values of h_f for a given set of parameter. From figure, it is clear that convergent solution can be obtained when $-1.5 \leq h_f \leq 0$. Tables 1 and 2 show a comparison of numerical values of $f_m^*(0, \tau)$ with the already reported values in refs. TURKYILMAZOGLU (2013), HAYAT et al. (2010), ZHENG et al. (2013), ABBAS et al. (2008). It is observed that our results are in excellent agreement with the already available results. This testifies the validity of our solution and the graphical results presented in the subsequent section.

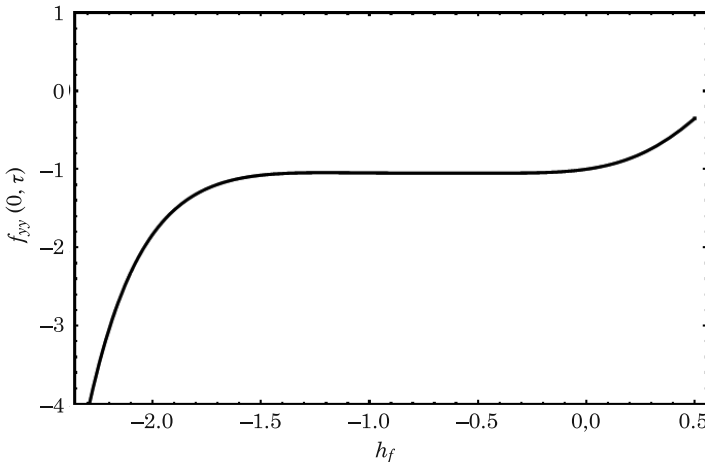


Fig. 1. h -curve for velocity profile at 8th order of approximation with $M = 0.1$, $S = 0.2$, $\beta_1, \beta_2 = 0.1$, $\tau = 0.5\pi$

Table 1

A comparison of values of $f^*(0, \tau)$ with the existing ones reported in Refs ZHENG et al. (2013), ABBAS et al. (2008)

S	M	τ	ZHENG et al. (2013)	ABBAS et al. (2008)	Present results $\beta_1 = \beta_2 = 0$
1.0	12	1.5π	11.678565	11.678656	11.678565
		5.5π	11.678706	11.678707	11.678706
		9.5π	11.678656	11.678656	11.678656

Table 2

A comparison of values of $f^*(0, \tau)$ for different values of M with the existing ones reported in Refs TURKYILMAZOGLU (2013), HAYAT (2010)

M	HAYAT (2010)	TURKYILMAZOGLU (2013)	Present results $\beta_1 = \beta_2 = S = 0, \tau = \pi / 2$
0	-1.000000	-1.00000000	-1.000000
0.5	-1.224747	-1.22474487	-1.224747
1.0	-1.414217	-1.41421356	-1.414217
1.5	-1.581147	-1.58113883	-1.581147
2.0	-1.732057	-1.73205081	-1.732057

Results and discussion

The analytical procedure explained in the previous section is adopted for the solution of the Eq. (14) with boundary conditions (15) and (16). The aim of this section is to present the graphical results and their interpretation. For this purpose, the effects of various parameters like Deborah numbers β_1 and β_2 ratio of angular frequency to stretching rate S and Hartmann number M on velocity profile are shown graphically.

Figure 2a-d presents the effects of Deborah numbers (β_1, β_2), Hartmann number M and ratio of angular frequency to stretching rate S on time-series of the velocity profile f' . The effects of Deborah number β_1 on the time-series of velocity profile f' is shown in Figure 2a. It is observed that the amplitude of the velocity decreases with increasing Deborah number β_1 . It is due to the fact that β_2 contains relaxation time which provides the resistance to the flow due to viscoelastic properties of the fluid. The variation of the time-series of the velocity profile with time τ for various values of β_2 is presented in Figure 2b. As expected, opposite behavior is observed as compared with Figure 2a i.e., the velocity decreases with increasing β_2 . Figure 2c illustrates the effects of ratio of angular frequency to stretching rate S on the time-series of the velocity by keeping $M = 0.5, \beta_1 = 1, \beta_2 = 0.5$. It is observed that an increase in

S results in a pronounced phase shift and rise in the amplitude of oscillations. Figure 2d displays the effects of Hartmann number on time-series of velocity profile. It is observed that the amplitude of velocity decreases with increasing Hartmann number. Such effects are expected because the fact that magnetic force produces a Lorentz force which act as resistance to amplitude of flow velocity.

Figure 3a, b displays the effect of Deborah number β_1 on the transverse profile of the velocity at two different time instants $\tau = 8.5\pi$ and $\tau = 9.5\pi$. Figure 2a reveals that at time instant $\tau = 8.5\pi$ the velocity decreases from unity to zero inside the boundary layer. The suppression of amplitude is a direct consequence of the elastic nature of fluid. Moreover, an increase in β_1 results in decrease in the momentum boundary layer thickness. Figure 3b shows the influence of β_1 at time instant $\tau = 9.5\pi$. Due to increase in β_1 the velocity of the fluid decreases and ultimately decreases the momentum boundary layer thickness.

The variation of transverse profile of velocity for various values of β_2 at two different time instants $\tau = 8.5\pi$ and $\tau = 9.5\pi$ is shown in Figure 4a, b. The transverse profiles of velocity illustrating the effects of β_2 at time instant $\tau = 8.5\pi$ are plotted in Figure 4a. It is observed that the magnitude of the velocity increases by increases β_2 . It can be justified physically as β_2 is associated with retardation time which increases with increase of β_2 . This increase in retardation time is responsible to increase the velocity of the fluid. Similarly at time instant $\tau = 9.5\pi$ the velocity increases from at the wall to zero far away from the surface. The momentum boundary layer thickness also increases at this time instant.

Figure 5a and b demonstrates the effect of Hartmann number on the velocity profile at $\tau = 8.5\pi$ and $\tau = 9.5\pi$, respectively. It is found that an increase in the Hartmann number M results in decrease in the velocity profile at both time instants. In fact the application of magnetic force produces a resistive force known as Lorentz force which has tendency to oppose the amplitude of the velocity. The effects of ratio of oscillating frequency to stretching rate parameter S on transverse profile of velocity at two different time instants $\tau = 8.5\pi$ and $\tau = 9.5\pi$ are shown in Figure 6a and b. From Figure 6a, it is clear at time instant $\tau = 8.5\pi$ the velocity profile increases with increasing ratio of oscillating frequency to stretching rate parameter S . The momentum boundary layer thickness also increases with increasing S . In contrast, Figure 6b shows a decrease in the amplitude of flow velocity with the ratio of oscillating frequency to stretching rate parameter S at time instant $\tau = 9.5\pi$.

Concluding remarks

We have investigated an unsteady two-dimensional boundary layer flow of Oldroyd-B fluid over an oscillatory stretching sheet by using boundary layer approximations. A well known analytic technique namely homotopy analysis method is used to compute the series solution. Study reveals that the time-series of amplitude of the velocity increases by increasing ratio of angular frequency to stretching parameter S and retardation time parameter β_2 , The effects of material parameters β_1 and β_2 on the velocity profile are quite opposite. It is also observed that the amplitude of velocity decreases by increasing Hartmann number.

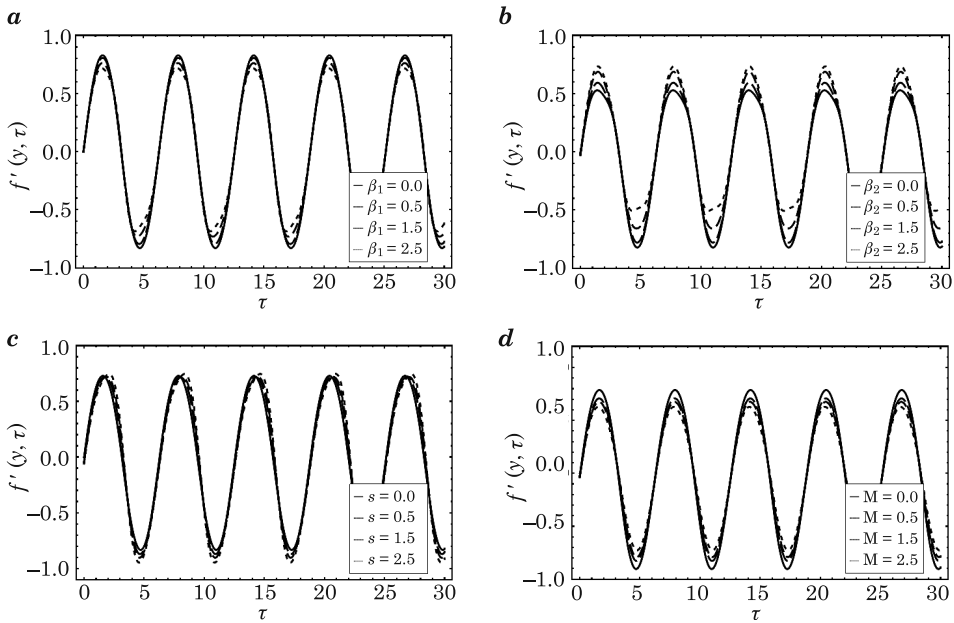


Fig. 2. Time-series of velocity profile for different values of: a - β_1 with $S = 0.2$, $M = 0.2$, $\beta_1 = 1.5$, b - β_2 with $M = 1.5$, $S = 0.1$, $\beta_1 = 2.6$, c - S with $M = 0.5$, $\beta_1 = 1$, $\beta_2 = 0.5$, d - M with $S = 0.5$, $\beta_1 = 1$, $\beta_2 = 0.5$

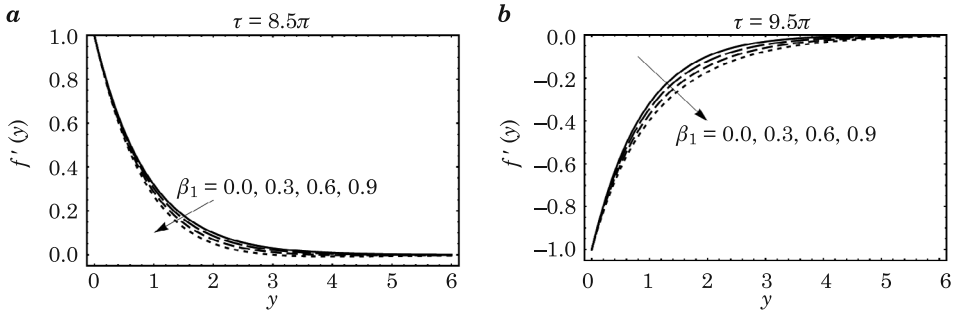


Fig. 3. Velocity profile for different values of β_1 with $M = 2, S = 0.7, \beta_2 = 0.5$

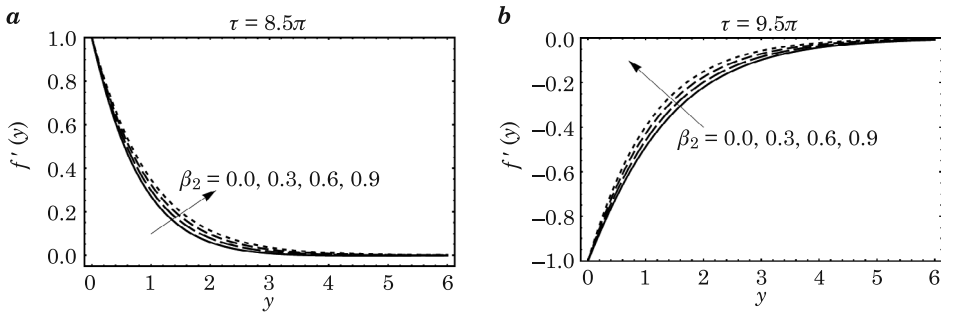


Fig. 4. Velocity profile for different values of β_2 with $M = 0.2, S = 0.1, \beta_1 = 1$

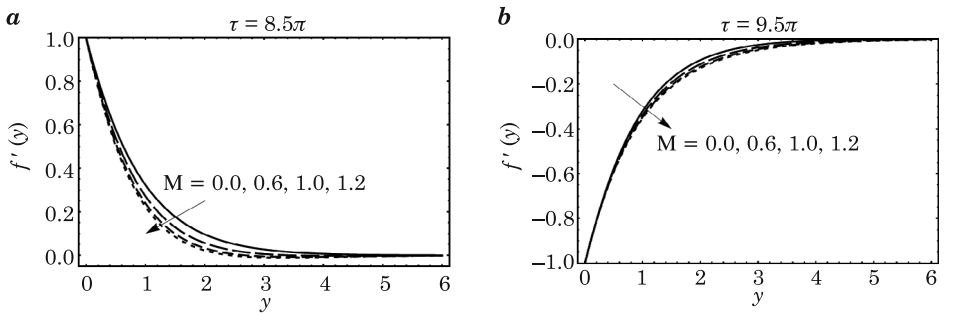


Fig. 5. Velocity profile for different values of M with $S = 0.1, \beta_1 = 3, \beta_2 = 1$

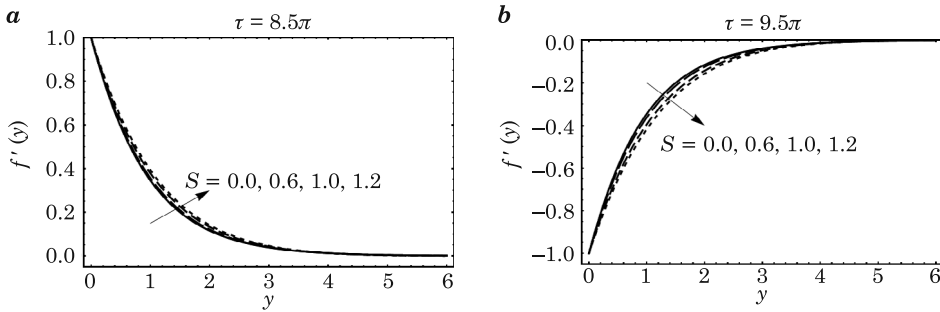


Fig. 6. Velocity profile for different values of S with $M = 0.1$, $\beta_1 = 3$, $\beta_2 = 1$

Acknowledgments

We are thankful to the anonymous reviewer for his/her useful comments to improve the earlier version of the paper.

References

- ABBAS Z., WANG Y., HAYAT T., OBERLACK M. 2008. *Hydromagnetic flow in a viscoelastic fluid due to the oscillatory stretching surface*. *Int. J. Nonlinear Mech.*, 43(8): 783–797, <http://dx.doi.org/10.1016/j.ijnonlinmec.2008.04.009>.
- ABBAS Z., WANG Y., HAYAT T., OBERLACK M. 2009. *Slip effects and heat transfer analysis in a viscous fluid over an oscillatory stretching surface*. *Int. J. Numer. Meth. Fluids*, 59: 443–458.
- ABBASBANDY S. 2007. *Homotopy Analysis Method for Heat Radiation Equations*. *Int. Commun. Heat Mass Transfer*, 34: 380–387.
- ALI N., KHAN S.U., ABBAS Z. 2015. *Hydromagnetic Flow and Heat Transfer of a Jeffrey Fluid over an Oscillatory Stretching Surface*. *Z. Naturforsch., A*, 70(7): 567–576.
- ALI N., KHAN S.U., ABBAS Z., SAJJID M. 2016. *Soret and Dufour effects on hydromagnetic flow of viscoelastic fluid over porous oscillatory stretching sheet with thermal radiation*. *J. Braz. Soc. Mech. Sci. Eng.*, 38: 2533–2546.
- CRANE L.J. 1970. *Flow past a stretching plate*. *Z. Angew. Math. Phys. (ZAMP)*, 21: 645–647.
- ELSHEHAWY E.F., ELSAYED M.E., ELBARBARY N.E. 2003. *Effect of inclined magnetic field on magneto fluid flow through a porous medium between two inclined wavy porous plates (numerical study)*. *Applied Mathematics and Computation*, 135(1): 85–103.
- HAYAT T., MUHAMMAD T., SHEHZAD S.A., ALSAEDI A. 2015a. *Temperature and Concentration Stratification Effects in Mixed Convection Flow of an Oldroyd-B Fluid with Thermal Radiation and Chemical Reaction*. *PLoS ONE* 10(6): e0127646, doi: 10.1371/journal.pone.0127646.
- HAYAT T., MUSTAFA M., POP I. 2010. *Heat and mass transfer for Soret and Dufour's effect on mixed convection boundary layer flow over a stretching vertical surface in a porous medium filled with a viscoelastic fluid*. *Commun. Nonlinear Sci. Numer. Simul.*, 15: 1183–1196.
- HAYAT T., SHAFIQ A., ALSAEDI A., ASGHAR S. 2015b. *Effect of inclined magnetic field in flow of third grade fluid with variable thermal conductivity*. *AIP Advances*, 5: 087108, doi: <http://dx.doi.org/10.1063/1.4928321>.
- HAYAT T., SHEHZAD S.A., MEZEL S.A., ALSAEDI A. 2014. *Three-dimensional flow of an Oldroyd-B fluid over a bidirectional stretching surface with prescribed surface temperature and prescribed surface heat flux*. *J. Hydrol. Hydromech.*, 62: 117–125.

- LIAO S.J. 2004. *On the homotopy analysis method for nonlinear problems*. App. Mathematics and Computation, 147: 499–513.
- MUKHOPADHYAY S., RANJAN DE P., LAYEK G.C. 2013. *Heat transfer, characteristics for the Maxwell fluid flow past an unsteady stretching permeable surface embedded in a porous medium with thermal radiation*. Journal of Applied Mechanics and Technical Physics, 54(3): 385–396.
- POP I., NA T.Y. 1996. *Unsteady flow past a stretching sheet*. Mechanics Research Communications, 23: 413–422.
- RAJAGOPAL K.R., BHATNAGAR R.K. 1995. *Exact solutions for some simple flows of an Oldroyd-B fluid*. Acta Mechanica, 113: 233–239.
- RAJU C.S.K., SANDEEP N., SULOCHANA C., SUGUNAMMA V., JAYACHANDRA BABU M. 2015. *Radiation, inclined magnetic field and cross-diffusion effects on flow over a stretching surface*. Journal of the Nigerian Mathematical Society, 34: 169–180.
- SAJID M., ABBAS Z., JAVED T., ALI N. 2010. *Boundary layer flow of an Oldroyd-B fluid in the region of stagnation point over a stretching sheet*. Canadian Journal of Physics, 88: 635–640.
- SHEIKH M., ABBAS Z. 2015. *Effects of thermophoresis and heat generation/absorption on MHD flow due to an oscillatory stretching sheet with chemically reactive species*. Journal of Magnetism and Magnetic Materials, S0304-8853(15): 3043.
- TURKYILMAZOGLU M. 2009. *Purely Analytic Solutions of the Compressible Boundary Layer Flow due to a Porous Rotating Disk with Heat Transfer*. Phys. Fluids, 21: 106104.
- TURKYILMAZOGLU M. 2012. *Solution of the Thomas-Fermi equation with a convergent approach*. Commun. Nonlinear Sci. Numer. Simul., 17: 4097–4103.
- TURKYILMAZOGLU M. 2013. *The analytical solution of mixed convection heat transfer and fluid flow of a MHD viscoelastic fluid over a permeable stretching surface*. Int. J. Mech. Sci., 77: 263–268.
- VARSHNEY C.L. 1979. *Fluctuating flow of viscous fluid through a porous medium bounded by a porous plate*. Indian J. Pure Appl. Math., 10(12): 1558–1564.
- WANG C.Y. 1988. *Nonlinear streaming due to the oscillatory stretching of a sheet in a Viscous fluid*. Acta Mech. 72: 261–268.
- ZHENG L., LIU Y., ZHANG X. 2011. *Exact solutions for MHD flow of generalized Oldroyd-B fluid due to an infinite accelerating plate*. Mathematical and Computer Modelling, 54: 780–788.
- ZHENG L.C., JIN X., ZHANG X.X., ZHANG J. H. 2013. *Unsteady heat and mass transfer in MHD flow over an oscillatory stretching surface with Soret and Dufour effects*. Acta Mechanica Sinica, 29(5): 667–675.

Guide for Autors

Introduction

Technical Sciences is a peer-reviewed research Journal published in English by the Publishing House of the University of Warmia and Mazury in Olsztyn (Poland). Journal is published continually since 1998. Until 2010 Journal was published as a yearbook, in 2011 and 2012 it was published semiyearly. From 2013, the Journal is published quarterly in the spring, summer, fall, and winter.

The Journal covers basic and applied researches in the field of engineering and the physical sciences that represent advances in understanding or modeling of the performance of technical and/or biological systems. The Journal covers most branches of engineering science including biosystems engineering, civil engineering, environmental engineering, food engineering, geodesy and cartography, information technology, mechanical engineering, materials science, production engineering etc.

Papers may report the results of experiments, theoretical analyses, design of machines and mechanization systems, processes or processing methods, new materials, new measurements methods or new ideas in information technology.

The submitted manuscripts should have clear science content in methodology, results and discussion. Appropriate scientific and statistically sound experimental designs must be included in methodology and statistics must be employed in analyzing data to discuss the impact of test variables. Moreover there should be clear evidence provided on how the given results advance the area of engineering science. Mere confirmation of existing published data is not acceptable. Manuscripts should present results of completed works.

There are three types of papers: a) research papers (full length articles); b) short communications; c) review papers.

The Journal is published in the printed and electronic version. The electronic version is published on the website ahead of printed version of Technical Sciences.

Technical Sciences does not charge submission or page fees.

Types of paper

The following articles are accepted for publication:

Reviews

Reviews should present a focused aspect on a topic of current interest in the area of biosystems engineering, civil engineering, environmental engineering, food engineering, geodesy and cartography, information technology, mechanical engineering, materials science, production engineering etc. They should include all major findings and bring together reports from a number of sources. These critical reviews should draw out comparisons and conflicts between work, and provide an overview of the 'state of the art'. They should give objective assessments of the topic by citing relevant published work, and not merely present the opinions of individual authors or summarize only work carried out by the authors or by those with whom the authors agree. Undue speculations should also be avoided. Reviews generally should not exceed 6,000 words.

Research Papers

Research Papers are reports of complete, scientifically sound, original research which contributes new knowledge to its field. Papers should not exceed 5,000 words, including figures and tables.

Short Communications

Short Communications are research papers constituting a concise description of a limited investigation. They should be completely documented, both by reference list, and description of the experimental procedures. Short Communications should not occupy more than 2,000 words, including figures and tables.

Letters to the Editor

Letters to the Editor should concern with issues raised by articles recently published in scientific journals or by recent developments in the engineering area.

Contact details for submission

The paper should be sent to the Editorial Office, as a Microsoft Word file, by e-mail: techsci@uwm.edu.pl

Referees

Author/authors should suggest, the names, addresses and e-mail addresses of at least three potential referees. The editor retains the sole right to decide whether or not the suggested reviewers are used.

Submission declaration

After final acceptance of the manuscript, the corresponding author should send to the Editorial Office the author's declaration. Submission of an article implies that the work has not been published previously (except in the form of an abstract or as part of a published lecture or academic thesis or as an electronic preprint), that it is not under consideration for publication elsewhere, that publication is approved by all authors and tacitly or explicitly by the responsible authorities where the work was carried out, and that, if accepted, it will not be published elsewhere in the same form, in English or in any other language.

To prevent cases of ghostwriting and guest authorship, the author/authors of manuscripts is/are obliged to: (i) disclose the input of each author to the text (specifying their affiliations and contributions, i.e. who is the author of the concept, assumptions, methods, protocol, etc. used during the preparation of the text); (ii) disclose information about the funding sources for the article, the contribution of research institutions, associations and other entities.

Language

Authors should prepare the full manuscript i.e. title, abstract and the main text in English (American or British usage is accepted). Polish version of the manuscript is not required.

The file type

Text should be prepared in a word processor and saved in doc or docx file (MS Office).

Article structure

Suggested structure of the manuscript is as follows:

- Title
- Authors and affiliations
- Corresponding author
- Abstract
- Keywords
- Introduction
- Material and Methods
- Results and Discussion
- Conclusions

Acknowledgements (*optional*)
References
Tables
Figures

Subdivision – numbered sections

Text should be organized into clearly defined and numbered sections and subsections (optionally). Sections and subsections should be numbered as 1. 2. 3. then 1.1 1.2 1.3 (then 1.1.1, 1.1.2, ...). The abstract should not be included in numbering section. A brief heading may be given to any subsection. Each heading should appear on its own separate line. A single line should separate paragraphs. Indentation should be used in each paragraph.

Font guidelines are as follows:

- Title: 14 pt. Times New Roman, bold, centered, with caps
- Author names and affiliations: 12 pt. Times New Roman, bold, centered, italic, two blank line above
- Abstract: 10 pt. Times New Roman, full justified, one and a half space. Abstract should begin with the word Abstract immediately following the title block with one blank line in between. The word Abstract: 10 pt. Times New Roman, centered, indentation should be used
- Section Headings: Not numbered, 12 pt. Times New Roman, bold, centered; one blank line above
- Section Sub-headings: Numbered, 12 pt. Times New Roman, bold, italic, centered; one blank line above
- Regular text: 12 pt. Times New Roman, one and a half space, full justified, indentation should be used in each paragraph

Title page information

The following information should be placed at the first page:

Title

Concise and informative. If possible, authors should not use abbreviations and formulae.

Authors and affiliations

Author/authors' names should be presented below the title. The authors' affiliation addresses (department or college; university or company; city, state and zip code, country) should be placed below the names. Authors with the same affiliation must be grouped together on the same line with affiliation information following in a single block. Authors should indicate all affiliations with a lower-case superscript letter immediately after the author's name and in front of the appropriate address.

Corresponding author

It should be clearly indicated who will handle correspondence at all stages of refereeing and publication, also post-publication process. The e-mail address should be provided (footer, first page). Contact details must be kept up to date by the corresponding author.

Abstract

The abstract should have up to 100-150 words in length. A concise abstract is required. The abstract should state briefly the aim of the research, the principal results and major conclusions. Abstract must be able to stand alone. Only abbreviations firmly

established in the field may be eligible. Non-standard or uncommon abbreviations should be avoided, but if essential they must be defined at their first mention in the abstract itself.

Keywords

Immediately after the abstract, author/authors should provide a maximum of 6 keywords avoiding general, plural terms and multiple concepts (avoid, for example, 'and', 'of'). Author/authors should be sparing with abbreviations: only abbreviations firmly established in the field may be eligible.

Abbreviations

Author/authors should define abbreviations that are not standard in this field. Abbreviations must be defined at their first mention there. Author/authors should ensure consistency of abbreviations throughout the article.

Units

All units used in the paper should be consistent with the SI system of measurement. If other units are mentioned, author/authors should give their equivalent in SI.

Introduction

Literature sources should be appropriately selected and cited. A literature review should discuss published information in a particular subject area. Introduction should identify, describe and analyze related research that has already been done and summarize the state of art in the topic area. Author/authors should state clearly the objectives of the work and provide an adequate background.

Material and Methods

Author/authors should provide sufficient details to allow the work to be reproduced by other researchers. Methods already published should be indicated by a reference. A theory should extend, not repeat, the background to the article already dealt within the Introduction and lay the foundation for further work. Calculations should represent a practical development from a theoretical basis.

Results and Discussion

Results should be clear and concise. Discussion should explore the significance of the results of the work, not repeat them. A combined Results and Discussion section is often appropriate.

Conclusions

The main conclusions of the study may be presented in a Conclusions section, which may stand alone or form a subsection of a Results and Discussion section.

Acknowledgements

Author/authors should include acknowledgements in a separate section at the end of the manuscript before the references. Author/authors should not include them on the title page, as a footnote to the title or otherwise. Individuals who provided help during the research study should be listed in this section.

Artwork

General points

- Make sure you use uniform lettering and sizing of your original artwork
- Embed the used fonts if the application provides that option

- Aim to use the following fonts in your illustrations: Arial, Courier, Times New Roman, Symbol
- Number equations, tables and figures according to their sequence in the text
- Size the illustrations close to the desired dimensions of the printed version

Formats

If your electronic artwork is created in a Microsoft Office application (Word, PowerPoint, Excel) then please supply 'as is' in the native document format

Regardless of the application used other than Microsoft Office, when your electronic artwork is finalized, please 'Save as' or convert the images to one of the following formats (note the resolution requirements given below):

EPS (or PDF): Vector drawings, embed all used fonts

JPEG: Color or grayscale photographs (halftones), keep to a minimum of 300 dpi

JPEG: Bitmapped (pure black & white pixels) line drawings, keep to a minimum of 1000 dpi or combinations bitmapped line/half-tone (color or grayscale), keep to a minimum of 500 dpi

Please **do not**:

- Supply files that are optimized for screen use (e.g., GIF, BMP, PICT, WPG); these typically have a low number of pixels and limited set of colors
- Supply files that are too low in resolution
- Submit graphics that are disproportionately large for the content

Color artwork

Author/authors should make sure that artwork files are in an acceptable format (JPEG, EPS PDF, or MS Office files) and with the correct resolution. If, together with manuscript, author/authors submit color figures then Technical Sciences will ensure that these figures will appear in color on the web as well as in the printed version at no additional charge.

Tables, figures, and equations

Tables, figures, and equations/formulae should be identified and numbered consecutively in accordance with their appearance in the text.

Equations/mathematical and physical formulae should be presented in the main text, while tables and figures should be presented at the end of file (after References section). Mathematical and physical formulae should be presented in the MS Word formula editor.

All types of figures can be black/white or color. Author/authors should ensure that each figure is numbered and has a caption. A caption should be placed below the figure. Figure must be able to stand alone (explanation of all symbols and abbreviations used in figure is required). Units must be always included. It is noted that figure and table numbering should be independent.

Tables should be numbered consecutively in accordance with their appearance in the text. Table caption should be placed above the table. Footnotes to tables should be placed below the table body and indicated with superscript lowercase letters. Vertical rules should be avoided. Author/authors should ensure that the data presented in tables do not duplicate results described in figures, diagrams, schemes, etc. Table must be able to stand alone (explanation of all symbols and abbreviations used in table is required). Units must be always included. As above, figure and table numbering should be independent.

References

References: All publications cited in the text should be presented in a list of references following the text of the manuscript. The manuscript should be carefully checked to ensure that the spelling of authors' names and dates of publications are exactly the same in the text as in the reference list. Authors should ensure that each reference cited in the text is also present in the reference list (and vice versa).

Citations may be made directly (or parenthetically). All citations in the text should refer to:

1. Single author

The author's name (without initials, with caps, unless there is ambiguity) and the year of publication should appear in the text

2. Two authors

Both authors' names (without initials, with caps) and the year of publication should appear in the text

3. Three or more authors

First author's name followed by et al. and the year of publication should appear in the text

Groups of references should be listed first alphabetically, then chronologically.

Examples:

"... have been reported recently (ALLAN, 1996a, 1996b, 1999; ALLAN and JONES, 1995).

KRAMER et al. (2000) have recently shown..."

The list of references should be arranged alphabetically by authors' names, then further sorted chronologically if necessary. More than once reference from the same author(s) in the same year must be identified by the letters "a", "b", "c" etc., placed after the year of publication.

References should be given in the following form:

KUMBHAR B.K., AGARVAL R.S., DAS K. 1981. *Thermal properties of fresh and frozen fish*. International Journal of Refrigeration, 4(3), 143–146.

MACHADO M.F., OLIVEIRA F.A.R., GEKAS V. 1997. *Modelling water uptake and soluble solids losses by puffed breakfast cereal immersed in water or milk*. In Proceedings of the Seventh International Congress on Engineering and Food, Brighton, UK.

NETER J., KUTNER M.H., NACHTSCHEIM C.J., WASSERMAN W. 1966. *Applied linear statistical models* (4th ed., pp. 1289–1293). Irwin, Chicago.

THOMSON F.M. 1984. *Storage of particulate solids*. In M. E. Fayed, L. Otten (Eds.), *Handbook of Powder Science and Technology* (pp. 365–463). Van Nostrand Reinhold, New York.

Citation of a reference as 'in press' implies that the item has been accepted for publication.

Note that the full names of Journals should appear in reference list.

Submission checklist

The following list will be useful during the final checking of an article prior to the submission. Before sending the manuscript to the Journal for review, author/authors should ensure that the following items are present:

- Text is prepared with a word processor and saved in DOC or DOCX file (MS Office). One author has been designated as the corresponding author with contact details: e-mail address

- Manuscript has been 'spell-checked' and 'grammar-checked'

- References are in the correct format for this Journal

- All references mentioned in the Reference list are cited in the text, and vice versa

- Author/authors does/do not supply files that are too low in resolution

- Author/authors does/do not submit graphics that are disproportionately large for the content